SIGNALING PATHWAYS INVOLVED IN ENHANCED NMDA RECEPTOR-DEPENDENT EXCITOTOXICITY IN A MOUSE MODEL OF HUNTINGTON DISEASE

by

Jing Fan

M.Sc., University of British Columbia, 2007

A THESIS SUBMITTED IN PARTIAL FULLFILLMENT OF THE

REQUIREMENTS FOR THE DEGREE OF

DOCTOR OF PHILOSOPHY

in

The Faculty of Graduate Studies

(Neuroscience)

THE UNIVERSITY OF BRITISH COLUMBIA

(Vancouver)

October 2011

Abstract

Huntington disease (HD) is an inherited neurodegenerative disease lacking effective treatment, characterized by involuntary movements, psychiatric disorders, and cognitive symptoms. Pathology shows prominent degeneration of γ-aminobutyric acid (GABA)-ergic medium-sized spiny neurons (MSNs) of the striatum and certain cortical layers (Vonsattel and DiFiglia, 1998). HD is caused by a dominant mutation in the HD gene that leads to >35 glutamine repeats (polyQ) near the N-terminus of the protein huntingtin (htt) (The Huntington's Disease Collaborative Research Group, 1993). Increasing evidence suggests that the N-methyl-D-aspartate (NMDA)-type glutamate receptor (NMDAR) plays a role in mediating death of MSNs observed in HD (Fan and Raymond, 2007). Previous results from our laboratory demonstrate that NMDAR-mediated current and toxicity are increased in MSNs from the Yeast Artificial Chromosome (YAC) transgenic mouse model expressing polyglutamine-expanded full-length human htt (Shehadeh et al., 2006; Zeron et al., 2002). However, the mechanism underlying altered function and enhanced toxicity of NMDAR in HD remains unknown.

Previous studies have shown that membrane-associated guanylate kinases (MAGUKs), such as postsynaptic density protein 95 (PSD-95) modulate NMDAR surface expression and excitotoxicity in rat hippocampal and cortical neurons (Aarts et al., 2002; Roche et al., 2001), and that htt interacts with PSD-95 in a polyglutamine dependent manner (Sun et al., 2001). Here, I tested the hypothesis that an altered

association and/or regulation between PSD-95 and NMDARs in mutant htt-expressing cells contributes to increased susceptibility to excitotoxicity and investigated mechanism by which this occurs. Specifically, I investigated the association of PSD-95 with htt and the NMDAR GluN2 subunits; signaling downstream of activation of the NMDAR/PSD-95 complex; and NMDA-induced cell death. My results suggest that at the presymptomatic stage of HD, the enhanced interaction of PSD-95 with GluN2B, and its signaling through p38 mitogen-activated protein kinase (MAPK) but not neuronal nitric oxide synthase (nNOS) activation, contributes to mutant htt-mediated sensitivity to NMDAR-dependent excitotoxicity in YAC128 striatal neurons. This work contributes to the understanding of both NMDAR-dependent neuronal death mechanisms in striatal neurons and early synaptic changes in HD pathogenesis, as well as providing potential drug candidates for future HD treatment.

Preface

A version of chapter 2 (section 2.1, section 2.2, section 2.3.1-3, section 2.3.4.1-2, section 2.3.5.1, section 2.3.6, section 2.4 except 2.4.3), and part of chapter 3 (section 3.1, section 3.2.5-8, section 3.3.1 and 3.3.3, section 3.4.1.1-2, section 3.4.3) have been published in: J. Fan, C. M. Cowan, L. Y. J. Zhang, M. R. Hayden, and L. A. Raymond. Interaction of postsynaptic density protein-95 with N-Methyl-D-Aspartate Receptors influences excitotoxicity in the YAC mouse model of Huntington's disease. J Neurosci. 2009 Sep 2; 29(35): 10928-38. I conducted all of the experiments except that in figure 3 (figure 2A in published article), 5 out of 8 independent experiments were conducted by L. Y. J. Zhang. I analyzed all the data and wrote the manuscript except that parts of the discussion and manuscript revisions were contributed by Dr. Lynn Raymond.

Part of chapter 2 (section 2.1, section 2.2, section 2.3.4.3, section 2.3.5.2, section 2.4.3), and chapter 3 (section 3.1, section 3.2.5-8, section 3.3.2, section 3.4.1.1) has been published in: J. Fan, O. C. Vasuta, L. Y. J. Zhang, L. Wang, A. George, L. A. Raymond. N-Methyl-D-Aspartate receptor subunit- and neuronal-type dependence of excitotoxic signaling through postsynaptic density 95. J Neurochem. 115, 1045-56. I conducted all the experiments except those shown in figures 8 and 9 (figure 1B and 1D in published article), which were partially conducted by L. Y. J. Zhang. Figures 11 and 13 (figure 2A and 4D&E in published article), were conducted by A. George and L. Wang, respectively,

under my supervision. I analyzed all the data and wrote most of the manuscript except that parts of the discussion and revision of manuscript were contributed by Dr. Lynn Raymond.

Other parts of chapter 3 are based on Jing Fan's work conducted in Dr. Lynn Raymond's laboratory at UBC. These results are part of an in-preparation manuscript titled "P38 MAPK is involved in enhanced NMDA receptor-dependent excitotoxicity in YAC transgenic mouse model of Huntington disease", by Jing Fan, C. M. Gladding, L. Y. J. Zhang, and Lynn A. Raymond. I was responsible for designing and conducting most of the experiments (except figure 1 in the manuscript, which is conducted by Clare Gladding), analyzing data and preparing the manuscript (except Dr. Lynn Raymond also contributed to the discussion and revision of the manuscript).

Check the first pages of these chapters to see footnotes with similar information.

All mice were housed and cared for, and was tissue harvested, according to guidelines of the University of British Columbia and the Canadian Council for Animal Care. Research in this study is approved by University of British Columbia Animal Care Committee (certificate numbers are: A06-1534, A03-0299, A06-0261, A09-0560, and A11-0012).

Table of contents

List of tables

List of figures

List of abbreviations

ACSF	Artificial cerebrospinal fluid
AKAP	A-kinase anchoring protein
AMPA	α-amino-3-hydroxy-5-methyl-4-isoxazolepropionate
AMPAR	AMPA receptor
AP	Alkaline phosphatase
AP-1	Activator protein-1
ATF-2	Activating transcription factor-2
BAC	Bacterial artificial chromosomes
Bax	Bcl-2–associated X protein
BCA	Bicinchoninic acid
Bcl-2	B-cell lymphoma 2
BDNF	Brain-derived neurotrophic factor
BES	N, N-bis[2-hydroxyethyl]-2-aminoethanesulfonic acid
BSA	Bovine serum albumin
BSS	Balanced salt solution
℃	Degrees centigrade
CaMKII	Ca^{2+}/calmodulin-dependent protein kinase II
Ca^{2+}	Calcium
$CaCl_2$	Calcium chloride
cAMP	Cyclic adenosine monophosphate
CBP	CREB binding protein
cDNA	Complementary deoxyribonucleic acid
cGMP	Cyclic guanosine monophosphate
Chapsyn 110	Channel-associated proteins of the synapses-110
CK2	Casein kinase II

CNS	Central nervous system
CO_2	Carbon dioxide
Co-IP	co-immunoprecipitation
CREB	cAMP response element binding protein
Ctrl	Control
DHPG	Dihydroxyphenylglycine
DIV	Days *in vitro*
Dlg	Discs large
DMSO	Dimethyl sulfoxide
DTT	Dithiothreitol
dUTP	2´Deoxyuridine, 5´Triphosphate
EAA	Excitatory amino acid
ECL	Enhanced chemiluminescence system
EDTA	Ethylenediaminetetraacetic acid
EGTA	Ethyleneglycol-bis[β-aminoethyl ether]-N, N, N'N'-tetraacetic acid
Elk-1	E twenty-six (ETS)-like transcription factor 1
ER	Endoplasmic reticulum
ERK	Ras–extracellular signal-regulated kinase
FoxO3a	Forkhead box O3a
GABA	γ-aminobutyric acid
GFP	Green fluorescent protein
GKAP	Guanylate kinase-associated protein
GluN1/2	See 'NR1/2'
GluR	Glutamate receptor
GLT1	Glutamate transporter-1
h (hr)	hour
H_2O_2	Hydrogen peroxide

htt	huntingtin
HAP	Huntingtin-associated protein
HBSS	Hank's balanced salt solution
HD	Huntington's disease
HEK293T cells	Human embryonic kidney 293T cells
HIP1	Huntingtin-interacting protein 1
HIP14	Huntingtin-interacting protein 14
HIPPI	HIP1-protein interactor
HIV	Human Immunodeficiency Virus
3-HK	3-hydroxykynurenine
HN33	Mouse hippocampal neuron x neuroblastoma cell line 33
HRP	Horse radish peroxidase
Htt	Huntingtin
IFN	Ifenprodil
IgG	Immunoglobulin G
iGluRs	ionotropic glutamate receptors
IP	Immunoprecipitation
IP_3	Inositol (1,4,5) – trisphosphate
$IP_3$1R	Type 1 inositol (1,4,5) – trisphosphate receptor
JNK	c-Jun amino-terminal kinase
KCl	Potassium chloride
LL	Dileucine
LTD	Long-term depression
LTP	Long-term potentiation
Lys	Lysate
M	Molar
MAGUK	Membrane-associated guanylate kinases

MAPK	Mitogen-activated protein kinase
MEF2	Myocyte enhancer factor-2
MEKKs	MAPK kinase kinases
MEKs	MAPK kinase
Mg^{2+}	Magnesium
mGluRs	metabotropic glutamate receptors
mL	Milliliter
μL	Microliter
mM	Millimolar
μM	Micromolar
MLK2	mixed-lineage kinase 2
mPins	mammalian partner of inscruteable
mPTP	Mitochondria permeability transition pore
mRNA	Messenger ribonucleic acid
ms	Milliseconds
MSNs	GABAergic medium-sized spiny striatal neurons
NaCl	Sodium chloride
Na_2HPO_4	Sodium phosphate, dibasic
N-Arg	Nω-Nitro-L-arginine
NF-κB	Nuclear factor kappa-light-chain-enhancer of activated B cells
NGS	Normal goat serum
nM	Nanomolar
NMDA	N-methyl-D-aspartate
NMDAR	NMDA receptor
nNOS	Neuronal nitric oxide synthase
NO	Nitric oxide
NOS	Nitric oxide synthase

nt	Nucleotide
NR1	NMDA receptor subunit-1 (also as GluN1)
NR2	NMDA receptor subunit-2 (also as GluN2)
NRSE	Neuron restrictive silencer element
P	Postnatal day
p53	Protein 53
PFA	Paraformaldehyde
PI	Propidium Iodide
PKA	Protein Kinase A
PKC	Protein Kinase C
PBS	Phosphate-buffered saline
PDZ domain	PSD/Discs-large/ZO-1 domain
PFA	Paraformaldehyde
PI	Propidium iodide
PM	Plating medium
PMSF	Phenylmethylsulfonyl fluoride
PolyQ	Polyglutamine expansion
PSD	Postsynaptic density
PSD-93	Postsynaptic density-93
PSD-95	Postsynaptic density-95
PVDF	Polyvinylidene difluoride
Q	Glutamine (PolyQ repeats)
QA	Quinolinic acid
RasGAP	Ras GTPase activating protein
RE1	Repressor element-1
REST	Repressor element-1 transcription factor
RNAi	RNA interference

ROS	Reactive oxygen species
RT	Room temperature
SAP97	Synapse-associated protein-97
SAP102	Synapse-associated protein-102
SAPKs	Stress-activated protein kinases
SCA-1	Spinocerebellar ataxia 1
SDS-PAGE	Sodium dodecyl sulfate-polyacrylamide gel electrophoresis
sec	Seconds
SEM	Standard error of the mean
SH3	Src homology 3
Shank	SH3 and ankyrin repeat-containing protein
siRNA	Small interfering RNA
Sp1	Specificity protein-1
SPN	Supernatant
Src	Sarcoma
STEP	Striatal-enriched protein tyrosine phosphatase
SynGAP	Synaptic RAS GTPase-activating protein
TBS	Tris-buffered saline
Thr (T)	Threonine
TUNEL	Terminal deoxynucleotidyltransferase-mediated dUTP-fluorescein nick end labeling
Tyr (Y)	Tyrosine
WT	Wild-type (FVB/N mice)
YAC	Yeast artificial chromosome
YFP	Yellow fluorescent protein

Acknowledgements

This dissertation would not have been a real fulfillment without the support and cooperation from many people through various means.

At the very first, I'm honoured to express my deepest gratitude to my devoted supervisor, Dr. Lynn A. Raymond, whose encouragement, guidance and patience all the way from the very beginning enabled me to develop an understanding of the field. She has guided me through my graduate study with valuable ideas, recommendations and criticisms with her profound knowledge and rich research experience. Her backing and kindness are heartily appreciated.

I would like to thank my committee members Dr. Brian MacVicar, Dr. Yutian Wang, and Dr. Blair Leavitt for their priceless input and discussions over the years. This thesis cannot be completed without all your support and encouragement. I owe special thanks to Dr. Brian MacVicar, for his valuable comments and guidance on collaborated study and my other projects. I wish to extend my gratefulness to the faculties and staffs of Neuroscience program, especially Dr. Tim Murphy, Dr. Alaa El-Husseini and Dr. Ann Marie Craig, for their supportive expertise.

I would also like to thank all previous and current members of the Lynn Raymond lab, especially Mannie Fan, Lily Zhang and Clare Gladding for their support and friendship. Additionally, I am very grateful for the friendship of all of the members in both Lynn's and Tim's lab, with whom I worked closely, laughed together and puzzled over many of the same problems.

Appreciations are also due to my out-of-lab friends, who never failed to offer me great encouragement and lessen my stress during the Ph.D study. Special thanks should go to Kun Huang, Shu Zhang, Guang Yang, Shanshan Zhu, Chao Tai, Ning Zhou, Dongchuan Wu and Xuefeng Liu for all the discussion and sharing of knowledge and experience with me when I was struggling with projects.

At last but not least, I would like to thank my parents, for their love and faith in me and respect of my decisions. Finally, and most importantly, I owe my deepest gratitude to my husband Xiaojun Xie. His support, tolerance and firm love were really what I relied on and the source of my strength in the past nine years.

Lastly, I offer my greatest regards and blessings to all of those who supported me in any respect during my growth in neuroscience and the completion of the Ph.D project.

Dedication

I dedicate this dissertation to my family, especially…

To my parents for teaching me love, patience, and helping to make me who I am;

To my dear husband for always being there for me with constant love and caring;

To my baby Jenny for accompanying me during the writing of this dissertation and brightening my world.

1 General introduction

1.1 Huntington's disease

HD is an autosomal-dominantly inherited neurodegenerative disease affecting approximately 5 to 10 in 100,000 population (Vonsattel and DiFiglia, 1998), for which there are few effective therapies and no cure. The typical symptoms of HD include chorea, or involuntary dance-like movements. Individuals with the disease frequently also display cognitive disturbances, motor learning deficits, and disorders of mood, most commonly depression and irritability, all of which precede the onset of the motor abnormalities (Harper, 1991; Johnson and Davidson, 2010; Paulsen et al., 2008).

1.1.1 Huntington's disease and huntingtin

HD is caused by an unstable expansion of a CAG repeat (>35) near the 5' end of the *HTT* gene, which is located on the short arm of chromosome 4 (The Huntington's Disease Collaborative Research Group, 1993). The gene encodes for a protein called huntingtin, and the mutation results in an elongated stretch of glutamine (polyQ) in the N-terminus of the 350 kDa protein (The Huntington's Disease Collaborative Research Group, 1993). The age of disease onset varies inversely with the length of CAG repeat and the severity of the progress of disease (Andrew et al., 1993; Aziz et al., 2009; Brinkman et al., 1997; Sieradzan et al., 1997). HD patients with CAG repeats < 60 usually show adult onset, normally at the age of ~ 39 (Harper, 1991), while those with CAG repeats > 60 have juvenile onset and accelerated clinical

progression (Brandt et al., 1996).

In the early studies, humans homozygous or heterozygous for the HD mutation show no significant differences in disease onset or progression (MacDonald and Gusella, 1996; Myers et al., 1989; Wexler et al., 1987). However, HD homozygotes had a more severe clinical course compared with heterozygotes in a human study (Squitieri et al., 2003), and homozygous transgenic mice expressing full-length mutant HD cDNA have a shorter life span compared with heterozygous mice by ~two months (Reddy et al., 1998).

Despite some dispute, it is now thought that HD is caused by both a loss-of-function of the normal htt protein that are fundamental for the survival and functioning of the predominantly degenerated neurons, and a gain-of-function of mutant htt with new toxic functions contributing to the disease (Zuccato et al., 2010).

1.1.1.1 Wild-type huntingtin and 'loss-of-function'

Huntingtin is ubiquitously expressed in the central nervous system (CNS) as well as in other tissues (Gutekunst et al., 1995; Sieradzan and Mann, 2001; Trottier et al., 1995; Vonsattel and DiFiglia, 1998), and has been shown to be critical for development. Huntingtin deletion in mice results in embryonic-lethality (Duyao et al., 1995; Hodgson et al., 1996; Nasir et al., 1995; Zeitlin et al., 1995), which can be rescued by introducing the human HD gene in the YAC transgenic mice (Hodgson et al., 1996; Leavitt et al., 2001). Further study provided *in vivo* evidence that the levels of huntingtin modulate neuronal sensitivity to excitotoxic neurodegeneration (Leavitt

et al., 2006).

Htt is a cytoplasmic protein closely associated with various organelles within the cell, including the mitochondria, endoplasmic reticulum (ER), Golgi complex, and nucleus (Atwal et al., 2007; Hilditch-Maguire et al., 2000; Hoffner et al., 2002; Kegel et al., 2002; Panov et al., 2002; Strehlow et al., 2007). Htt is also found within neurites and at synapses, where it associates with microtubules, clathrin-coated vesicles, endosomal compartments, as well as synaptic proteins suggesting that it may have a role in vesicle transport, protein trafficking, exocytosis, endocytosis, and synaptic function (DiFiglia et al., 1995; Hoffner et al., 2002; Sharp et al., 1995; Velier et al., 1998; Wood et al., 1996).

Wild-type htt has been shown to stimulate cortical brain-derived neurotrophic factor (BDNF) protein production by acting at a transcriptional level through its association and sequestration of the repressor element-1 (RE1) transcription factor REST-NRSE (neuron restrictive silencer element) complex (Zuccato et al., 2003). In addition, a group also showed that full-length wild-type huntingtin promotes BDNF vesicular trafficking through its binding with huntingtin-associated protein 1 (HAP1) in neuronal cells and this transport can be attenuated by reducing the levels of wild-type huntingtin using RNAi (Gauthier et al., 2004).

Moreover, both *in vivo* and *in vitro* studies show that htt plays an anti-apoptotic role in response to a variety of insults (Cattaneo et al., 2001; Leavitt et al., 2001; Rigamonti et al., 2000; Rigamonti et al., 2001; Zhang et al., 2003).

1.1.1.2 Mutant huntingtin and 'gain-of-function'

Results of many studies suggest that mutant huntingtin is responsible for mitochondrial dysfunction, elevated oxidative stress, compromised energy metabolism, impaired ubiquitination and proteasomal function, dysregulation of the transcriptional machinery, compromised endocytosis and axonal transport, as well as enhanced excitotoxicity and cortical-striatal dysfunction (Davies and Ramsden, 2001; Fan and Raymond, 2007; Gutekunst et al., 1995; Harjes and Wanker, 2003; Hoffner et al., 2002; Li and Li, 2004b; Menalled et al., 2002; Milnerwood and Raymond, 2007; Milnerwood and Raymond, 2010; Ross, 2002; Rubinsztein, 2002; Sugars and Rubinsztein, 2003; Tobin and Signer, 2000; Zuccato et al., 2010). All of these changes together or sequentially lead to neuronal dysfunction and eventually neurodegeneration. Additionally, there is a hypothesis that neuronal dysfunction results, at least in part, from altered astrocytic or glial glutamate uptake function caused by mutant huntingtin. Microdialysis studies have shown that glial glutamate transporter-1 (GLT1) function is downregulated in R6/2 mice, resulting in deficient clearance of glutamate by the GLT1 in the striatum of R6 transgenic mice (Behrens et al., 2002; Lievens et al., 2001; Shin et al., 2005).

Another pathophysiological mechanism thought to underlie neuronal dysfunction in HD is that soluble mutant htt, when localized to the nucleus, alters neuronal gene expression (Cattaneo et al., 2005). This may occur, in part, through interaction with several transcription factors, such as cAMP response element binding protein (CREB)-binding protein (CBP) and specificity protein-1 (Sp1) (Dunah et al., 2002; Li et al., 2002b; Luthi-Carter et al., 2002; Nucifora et al., 2001; Steffan et al., 2001). One

study found that mutant htt interacts weakly with REST–NRSE, leading to increased accumulation of REST–NRSE in the nucleus, which subsequently inhibits the expression of BDNF and other genes and thus contributes to neuronal dysfunction (Zuccato et al., 2003).

1.1.2 Selective neurodegeneration in Huntington's disease

Post-mortem analyses of HD brains show selective degeneration of the striatum (up to ~95% loss of neurons), affecting striatal GABAergic medium-sized spiny neurons (MSNs) most severely, as well as the cortex, with lesser losses of the hippocampus and hypothalamus (Vonsattel and DiFiglia, 1998). In the striatum, the most affected neuronal population is MSNs, which comprise ~90% of neurons in this region (Surmeier et al., 1988), while the interneurons are spared (Sieradzan and Mann, 2001). The reasons why MSNs are most vulnerable in HD are not fully understood, but these neurons are enriched in GluN2B-containing NMDARs compared with other GluN2 subunits and other brain regions (Christie et al., 2000; Landwehrmeyer et al., 1995; Li et al., 2003b). Thus, striatum and MSNs will be my focus in this HD study.

1.1.3 Proteins that interact with huntingtin

The expression levels of htt in the CNS and in different types of striatal neurons are similar, without any enrichment in the striatum or MSNs as might be expected given the selective degeneration of this neuronal population (DiFiglia et al., 1995; Ferrante et al., 1997; Kumar et al., 1997; Li et al., 1993; Sharp et al., 1995). Thus, one would suggest that htt interactions with proteins which have critical functions in

specific striatum or MSNs context and cellular signaling networks, and whose interactions are changed by the htt polyQ expansion may lead to the selective neuronal death.

Discovery of several proteins that interact with huntingtin in a polyQ-dependent manner has provided clues to the role of wild-type htt in normal neuronal function, as well as to the possible mechanisms by which polyQ-expanded htt ("mutant htt") results in neurodegeneration (Gutekunst et al., 1995; Li et al., 2003a). Some of these htt-interactors and their possible functions are summarized in the table below (Table 1), which is not a complete list but just to name a few examples.

Huntingtin-associated proteins (HAP-1,2) and huntingtin-interacting proteins (HIP-1,2,3) are two families of cytoskeletal proteins that interact with vesicle or membrane associated proteins (Gutekunst et al., 1995; Li and Li, 2004a). HAP and HIP families are reported to interact with the N-terminus of htt in a polyQ length-dependent manner, by yeast two-hybrid screens (Gutekunst et al., 1995; Li and Li, 2004a). As interaction of HAP1 with htt is enhanced by polyQ expansion, and HAP1 was recently found to interact with the type 1 inositol (1,4,5) − trisphosphate receptor (IP$_3$R1), it is suggested that mutant htt enhances the sensitivity of IP$_3$R1 to inositol (1,4,5) − triphosphate through the IP$_3$R1 − HAP1A − Htt ternary complex (Tang et al., 2004). On the other hand, it was reported that decreased binding of mutant htt to HIP1 might increase association of HIP1 and HIPPI (HIP1-protein interactor), which induces caspase-8 cleavage and apoptosis (Gervais et al., 2002).

Another interesting htt-interacting protein is postsynaptic density protein-95

(PSD-95) (Sun et al., 2001), which has been shown to cluster and stabilize ion channels and receptors at the synapse (Kim and Sheng, 2004). PSD-95 directly binds to the proline-rich region adjacent to the polyQ domain in the N-terminus of wild-type htt, through its type-II Src homology 3 (SH3) domain (Sun et al., 2001). As polyQ length increases, a decreased interaction of mutant huntingtin with PSD95 has been observed (Sun et al., 2001). The authors postulate that expression of polyQ-expanded htt allows more PSD95 to be released, resulting in more stabilized ion channels (such as NMDA receptors), and possibly leading to their over-activation/sensitization, thus making neurons more vulnerable to excitation insults (Sun et al., 2001).

Interacting protein	Function	PolyQ-length dependence	References
HAP1	Endosome-lysosome trafficking	Yes (↑)	(Li et al., 1995)
HIP1	Clathrin-mediated endocytosis	Yes (↓)	(Kalchman et al., 1997; Legendre-Guillemin et al., 2002; Wanker et al., 1997)
HIP14	Intracellular trafficking and endocytosis	Yes (↓)	(Singaraja et al., 2002)
PSD-95	Synaptic scaffolding protein	Yes (↓)	(Sun et al., 2001)
MLK2	JNK activator	Yes (↓)	(Liu et al., 2000)
Rhes	G protein in striatum	Unknown	(Subramaniam et al., 2009)
Akt	Serine/threonine kinase	No	(Humbert et al., 2002)
Sp1	Transcription factor	Yes (↑)	(Li et al., 2002b)
RasGAP	Ras GTPase activating protein	Unknown	(Liu et al., 1997)

Table 1. Selected huntingtin-interacting proteins and major functions.

Abbreviations: HAP1, Huntingtin-associated protein 1; HIP1, Huntingtin-interacting protein 1; HIP14, Huntingtin-interacting protein 14; PSD-95, postsynaptic density-95; MLK2, mixed-lineage kinase 2; JNK, c-Jun amino-terminal kinase; Sp1, specificity protein1; RasGAP, Ras GTPase activating protein. (↑), stronger interaction with mutant htt; (↓), weaker interaction with mutant htt.

1.1.4 Mouse models of Huntington's disease

Recently, a wide variety of species, including: the invertebrates *Caenorhabditis elegans* and *Drosophila melanogaster*; rodents, such as mouse and rat; and large mammals such as sheep and the non-human primate; have been genetically engineered and used to reveal the mechanisms and suggest possible clinical therapies of HD. HD mouse models are still the most widely used models and can be classified into three major groups: one expressing full-length mutant human huntingtin, generated by using yeast or bacterial artificial chromosomes (YAC or BAC); transgenic mouse models expressing truncated mutant huntingtin under the control of promoters; and knock-in mouse models with expanded CAG repeats introduced into the endogenous mouse HD gene (Levine et al., 2004). All of these mouse models exhibit changes in electrophysiological (e.g. currents, capacitance, and/or resistance) and neuropathological (e.g. atrophy, cell loss, neuropil aggregates, and/or nuclear inclusions) properties of striatal neurons and/or impairments in behavioral tests (e.g. open field activity and rotarod performance), many of which are consistent with clinical manifestations in HD patients (Levine et al., 2004). However, these mouse models show phenotypic differences that may be attributable to the influence of the transgene copy number, protein context, mouse strain, or regulatory sequences between the mouse and human huntingtin genes (Zuccato et al., 2010). The advantages and disadvantages of each type of HD mouse models will be briefly discussed below (also see Table 2).

1.1.4.1 YAC transgenic mouse model

YAC transgenic mice were developed on the FVB/N mouse strain background, expressing full-length human htt including the upstream and downstream endogenous regulatory sequences, containing either 18 CAG repeats (termed "YAC18") or a pathological number of repeats (YAC46, YAC72 and YAC128) (Hodgson et al., 1999; Hodgson et al., 1996; Slow et al., 2003). In the YAC72 line 2511 mice, expressing mutant human htt at low levels, electrophysiological abnormalities appear in hippocampal slices at 6 months followed by behavioral impairments, while selective degeneration of MSNs in the striatum begins at about 12 months (Hodgson et al., 1999). YAC128 mice are of special interest because they show age-dependent striatal and subsequent cortical degeneration at earlier ages than YAC72. As well, YAC128 mice exhibit well-characterized progressive cognitive and motor deficits, with increased open field activity as early as 3 month of age, and rotarod performance abnormalities at 6 months of age (Slow et al., 2003; Van Raamsdonk et al., 2005a; Van Raamsdonk et al., 2005b). Accelerated death is only observed in a subgroup of the most extreme YAC128 model, depending on the level of expression of human mutant htt (Van Raamsdonk et al., 2005a).

Many features make YAC transgenic mice a favorable model for studying mechanisms of pathogenesis of HD. Some of these advantages include: expressing full-length human huntingtin in a manner similar to endogenous htt in HD patients, due to the presence of the 5' and 3' regulatory regions of the HD gene; behavioral and neuropathological changes that are similar to those found in human HD; and a more severe phenotype that can be more easily measured than the knock-in mouse models

(Hickey and Chesselet, 2003; Hodgson et al., 1999; Slow et al., 2003). Mice expressing full-length mutant htt using the BAC show a similar phenotype to the YAC mice, although more severe, probably because of higher levels of transgene expression (Gray et al., 2008). Expression of full-length human huntingtin is especially important as the so-called "Short-Stop" mouse produced by Dr. Hayden's laboratory, bearing a 128 CAG-expanded huntingtin gene truncated after intron II, displayed no neuronal dysfunction or degeneration despite the presence of aggregates, when compared with YAC128 (Slow et al., 2005).

1.1.4.2 R6/2 and R6/1 mouse model

The R6/1 and R6/2 lines of transgenic mice were the first mouse HD models to be developed. They express exon 1 of the human HD gene with ~115 or ~155 CAG repeats, respectively, controlled by 1 kB of the human HD promoter region. These mice show certain motor defects typical of HD earlier than found in the YAC or BAC models and death at the age of 4-5 months, but no specific neuronal loss (Davies et al., 1997). The accelerated phenotype of R6 mice is more useful for therapeutic trials, but less suitable for the investigation of early disease mechanisms (Gil and Rego, 2009).

1.1.4.3 Knock-in mouse models

The HD knock-in mouse models have been developed by introducing pathogenic CAG repeats into the endogenous mouse HD gene (Hdh) or by replacing mouse exon 1 with human exon 1 carrying expanded CAG repeats (Zuccato et al., 2010). Initial studies were disappointing as these knock-in mice showed few neuropathological

signs of HD, with a very mild behavioural phenotype and little neuronal degeneration (Albin and Greenamyre, 1992; Albin et al., 1990; Hilditch-Maguire et al., 2000 2006; Li et al., 2001; Menalled et al., 2003; Menalled et al., 2002). It was later appreciated that two knock-in mouse models, HdhQ(CAG)150 and HdhQ140, showed early behavioral abnormalities and striatal neuronal loss at 2 years of age (Heng et al., 2007; Menalled et al., 2003). These models can be valuable for studying the early and mild neuronal abnormalities that might underlie early functional deficits in HD.

	R6/1 (Mangiarini et al., 1996)	YAC128 (Hodgson et al., 1999; Slow et al., 2003)	HdhQ140 (**Hilditch-Maguire et al., 2000**)
Construct	Exon 1 of human Htt	YAC expressing full-length human Htt	PolyQ sequence inserted into endogenous mouse Htt gene
Promoter	Human Htt	Human Htt	Mouse Htt promotor
CAG	116	128	140 (later 121)
Motor symptoms	Clasping behaviour and rotarod deficit (20 weeks)	Clasping behaviour and rotarod deficit (24 weeks)	80-100 weeks
Onset of Cognitive symptoms	12 weeks	8 weeks	16-24 weeks
Life span	32-40 weeks	Normal life span	Normal life span
Brain atrophy and cell loss	~10-30% global brain volume loss (20 weeks)	Striatal (10–15%) and cortical (7–9%) volume and neuron number reduction (48 weeks)	19-38% striatal & cortical volume reduction (80-100 weeks)

	R6/1 (Mangiarini et al., 1996)	YAC128 (Hodgson et al., 1999; Slow et al., 2003)	HdhQ140 (**Hilditch-Maguire et al., 2000**)
Neuronal dysfunction	Altered synaptic plasticity/augmented NMDAR (8-20 weeks)	Striatal synaptic alteration and ↑ extrasynaptic NMDARs (4 weeks)	↓striatal synaptic currents, ↑ cortical synaptic currents (48 weeks); altered synaptic plasticity (8 weeks)

Table 2. Brief comparisons of selected mouse models of HD.

For detailed references, please see (Milnerwood and Raymond, 2010; Zuccato et al., 2010).

1.1.5 Excitotoxic hypothesis of Huntington's disease

Based on experiments dated back to the 1950s, excitotoxicity is defined as overactivation of receptors by excitatory amino acid (EAA) neurotransmitters, which leads to neuronal death (Choi, 1992; Doble, 1999; Olney et al., 1971). Glutamate is considered to be the major excitatory neurotransmitter in the mammalian CNS (Engelsen, 1986; Hebb, 1970), and disrupted glutamate homeostasis has been seen in many neurological disorders, thereby making the glutamatergic system of great interest for neuronal excitotoxicity.

The 'excitotoxic hypothesis' of HD usually refers to the dysfunction and death of MSNs in the striatum caused by excessive glutamate from cortical afferents, impaired uptake of glutamate, and/or hyper-sensitivity of glutamate receptors, resulting in excessive influx of ions (especially calcium) into the cells (DiFiglia, 1990; Schwarcz et al., 1977). The excessive calcium entry is particularly neurotoxic, leading to activation of degradative enzymes like caspases and calpains, and production of reactive oxygen species (Albin and Greenamyre, 1992; Berliocchi et al., 2005; Coyle and Puttfarcken, 1993).

1.1.6 Calcium homeostasis and Huntington's disease

Calcium is perhaps the most studied physiological ion because of its vital intracellular messenger role, regulating cellular functions like exocytosis including transmitter release, membrane excitability and synaptic plasticity, and even cell growth

and differentiation (Berridge, 1998; Clapham, 1995). Calcium homeostasis is normally adjusted by calcium influx processes (through voltage-gated calcium channels, NMDARs or α-amino-3-hydroxy-5-methyl-4-isoxazolepropionic acid receptors (AMPARs)), calcium efflux processes (through the calcium/ATPase pump or sodium/calcium antiporter), calcium storage organelles (mitochondria, endoplasmic reticulum and nucleus), and calcium binding proteins (like calbindin and calmodulin) (Sattler and Tymianski, 2000). Increased intracellular calcium has been found to play a role in both necrosis and apoptosis (Yu et al., 2001).

Calcium influx through NMDARs after intensive glutamate stimulation is thought to be especially toxic and a major cause of neuronal degeneration (Choi et al., 1987), due to the receptor's high permeability to calcium (Hartley et al., 1993) and especially the extrasynaptic GluN2B-containing receptors (Hardingham et al., 2002; Liu et al., 2007; Rumbaugh and Vicini, 1999; Tovar and Westbrook, 1999; Vanhoutte and Bading, 2003). It has been shown that increased intracellular calcium is an important trigger for caspase activation and mitochondrial dysfunction in striatal cultures (Petersen et al., 2000). Calcium-induced excitotoxicity may be mediated by many calcium-dependent enzymes, such as calpains and nitric oxide synthase (NOS) (Dawson et al., 1991; Siman et al., 1989), or other enzymes involved in cell death, such as proteases and endonucleases (Leist and Nicotera, 1998; Orrenius et al., 1996). Another excitotoxic-inducing pathway is triggered by calcium overload in mitochondria, resulting in energetic failure and production of reactive oxygen species, as well as mitochondrial membrane depolarization

with more calcium released through the mitochondria permeability transition pore (mPTP) (Nicholls and Budd, 2000).

Calcium homeostasis has been found to be compromised in many HD models. Immortalized striatal cells from STHdhQ111/Q111 knock-in mice (Seong et al., 2005), striatal neurons from R6/2 mice (Hansson et al., 2001), and hippocampal neurons from symptomatic YAC72 mice (Hodgson et al., 1999), all showed elevated basal calcium concentration. Altered NMDAR-mediated calcium signaling was observed in striatal cells cultured from YAC transgenic mouse expressing expanded htt at birth (Oliveira et al., 2006; Zeron et al., 2004). Striatal slices from pre-symptomatic and symptomatic R6/2 mice (Cepeda et al., 2001), as well as cultured striatal MSNs from YAC46 and YAC72 mice (Zeron et al., 2004) all displayed larger increases in intracellular calcium levels in response to NMDA. Similarly, cytosolic calcium levels in cultured MSNs from YAC128 mice were enhanced after repeated glutamate application (Tang et al., 2005). Moreover, IP3 receptor (IP3R)-mediated calcium release from ER stores was potentiated by polyQ-expanded htt in cultured MSNs from both rat and mouse (Tang et al., 2003; Tang et al., 2004). Taken together, all these studies suggest that dysregulation of calcium homeostasis may be caused by mhtt, and plays a key role in the dysfunction and neuronal loss of striatal neurons in HD.

1.1.7 Apoptosis and Huntington's disease

Apoptosis, also called 'programmed cell death' or 'cell suicide', is different from

necrosis in many ways, including the absence of toxic factor release into the extracellular space during cell death, and morphological changes such as cell shrinkage, condensed nuclear chromatin, and break down of nucleus and cytoplasm into "apoptotic bodies" (Burlacu, 2003; Derradji and Baatout, 2003; Kanduc et al., 2002). In addition, apoptosis takes place in individual cells and leaves surrounding healthy cells unaffected, whereas necrosis induced by injury and trauma involves neighboring cells by releasing inflammatory factors (Kanduc et al., 2002; Sastry and Rao, 2000). Excitotoxic stimuli, environmental toxins, and metabolic or oxidative stresses, could initiate apoptosis by activating calpains, initiator caspases (e.g. caspases-8 or -9) or the effector caspases (e.g. caspases-3) (Chan and Mattson, 1999; Sastry and Rao, 2000; Thornberry, 1997).

Increased apoptosis has been reported in several HD models expressing expanded htt. We have shown before that NMDA-induced caspases-3 and -9 activities are elevated in striatal MSNs from YAC46 and YAC72 mice compared to WT mice (Zeron et al., 2004; Zeron et al., 2002). There is also evidence showing increased calpain (Gafni and Ellerby, 2002), caspase-1 (Ona et al., 1999) and caspase-8 (Sanchez et al., 1999) activity in the striatum of HD patients. Furthermore, the increased apoptosis in HD has been linked to NMDARs. In one study, the glutamate-induced apoptosis seen in the hippocampal HN33 cell line expressing htt-48Q, but not htt-16Q, could be prevented by AP-5 treatment, which is an NMDAR antagonist (Sun et al., 2001). The enhancement of excitotoxicity by polyQ expansion in mhtt seems to be NMDAR-specific, since AMPA-induced apoptosis in MSNs is unaffected by genotype (Zeron et al., 2002). Data from our lab has also

18

shown that NMDA-induced apoptosis was increased only in cells that co-expressed htt-138Q with GluN1/GluN2B but not GluN1/GluN2A (Zeron et al., 2001). Further experiments indicated that enhancement of NMDA-induced apoptosis in cultured MSNs showed YAC72 > YAC46 > WT > YAC18, i.e., the NMDA-induced apoptosis is proportional to the polyQ length of mutant htt (Shehadeh et al., 2006; Zeron et al., 2002). Treatment with the NMDAR antagonist AP-5 at concentrations shown to decrease NMDA-induced calcium influx in YAC72 MSNs to WT levels resulted in a proportional reduction of NMDA-induced apoptosis to WT levels (Shehadeh et al., 2006). The toxic effect of increased calcium from both extracellular space (application of KCl and an L-type voltage-gated calcium channel agonist) and intracellular stores (caffeine and DHPG treatments) were also explored. The potentiation of apoptosis induced by these non-NMDAR dependent stimuli in YAC72 and YAC128 MSNs relative to YAC18 MSNs was much smaller than that observed with NMDA (Shehadeh et al., 2006). Additionally, high concentrations of staurosporine induced similar apoptosis in cultured MSNs from YAC72 and WT mice, and there was only a small potentiation in YAC128 MSNs compared to WT (Shehadeh et al., 2006). Staurosporine induces apoptosis by inhibiting protein kinase C and/or activating the mPTP via suppression of Bcl-2 expression, resulting in caspase-3 activation (Nicotera et al., 1999; Roucou et al., 2001; Swannie and Kaye, 2002). These results suggest that cell death, and especially NMDAR-dependent apoptosis, is augmented in mhtt-expressing neurons. As well, mitochondria are more vulnerable to calcium influx through NMDARs than through other ways of increasing

cytosolic calcium, which may be due to microstructure or specific pathways (Peng and

Greenamyre, 1998; Sattler and Tymianski, 2000).

1.2 Glutamate, NMDAR and HD

1.2.1 Glutamate and glutamate receptors

Glutamate mediates most excitatory synaptic transmission in the adult mammalian

CNS by activation of ionotropic receptors that flux cations (Bergles et al., 1999). During

stress or disease, glutamate can reach very high concentrations (100-300 μM) in the

synaptic cleft due to excessive glutamate release or impaired glutamate uptake ability of

astrocytes (Schubert and Piasecki, 2001)

There are two categories of glutamate receptors: ionotropic glutamate receptors

(iGluRs), which allow cationic ions to enter the cell upon ligand binding (Dingledine et

al., 1999), and metabotropic glutamate receptors (mGluRs), which are linked to many

downstream effectors through G-proteins (Conn and Pin, 1997). Activation of iGluRs

leads to membrane depolarization and increases the probability of action potential firing;

both types of GluRs are involved in synaptic plasticity in the adult brain, e.g. long-term

potentiation (LTP) and long-term depression (LTD) (Asztely and Gustafsson, 1996;

Bortolotto et al., 1999; Gubellini et al., 2004).

1.2.2 Glutamate and Huntington's disease

MSNs are central to the function of the striatum because they receive a diverse input

from the cerebral cortex, thalamus, and dopaminergic neurons of the substantia nigra, and

provide the major output from the caudate nucleus and putamen (Braak and Braak, 1982).

The cortex and thalamus send glutamatergic outputs to the striatum (Beal, 1992; DiFiglia,

1990). Results of radiolabelled ligand binding assays in human HD postmortem brain

tissue indicated a profound 50-60% loss of glutamate receptors specifically in striatum

whereas no loss was observed in cortex (Albin et al., 1990; Young et al., 1988). Recent

studies suggest that quinolinate, kynurenic acid and 3-hydroxykynurenine (3-HK) show

increased levels in low-grade human HD and three mouse models of HD (R6/2, YAC128,

Hdh-Q111 and Hdh-Q92) brains (Guidetti et al., 2006; Guidetti et al., 2004). However,

the elevated neuroactive kynurenine pathway metabolites cannot fully explain the mutant

htt-mediated cellular changes, and may itself be a byproduct of the early pathological

changes in HD.

1.2.3 NMDA receptors

Compared to other ionotropic glutamate receptors, NMDARs have received more

attention because of their voltage-dependent block by extracellular magnesium, higher

affinity for glutamate and permeability to calcium, slower activation and deactivation

kinetics, as well as slower and incomplete desensitization with agonist binding

(Cull-Candy et al., 2001; Dingledine et al., 1999; Mayer et al., 1984; McBain and Mayer,

1994; Nowak et al., 1984; Waxman and Lynch, 2005b). When NMDARs located at

postsynaptic sites are activated by coincidence of pre-synaptic glutamate release and

post-synaptic depolarization, the receptors flux calcium to stimulate protein kinases,

proteases, and phosphatases; these calcium-activated downstream signals are critical for synapse formation during development and also for synaptic plasticity, which are required for learning and memory (Asztely and Gustafsson, 1996; Bliss and Collingridge, 1993; Maren and Baudry, 1995). However, over-activation of NMDARs, especially the extrasynaptic ones, has been proposed to result in neuronal dysfunction and excitotoxic death from calcium-activated lipases, proteases, and DNases (Besancon et al., 2008; Rothman and Olney, 1995; Sattler and Tymianski, 2000). In conclusion, these receptors play a critical role in excitatory neurotransmission, synaptic plasticity and excitotoxicity in the CNS (Bliss and Collingridge, 1993; Dingledine et al., 1999; Sattler and Tymianski, 2001; Waxman and Lynch, 2005b) as well as mechanisms underlying neurologic disorders including Huntington's disease (Cowan and Raymond, 2006; Waxman and Lynch, 2005b; Zeron et al., 2002).

NMDARs are heteromeric tetramers mostly made of two glycine-binding GluN1 subunits (with eight splice variants: GluN1A-H) and two glutamate-binding GluN2 subunits (GluN2A-D) (Dingledine et al., 1999; Hollmann et al., 1993; Kohr, 2006; Kutsuwada et al., 1992; Monyer et al., 1992; Sugihara et al., 1992); GluN3 subunits (GluN3A and B) are less commonly included in the receptor complex (Cavara and Hollmann, 2008). The four different types of GluN2 subunits show differential spatial and temporal expression during neuronal development: high levels of GluN2B and GluN2D are expressed at prenatal stages, while GluN2A and GluN2C levels increase later at postnatal stages; GluN2A is more universally expressed, whereas GluN2B is

highly expressed in the forebrain, and GluN2C is restricted to cerebellum (Monyer et al., 1994). The GluN2 subunits determine NMDA receptor-channel pharmacological and physiological properties, such as channel conductance, open probability, degree of desensitization, deactivation time, and sensitivity to agonist, antagonist and modulators like zinc and polyamines (Buller et al., 1994; Chazot et al., 1992; Chen et al., 1999a; Chen et al., 1999b; Dingledine et al., 1999; Kohr, 2006; Krupp et al., 1996; Paoletti and Neyton, 2007; Wyllie et al., 1998). The GluN2 subunits also differ in their subcellular localization and interactions with proteins and signaling networks, and thus have great impact on the balance between neuronal survival and dysfunction or death (Cull-Candy et al., 2001; Dingledine et al., 1999; Hardingham and Bading, 2003; Kohr, 2006; Prybylowski and Wenthold, 2004). Some studies have suggested that NMDAR complexes containing GluN2B facilitate cell death signaling whereas GluN2A-containing NMDARs promote neuronal survival (Chen et al., 2007; Liu et al., 2007), although both subtypes mediate toxicity in more mature cultured neurons (von Engelhardt et al., 2007). Although there are some differences in the complex of proteins preferentially associated with GluN1/GluN2A and GluN1/GluN2B, these two NMDAR subtypes also interact with many synaptic proteins in common, including the PSD-95 family proteins (Al-Hallaq et al., 2007).

1.2.4 NMDA receptors and Huntington's disease

Several lines of evidence support a role for altered NMDAR function and

NMDAR-dependent excitotoxicity in HD (DiFiglia, 1990; Fan and Raymond, 2007). Firstly, postmortem analysis of brain tissue from HD patients suggests that neurons with high expression of NMDARs are particularly vulnerable to degeneration (Albin et al., 1990; Young et al., 1988). As well, NMDARs are more effective and selective than other glutamate receptor subclasses in mediating excitotoxic damage in MSNs (DiFiglia, 1990). Secondly, quinolinic acid injection into the striatum of the rat or non-human primate replicates some of the features of HD (Beal et al., 1986; Sanberg et al., 1989). Furthermore, data from our laboratory and the Levine lab suggested that NMDAR activation is involved in degeneration of MSNs in HD (Chen et al., 1999b; Levine et al., 1999; Shehadeh et al., 2006; Zeron et al., 2001; Zeron et al., 2002). Moreover, the report of increased NMDAR currents and extrasynaptic localization, caspase-3 activity and excitotoxicity in striatal neurons of YAC HD mice compared to WT or YAC18 controls all provides additional evidence to show that mutant huntingtin can affect the function and signaling of NMDARs (Milnerwood et al., 2010; Shehadeh et al., 2006; Zeron et al., 2002). However, the molecular mechanisms underlying mutant huntingtin's effect on NMDAR function have not been fully elucidated.

1.2.4.1 GluN2B-type NMDA Receptors and HD

Previous work in mouse and cellular models of HD suggests GluN2B-containing NMDARs are functionally altered in HD and contribute to neuronal dysfunction and susceptibility to apoptosis (Cepeda et al., 2001; Chen et al., 1999b; Fan et al., 2007;

Levine et al., 1999; Milnerwood et al., 2006; Shehadeh et al., 2006; Song et al., 2003; Starling et al., 2005; Tang et al., 2005; Zeron et al., 2001; Zeron et al., 2002). GluN2 subunits are differentially distributed in the brain, and GluN2B is more enriched in mature striatal MSNs compared with other GluN2 subunits and mature neurons in other brain regions (Christie et al., 2000; Landwehrmeyer et al., 1995; Li et al., 2003b). Studies in human embryonic kidney (HEK)-293 cells from our laboratory have shown that when mutant huntingtin and NMDARs are co-expressed, the increase of NMDAR-mediated apoptosis is larger for cells expressing GluN1/GluN2B subtype compared to cells expressing the GluN1/GluN2A (Chen et al., 1999b; Zeron et al., 2001). In MSNs from YAC72 mice, excitotoxic death was increased after intrastriatal injection of quinolinate, and after NMDA treatment in cultured MSNs, and the NMDA-induced cell death was abolished by an GluN2B subtype-selective antagonist (Zeron et al., 2002). In contrast, NMDAR-mediated death of cerebellar granule neurons was not enhanced by mutant htt expression, which is consistent with cell-type and NMDAR subtype specificity (cerebellar granule neurons do not express GluN2B). In addition, our recent study showed that GluN2B expression was significantly increased in striatal ''non-PSD'' fractions and decreased in the synaptic ''PSD'' fractions in YAC128 mice compared to YAC18 mice, which may lead to increased extrasynaptic NMDAR current, and reduced nuclear CREB activation in HD mouse striatum (Milnerwood et al., 2010). All these results suggest a selective interaction of huntingtin with the GluN1/GluN2B NMDAR subtype.

1.2.4.2 Extrasynaptic vs. synaptic NMDA Receptors

In addition to their synaptic localization, NMDARs are found at extrasynaptic and perisynaptic sites, which can be defined immunocytochemically and electrophysiologically. Synaptic NMDARs are classically defined as functional receptors that are activated by glutamate released during low frequency synaptic events including low frequency evoked events, spontaneous synaptic events and action potential-independent synaptic release of single quanta of glutamate (Hardingham and Bading, 2010). Extrasynaptic NMDARs are receptors that are not activated during low frequency synaptic events, and can be found at various locations, including the cell body, dendritic shaft, the neck of the dendritic spine and also adjacent to the postsynaptic density (PSD) (Petralia et al., 2010).

Some early evidence suggests that GluN2A-type NMDARs gradually replace GluN2B-type receptors at synapses during development, whereas GluN2B-type NMDARs are more enriched at extrasynaptic sites of cultured cortical or hippocampal neurons (Barria and Malinow, 2002; Li et al., 1998; Rumbaugh and Vicini, 1999; Stocca and Vicini, 1998; Tovar and Westbrook, 1999). However, a later study in cultured hippocampal neurons also indicates that receptors with either GluN2 subunits can be found in both synaptic and extrasynaptic compartments (Kohr, 2006; Thomas et al., 2006).

A recent study in whole genome expression revealed that the location of the activated

NMDA receptor (calcium signal initiation sites) decides the neuronal fate at the level of transcription: synaptic NMDA receptors induce up-regulation of pro-survival genes and down-regulation of pro-death genes, while extrasynaptic NMDA receptors work in the opposite way (Zhang et al., 2007). Studies in cultured cortical and hippocampal neurons reveal that selective activation of synaptic NMDARs preferentially promotes neuroprotection, while activation of extrasynaptic NMDARs or NMDARs at both locations triggers neuronal death (Dick and Bading, 2010; Hardingham and Bading, 2010; Hardingham et al., 2002; Leveille et al., 2008; Soriano and Hardingham, 2007; Vanhoutte and Bading, 2003; Xu et al., 2009).

Recently, our group reported that extrasynaptic NMDAR expression and current are specifically increased in YAC HD mouse striatum (Milnerwood et al., 2010). In addition, low-dose memantine, which preferentially blocks extrasynaptic NMDARs, reversed motor learning deficits in these HD mice (Milnerwood et al., 2010). This suggests that the altered balance between synaptic and extrasynaptic NMDAR is an important candidate mechanism of HD, and can be a target for early therapy interventions (Levine et al., 2010).

1.3 MAGUKs

MAGUKs are a family of synaptic proteins that share high homology structures of three PSD/Discs-large/ZO-1 (PDZ), one Src homology 3 (SH3) and one guanylate kinase-like domains (Kim and Sheng, 2004). The MAGUKs include

PSD-95/synapse-associated protein (SAP)-90, PSD-93/Chapsyn-110, SAP102 and SAP97, which are believed to stabilize or anchor glutamate receptors at the synapse and regulate downstream signaling through interaction with scaffolding proteins and enzymes (Fujita and Kurachi, 2000; Gardoni et al., 2009a; Kim and Sheng, 2004).

PSD-95, and PSD-93/Chapsyn110 can be palmitoylated and are enriched in the PSD, while SAP102 and SAP-97 are not palmitoylated, can locate in both dendrites and axons, and are abundant at both cytoplasm and synapse (El-Husseini et al., 2000; Fujita and Kurachi, 2000; Muller et al., 1995). A study in rat hippocampus showed that SAP102 was highly expressed at P2 and dominated at the synapse at early postnatal stages, while PSD-93 and PSD-95 expression increased later and largely replaced SAP102 at synapses, which coincides with the replacement of GluN2B with GluN2A at the synapse during development (Sans et al., 2000). One study found that the postsynaptic targeting of PSD-95 is maintained independently of palmitoylation when the N-terminus of PSD-95 is replaced by the N-terminus of PSD-93/Chapsyn-110 or SAP102 (Firestein et al., 2000) which suggests that MAGUKs contain diverse signals within their N-termini for postsynaptic targeting. Other evidence suggests that the N-terminal domain of PSD-95 regulates postsynaptic protein clustering (Chetkovich et al., 2002), and that different splice variants within the N-terminal domains of PSD-95 and SAP-97 govern their roles in activity-dependent regulation of synaptic AMPA receptor function (Schluter et al., 2006). Thus, the differences of MAGUK family proteins in their subcellular localization, developmental expression patterns, N-terminal signals and post-translational regulations,

suggest fine-tuned roles of these proteins in the CNS.

All the MAGUK proteins interact with the GluN2 subunits of NMDARs, while SAP-97 binds directly with the GluR1 subunit of AMPAR, and PSD-95 associates with AMPAR through binding with stargazin (Chen et al., 2000; Kim et al., 1996; Kim and Sheng, 2004; Kornau et al., 1995; Leonard et al., 1998; Niethammer et al., 1996). It is suggested that PSD-95 and PSD-93 are more involved in synaptic function and regulation of downstream signals of glutamate receptors, whereas SAP-97 and SAP102 are more important in trafficking of these receptors (Elias and Nicoll, 2007; Gardoni et al., 2009a; Garner et al., 2000; Kim and Sheng, 2004; Lau and Zukin, 2007).

1.3.1 PSD-95

PSD-95 plays an essential role as a central organizer in the PSD by interacting with a wide variety of membrane receptors or channels, cell-adhesion molecules, and cytoplasmic signaling enzymes. The interaction of the PDZ1-2 domain in PSD-95 with the tSXV motif in the cytoplasmic tail of GluN2 subunits of NMDAR (Kornau et al., 1995; Niethammer et al., 1996) has been shown to regulate synaptic localization, internalization, desensitization and downstream toxic signaling of NMDARs at the neuronal surface (Aarts et al., 2002; Li et al., 2003b; Lin et al., 2004; Prybylowski et al., 2005; Roche et al., 2001; Sattler et al., 1999; Soriano et al., 2008; Sornarajah et al., 2008). Study has shown that GluN2B binding to PSD-95 reduces the level of S1480 phosphorylation of GluN2B, and promotes stabilization of NMDARs at the surface

(Chung et al., 2004).

Src-family kinases are coupled by PSD-95 to NMDARs to increase tyrosine-1472 phosphorylation of GluN2B at the C-terminus, which inhibits GluN2B-type NMDAR endocytosis and promotes localization of GluN2B at the synaptic membrane (Prybylowski et al., 2005). The Src-family kinase-dependent tyrosine phosphorylation of GluN2B, and NMDAR-mediated toxicity has been shown to be enhanced in 293T cells co-expressing mhtt, PSD-95, GluN1 and GluN2B (Song et al., 2003).

Synaptic RAS GTPase-activating protein (SynGAP) is another abundant PSD protein that binds to PSD-95 (Bezprozvanny and Hayden, 2004; Kim et al., 1998), which can be activated by Ca^{2+}/calmodulin-dependent protein kinase II (CaMKII) (Oh et al., 2004) and suppresses the Ras–extracellular signal-regulated kinase (ERK) pathway. PSD-95 also interacts with neuroligins (Irie et al., 1997); guanylate kinase-associated protein (GKAP) (Kim et al., 1997), which then binds to SH3 and ankyrin repeat-containing protein (Shank) (Naisbitt et al., 1999); as well as many other cell-adhesion and cytoskeletal-associated proteins, and is thus an important scaffolding protein in the PSD (Kim and Sheng, 2004).

1.3.1.1 NMDAR/PSD-95/nNOS pathway

Neuronal nitric oxide synthase (nNOS), which binds directly to the PDZ-2 domain of PSD-95 (Brenman et al., 1996; Christopherson et al., 1999), is a Ca^{2+}/calmodulin-activated enzyme that produces nitric oxide (NO). It is suggested that PSD-95 functionally couples calcium entry from NMDARs to nNOS activation and

production of NO, which contributes to NMDAR-dependent excitotoxicity (Dawson et al., 1991; Sattler et al., 1999), through p38 MAPK activation(Cao et al., 2005; Soriano et al., 2008). The NMDAR/PSD-95/nNOS complex has been shown to be critical for mediating excitotoxicity, since disruption of the NMDAR/PSD-95 interaction with a cell-permanent peptide (Tat-NR2B9c) resulted in reduced NMDAR-mediated excitotoxicity without affecting NMDAR function in cultured cortical neurons (Aarts et al., 2002). In the striatum of N171-82Q transgenic mouse model of HD, down-regulation of PSD-95 family proteins and nNOS correlates with resistance to NMDA toxicity (Jarabek et al., 2004).

1.3.1.2 PSD-95 and Huntington's disease

Evidence indicates that the PSD-95 SH3 domain interacts directly with the polyproline region of huntingtin in transfected 293T cells and human cortical tissue by co-IP experiments, in a polyQ length-dependent manner (Sun et al., 2001). Furthermore, NMDAR-dependent apoptosis induced by over-expression of mhtt with 48Q in HN33 hippocampal cell line could be reduced by over-expressing htt-16Q, and this rescue was abolished by co-expression with PSD-95 (Sun et al., 2001). Sun and colleagues thus concluded that htt and NMDA receptors are associated via PSD-95, and polyglutamine expansion interferes with the ability of htt to interact with PSD-95 (Sun et al., 2001). Moreover, they hypothesized that diminished binding of polyQ-expanded htt to PSD-95 might increase the free PSD-95 available for binding to NMDARs and thereby augment

NMDAR-dependent toxicity (Sun et al., 2001), since previous studies have suggested that coupling of NMDARs with PSD-95 leads to activation of nNOS and is required for NMDA-induced toxicity (Sattler et al., 1999). However, the mechanisms underlying how mutant huntingtin's influence on the NMDAR/PSD-95 complex contributes to elevated NMDA toxicity in HD has not been carried forward in the striatum.

1.3.2 SAP102

Similar to PSD-95, SAP102 is also enriched in the postsynaptic density and has also been reported to interact with the carboxyl-terminus of the GluN2B subunit of NMDA receptors (Muller et al., 1996). During development, the expression profile of GluN2B coincides with that of SAP102 at hippocampal synapses, and there is a preference for complexes of GluN2A/PSD-93/95 and GluN2B/SAP102 (Sans et al., 2000). It is suggested that GluN2B-SAP102 complexes may inhibit the extracellular signal-regulated protein kinases (ERK) pathway, through synaptic Ras-GTPase-activating protein, to facilitate removal of AMPARs from the postsynaptic membrane, whereas GluN2A-PSD-95 complexes work in the opposite way (Kim et al., 2005).

A recent study found that SAP102 interacts with Sec8 subunit of the exocyst complex, which targets secretory vesicles to the cell surface, and that dominant-negative Sec8 inhibits NMDAR currents in neurons (Sans et al., 2003). This result suggests that the synaptic trafficking of NMDARs is regulated by interaction of SAP102 with Sec8. Additionally, SAP102 interacts with the protein mPins (mammalian partner of

inscruteable, which mediates G-protein signaling) and this interaction was shown to influence the trafficking of NMDA receptors between the ER and the trans-Golgi network (Sans et al., 2005). One study reported a robust elevation of SAP102 in PSD-95 mutant mice, and that more PSD-95 is associated with GluN1 in SAP102 mutant mice (Cuthbert et al., 2007). Furthermore, mice carrying a double mutation of PSD-95 and SAP102 die perinatally, indicating partial overlapping functions of these two MAGUKs and that the presence of at least one is required for postnatal development (Cuthbert et al., 2007). It is suggested that specific MAGUK proteins may couple the NMDA receptor to distinct downstream signaling pathways (Cuthbert et al., 2007).

1.3.3 SAP-97 and PSD-93/Chapsyn-110

SAP-97 and PSD-93/Chapsyn110 have also been reported to interact with the C-terminus of NMDAR GluN2 subunits and play a role in NMDAR clustering (Kim et al., 1996; Niethammer et al., 1996). Furthermore, CaMKII-dependent phosphorylation of the SAP-97 N-terminus at different developmental stages and locations controls the trafficking and postsynaptic membrane insertion of the GluN2A subunit of NMDA receptors (Mauceri et al., 2007). SAP-97 is also directly associated with the C-terminus of the GluR1 subunit of AMPA receptors (Leonard et al., 1998). A recent paper suggests that SAP-97 may play a central role in the growth of synapses during development and plasticity by recruiting postsynaptic proteins that enhance presynaptic terminal growth and function via multiple trans-synaptic molecular interactions (Regalado et al., 2006).

1.3.4 Tat-NR2B9c peptide

The Tat-NR2B9c is a 20 amino acid fused protein constructed with the nine C-terminal residues of GluN2B (where the PSD-95 PDZ1&2 domains bind) and the cell-membrane transduction domain of the Human Immunodeficiency Virus (HIV)-1 Tat protein. This peptide has been shown to perturb the interaction of MAGUKs with NMDAR and nNOS, and to protect cortical neurons from NMDA-induced excitotoxicity *in vitro* and ischemic neuronal death *in vivo*. A control peptide -- Tat-NR2BAA in which two serine residues in the Tat-NR2B9c peptide have been substituted with alanines to eliminate the possibility of PDZ domain binding -- does not block this interaction and also shows no protection against NMDA-induced excitotoxic cortical neuronal death (Aarts et al., 2002; Cui et al., 2007; Soriano et al., 2008). Even though there is some similarity in binding of different MAGUKs and GluN2 subunits of NMDARs, an *in vitro* study showed that Tat-NR2B9c peptide disturbs the GluN2/PSD-95 and PSD-95/nNOS much more efficiently than for other MAGUKs (Cui et al., 2007). In my studies, Tat-NR2B9c peptide is used to help explore the roles of the PSD-95/NMDAR interaction in NMDAR functional changes in the YAC transgenic mouse model.

1.4 MAPKs

Mitogen-activated protein kinases (MAPKs) is a superfamily of serine/threonine protein kinases that are highly responsive to diverse extracellular signals, such as growth factors, stresses, and synaptic stimuli in postmitotic neurons of adult mammalian brain, including activation of NMDARs in a Ca^{2+}-dependent manner (Haddad, 2005; Wang et

al., 2007; Wang et al., 2004). In mammalian cells, the four best-characterized MAPK pathways are the extracellular signal-regulated protein kinases (ERK1/2), the p38 MAPKs, the c-Jun N-terminal kinases (JNK) and the ERK5 pathways (the last of which will not be introduced here). Members of both the JNK and p38 MAPK pathways are also classified as stress-activated protein kinases (SAPKs), because they are activated in response to osmotic shock, UV irradiation, inflammatory cytokines and other stressful conditions (Haddad, 2005).

The MAPK cascade involves a sequential activation of four levels of evolutionarily conserved signaling proteins: small GTPases (Ras and Rac proto-oncogenes), MAPK kinase kinases (Raf or MEKKs), MAPK kinases (MEKs), and MAPKs. Active MAPKs then normally translocate to the nucleus to directly or indirectly activate a specific set of transcription factors for target gene expression, such as CREB, activating transcription factor-2 (ATF-2; also CREB2), or activator protein-1 (AP-1) (Raman et al., 2007; Roux and Blenis, 2004; Wang et al., 2007). The recent discovery of specific inhibitors (PD-98059 for ERK, SB-239063 for p38, and SPC-9766 for JNK) has made the study of specific function of different MAPKs possible, while the most-used p38 inhibitor SB-203580 also inhibits JNK (Harper and Wilkie, 2003), and SP-600125 is still widely used as a JNK inhibitor.

Recent evidence points to the fact that MAPKs play a crucial role in regulating the signaling of NMDARs, their physiological and biochemical/biophysical properties, and their potential role in pathophysiology (Haddad, 2005). It has been suggested that

NMDAR-dependent apoptosis is likely to involve the stress-induced pathways such as p38 MAP kinase and c-Jun N-terminal kinase (Hardingham, 2006; Hardingham and Bading, 2003). In rat cerebellar granule cells, glutamate induced rapid activation of JNK and p38 to phosphorylate c-Jun (at Ser63) and p53 (at Ser15), respectively, and caused a subsequent marked increase in AP-1 binding that preceded apoptotic death (Chen et al., 2003). It has also been shown that NMDA activated JNK and p38 kinases in hippocampal neurons (Mukherjee et al., 1999), and that quinolinic acid-induced excitotoxicity in the cortex and the hippocampus was accompanied by increased JNK and p38 phosphorylation (Ferrer et al., 2001).

The existence of multiple MAPKs, and their different regulation by subtype-specific glutamate receptors, suggest that MAPK signaling pathways may play distinct roles in regulating synaptic plasticity, gene expression, and neuronal survival. This family of kinases has been emerging as new targets for several neurodegenerative diseases, such as Parkinson's disease and Alzheimer's disease, etc.(Haddad, 2005; Harper and Wilkie, 2003; Wang et al., 2004).

1.4.1   ERKs

Among many isoforms (ERK1/2/3/4/5/7), ERK1/2 proteins are the most thoroughly characterized. They are activated via Thr202 and Tyr204 phosphorylation by the Ras-Raf-MEK1/2 pathway (Wang et al., 2007; Wang et al., 2004), and then phosphorylate numerous substrates, including nuclear substrates Elk-1, MEF2, c-Fos, and c-Myc (Roux

and Blenis, 2004).

Interestingly, the synaptic pool of NMDA receptors activated, whereas the extrasynaptic pool of the receptors inactivated, ERK (Ivanov et al., 2006). On the other hand, in mature neurons, GluN2B-type NMDA receptor stimulation is coupled to inhibition rather than activation of ERK, whereas GluN2A-containing NMDA receptors have been shown to optimally activate ERK (Kim et al., 2005).

1.4.2   P38 MAPKs

The p38 kinases are widely expressed in many tissues including brain and are activated by dual phosphorylation on Threonine (Thr/T) 180 and Tyrosine (Tyr/Y) 182 (Raingeaud et al., 1995). There are four isoforms of p38: p38α, p38β, p38γ, and p38δ, which are activated by the Rac-MEKK-MEK3/6 pathway (Gallo and Johnson, 2002), and phosphorylate transcriptional factors like ATF-1 and -2, MEF2A, Sap-1, Elk-1, NF-κB, and p53 (Kyriakis and Avruch, 2001).

P38 was shown to be present in both the nucleus and cytoplasm of cells, but upon cell stimulation, the cellular localization of p38 is not well understood (Roux and Blenis, 2004). Some evidence suggests that, following activation, p38 translocates from the cytoplasm to the nucleus (Raingeaud et al., 1995), but other data indicate that activated p38 is also present in the cytoplasm of stimulated cells (Ben-Levy et al., 1998).

1.4.2.1 P38 MAPKs and NMDARs

In cultured striatal neurons, NMDAR stimulation results in p38-dependent activation of MAP kinase (Vincent et al., 1998). P38 MAPK could be activated by NMDAR through downstream generation of reactive oxygen species, such as NO and hydrogen peroxide (H_2O_2) (Bossy-Wetzel et al., 2004; Izumi et al., 2008), and may also be activated through SynGAP in hippocampal and cortical neurons (Kim et al., 1998; Rumbaugh et al., 2006). High concentrations of glutamate and NMDA activate p38 MAPK in acute hippocampal slices (Molz et al., 2008) and in rat cerebellar granule cells, which correlates with apoptosis (Kawasaki et al., 1997). Furthermore, activation of extrasynaptic NMDARs triggers FoxO3a nuclear translocation, and this translocation is greatly reduced by p38 inhibitors in hippocampal neurons (Dick and Bading, 2010). However, the amplitude of p38 phosphorylation by NMDAR signals in hippocampal neurons depends on the level of NMDAR activity, age of cultures, and the subunit composition of NMDARs (Waxman and Lynch, 2005a). More interestingly, it has been reported that extrasynaptic NMDAR stimulation, but not synaptic stimulation, leads to the phosphorylation of p38 and subsequent neuronal death (Xu et al., 2009).

1.4.2.2 P38 MAPKs and HD

The role of p38 MAPK is not well studied in HD. However, in one study, activation of the p38 MAPK and its correlation with striatal damage has been found in the striatal neurons of R6/2 mouse but not in the cortex (Gianfriddo et al., 2004). In addition, a study

shows that two unrelated proteins with expanded polyglutamine repeats induce p38 MAPK in cultured cell models of neurodegeneration (spinocerebellar ataxia 1, or SCA-1), and the expanded polyglutamine protein cytotoxicity is mediated primarily through activation of p38 MAPK (Tsirigotis et al., 2008).

1.4.3   JNKs

There are at least 10 different mammalian JNK isoforms encoded by three genes: *jnk1*, *jnk2*, and *jnk3*, which are activated by the Rac-MEKK-MEK4/7 pathway (Gallo and Johnson, 2002). JNKs activate transcriptional factors including c-Jun (its specific substrate), Elk-1, ATF-2, and SAP-1 (Haddad, 2005; Kyriakis and Avruch, 2001; Roux and Blenis, 2004). The JNK1 and JNK2 are ubiquitously expressed while the JNK3 is selectively expressed in the brain, heart and the testis (Gupta et al., 1996).

As mediators of apoptosis, JNKs can antagonize the function of the anti-apoptotic protein Bcl-2 (Park et al., 1997), possibly by phosphorylation (Maundrell et al., 1997). On the other hand, the JNK signaling pathway stabilizes and activates the tumor suppressor p53 (Fuchs et al., 1998), a pro-apoptotic transcription factor that suppresses *bcl-2* and enhances *bax* induction (Miyashita et al., 1994).

1.4.3.1 JNKs and NMDARs

High concentrations of glutamate and NMDA induce JNK activation in rat cerebellar granule cells, though less strongly than the activation of p38 MAPK (Kawasaki et al.,

1997). NMDA-mediated neurotoxicity in cortical cell cultures mediated by activated JNK is dependent on entry of extracellular calcium (Ko et al., 1998). In cortical cultures, NMDA induces JNK activation through the rapid and selective phosphorylation of MKK7, and NMDA-induced cell death can be prevented by a JNK peptide-based inhibitor (Centeno et al., 2007); on the other hand, a subsequent study indicated that JNK inhibition only partially rescues NMDAR-mediated cell death in cortical cultures (Soriano et al., 2008). Further work has shown that activation of extrasynaptic NMDA receptors triggers FoxO3a nuclear translocation in hippocampal neurons and this translocation can be largely reduced by JNK inhibitors (Dick et al., 2010). It has also been shown that glutamate or NMDA, but not dopamine, activates JNK and AP-1-mediated transcription in cultured striatal neurons (Schwarzschild et al., 1997; Schwarzschild et al., 1999).

1.4.3.2 JNKs and HD

It has been previously reported that normal huntingtin interacts with MLK2, a JNK activator, whereas the polyglutamine expansion interferes with this interaction and induces JNK activation and apoptosis in transfected HN33 cells (Liu et al., 2000). JNK has also been recently shown to be involved in HD-related neurotoxicity in a rat model (Perrin et al., 2009) as well as in intersectin-enhanced huntingtin aggregation and neurodegeneration in a *Drosophila* model of HD (Scappini et al., 2007).

1.5　Rationale, hypothesis, and objectives

As much evidence suggests that NMDAR (especially extrasynaptic GluN2B-type)-induced excitotoxicity plays a role in the pathogenesis of HD, the emerging question is what molecules link NMDARs and huntingtin together in a htt polyQ length-dependent manner to alter NMDAR function and toxic signaling, eventually leading to enhanced neuronal death? As reviewed here, the MAGUK family proteins play crucial roles in NMDAR trafficking, anchoring and interaction with downstream effectors, and others have reported a polyQ-dependent association of PSD-95 and htt. Notably, a recent publication shows that NMDA-induced cell death in cortical neurons is mediated by two distinct excitotoxic pathways: one is via the p38 MAPK, which relies on NMDAR/PSD-95/nNOS signaling and can be disrupted by Tat-NR2B9c without impacting prosurvival signaling; and the other is via the JNK pathway, which is not PSD-95/nNOS signaling-dependent and is observed also in non-neuronal cells (Soriano et al., 2008). Although these studies have not been done yet in striatal GABAergic MSNs, it is possible that NMDAR/PSD-95 signaling is altered by mutant htt in the YAC HD mice, leading to elevated NMDA-induced, p38 MAPK-mediated cell death. Therefore, my overarching hypothesis is that the interaction between PSD-95 and GluN2B-containing NMDARs, and altered regulation of downstream MAPK pathways, play important roles in mutant htt-mediated regulation of NMDAR function and enhanced excitotoxicity in striatal MSNs.

Objectives:

1. Determine whether expression of polyQ-expanded htt alters PSD-95 interaction with GluN2B or GluN2A subunit of NMDAR in presymptomatic mice striatum;

2. Investigate whether GluN2B/PSD-95 interaction plays any role in signaling to NMDAR-mediated cell death in striatal neurons, compared with hippocampal neurons, and in WT versus mutant htt-expressing MSNs;

3. Examine whether nNOS, p38 or JNK MAPKs plays any role in the pro-apoptotic signaling downstream of NMDAR, and whether their activation requires GluN2B/PSD-95 interaction, in mutant-htt expressing MSNs compared with WT MSNs.

2 Interaction of PSD-95 with NMDAR influences excitotoxicity in the YAC mouse model of Huntington's disease[1]

2.1 Introduction

N-methyl-D-aspartate (NMDA)-type glutamate receptors play a critical role in synaptic plasticity (Bliss and Collingridge, 1993) as well as mechanisms underlying neurodegeneration including Huntington's disease (Cowan and Raymond, 2006; Waxman and Lynch, 2005b). NMDARs contain two GluN1 subunits with two of GluN2A, GluN2B, GluN2C and/or GluN2D (Dingledine et al., 1999). GluN2 subunits determine receptor-channel properties and interactions with scaffolding proteins and signaling networks (Dingledine et al., 1999; Hardingham and Bading, 2003; Prybylowski and Wenthold, 2004), influencing the balance between neuronal survival and dysfunction or death.

Several lines of evidence support a role for altered NMDAR function in HD (DiFiglia, 1990; Fan and Raymond, 2007), which is caused by a polyQ repeat expansion >35 near the N-terminus of the protein huntingtin (Huntington's Disease Collaborative Research

---

[1] This chapter has been adapted from two published articles: J. Fan, C. M. Cowan, L. Y. J. Zhang, M. R. Hayden, and L. A. Raymond. Interaction of postsynaptic density protein-95 with N-Methyl-D-Aspartate Receptors influences excitotoxicity in the YAC mouse model of Huntington's disease. *J Neurosci.* Sep 2; 29(35): 10928-38, 2009. Article content reproduced here with permission from Society of Neuroscience. Copyright 2009. Other parts in: J. Fan, O. C. Vasuta, L. Y. J. Zhang, L. Wang, A. George, L. A. Raymond. N-Methyl-D-Aspartate receptor subunit- and neuronal-type dependence of excitotoxic signaling through postsynaptic density 95. *J Neurochem.* 115, 1045-56, 2010. Article content reproduced here with permission from John Wiley and sons. Copyright 2010.

Group, 1993). HD is characterized by selective neuronal degeneration, affecting striatal MSNs most severely (Vonsattel and DiFiglia, 1998). These neurons are enriched in GluN2B-containing NMDARs compared with other GluN2 subunits and other brain regions (Christie et al., 2000; Landwehrmeyer et al., 1995; Li et al., 2003b). Previous work in mouse and cellular models of HD suggests GluN2B-containing NMDARs are functionally altered in HD and contribute to neuronal dysfunction and susceptibility to apoptosis (Cepeda et al., 2001; Chen et al., 1999b; Fan et al., 2007; Levine et al., 1999; Milnerwood et al., 2006; Shehadeh et al., 2006; Song et al., 2003; Starling et al., 2005; Tang et al., 2005; Zeron et al., 2001; Zeron et al., 2002). However, the molecular mechanisms underlying mutant huntingtin's effect on NMDAR function have not been fully elucidated.

MAGUKs, including PSD-93, PSD-95, SAP97 and SAP102, act as scaffolds to facilitate signaling by anchoring key enzymes close to glutamate receptors (Fujita and Kurachi, 2000). The second PDZ domain in PSD-95 and SAP102 binds to the GluN2A or GluN2B carboxy-terminal tSXV motif (Niethammer et al., 1996). This interaction has been shown to contribute to toxic signaling downstream of NMDAR activation; a peptide that interferes with the binding of MAGUKs to NMDARs rescues hippocampal and cortical neurons from NMDA-induced excitotoxicity *in vitro* and ischemic neuronal death *in vivo* (Aarts et al., 2002; Soriano et al., 2008). Neuronal protection mediated by this peptide correlates well with reduced activation of nNOS, which also binds to the PDZ2 of PSD-95. Less is known about the mechanisms of excitotoxic death in striatal neurons,

which are the targets of neurodegeneration in a variety of neurological disorders as well as in response to ischemia. Notably, the PSD-95 SH3 domain interacts directly with the polyproline region of huntingtin *in vitro*, in a polyQ length-dependent manner, and these proteins co-associate in human brain tissue (Sun et al., 2001).

We hypothesized that polyQ-expanded htt in a complex with MAGUKs and NMDARs functionally alters the interaction between GluN2B and PSD-95 and/or SAP102, thereby contributing to the enhanced NMDAR surface expression and/or toxicity previously described in YAC mutant transgenic mouse MSNs (Fan et al., 2007; Shehadeh et al., 2006; Zeron et al., 2002).

Here, we investigate the importance of the PSD-95 interaction with GluN2B-containing NMDARs in mechanisms underlying enhanced excitotoxicity previously documented in mutant huntingtin-expressing MSNs (Fan et al., 2007; Shehadeh et al., 2006; Zeron et al., 2002). In these experiments, we used transfected HEK293T cells, primary cultured hippocampal neurons, as well as striatal MSNs and tissues from WT mice or the YAC transgenic HD mouse model expressing full-length human huntingtin with polyQ lengths of 18 (control), 72 and 128 (pathogenic) (Hodgson et al., 1999; Slow et al., 2003). We show that altered GluN2B binding with PSD-95 contributes to enhanced NMDA toxicity independently of nNOS activation in striatal neurons.

2.2 Methods and materials

2.2.1 Cell culture and transient transfection

HEK293T cells (human embryonic kidney cells expressing SV40 large T antigen) were maintained in Gibco's modified Eagle's medium with penicillin/streptomycin, L-glutamine, sodium pyruvate and 10% Gibco's fetal bovine serum. Cells were transfected using the calcium-phosphate precipitation method (Chen and Okayama, 1987), with a 1:1 transfection solution of 250 mM $CaCl_2$ and 2 x BES (N,N-bis[2-hydroxy-ethyl]-2-aminoethanesulfonic acid) (50 mM BES, 280 mM NaCl, 1.5 mM Na_2HPO_4, pH 6.98). Ten to twelve μg of plasmids were mixed with 1 ml of transfection solution per 10-cm plate. Cells were transfected for 6-8 hrs in a 37^0C, 3% CO_2 incubator and then washed once with PBS to stop transfection. cDNA plasmids encoding GluN1A, GluN2B, have been described previously (Chen et al., 1999b). The cDNA plasmid for PSD-95, described previously (Li et al., 2003b) was a gift from the late Dr. A. El-Husseini, University of British Columbia.

2.2.2 Transgenic mice

The following lines of YAC transgenic mice - YAC18 (line 212) (similar to line 29) (Leavitt et al., 2001), YAC72 (line 2511) (Hodgson et al., 1999) and YAC128 (line55) (Graham et al., 2006b) were used as models expressing full-length human htt containing 18 (control), 72, and 128 (pathogenic) polyQ repeats (18Q, 72Q, 128Q), respectively, and compared to FVB/N WT mice. Offspring of crosses between two homozygous YAC transgenic mice on a pure FVB/NJ strain background were used for experiments

(Hodgson et al., 1999). All mice were housed, tested and tissue harvested according to guidelines of the University of British Columbia and the Canadian Council for Animal Care.

2.2.3 Peptides

The Tat-NR2B9c and Tat-NR2BAA peptides were originally a gift from Dr. M. Tymianski (U. of Toronto) and were later purchased from AnaSpec (San Jose, CA, USA) and Peptides 2.0 (Chantilly, VA, USA). Tat-NR2BAA peptide is similar to Tat-NR2B9c but with a double point mutation in the COOH terminal tSXV motif (Tyr-Gly-Arg-Lys-Lys-Arg-Arg-Gln-Arg-Arg-Arg-Lys-Leu-Ser-Ser-Ile-Glu-<u>Ala</u>-Asp-<u>Ala</u>), making it incapable of binding PSD-95. The peptides were dissolved in sterile Milli-Q water to make 1mM stock aliquots and stored at -80^0C. Peptide aliquots were thawed only once.

2.2.4 Antibodies used in immuoprecipitation and western blotting

Antibodies used for immunoprecipitation and/or to probe western blots included: rabbit polyclonal anti-GluN2B (1 μg/ml, Upstate, #06-600); mouse monoclonal anti-GluN2B (1:250, Transduction Lab, #610417); mouse monoclonal anti-GluN2B (1 μg/ml, Affinity BioReagents, #MA1-2014); rabbit polyclonal anti-GluN2A (1 μg/ml, Upstate, #07-632); anti-huntingtin mouse monoclonal antibody (1 μg/ml, Chemicon, #MAB2166); anti-huntingtin human-specific mouse monoclonal antibody (HD650, used at

1:500)(Warby et al., 2005); anti-SAP102 rabbit polyclonal antibody (1:400, Chemicon, #AB5170); anti-SAP102 mouse monoclonal antibody (1 µg/ml, NeuroMAB, #75-058); anti-PSD-95 (1 µg/ml, NeuroMAB, #75-028), anti-PSD-95 (1:200, Affinity BioReagents, MA1-045), anti-actin (1 µg/ml, Santa Cruz, sc-1616). Horseradish Peroxidase (HRP) -linked secondary antibodies for western blotting are anti-mouse IgG antibody (NA931V) and anti-rabbit IgG antibody (NA934V), both from Amersham, and used at 1:5000. AP-conjugated secondary antibody (S372B), are from Promega (Madison, WI, USA) and used at 1:10,000 dilution.

2.2.5 Primary neuronal culture

All neuronal cultures were grown in serum-free plating medium (B27, penicillin/streptomycin, L-glutamine, Gibco's Neurobasal medium), maintained in a humidified 37^0C incubator with 5% CO_2, and refreshed every 4-5 days by replacing half of the medium.

2.2.5.1 Postnatal striatal neuronal culture

Nitric-acid treated 12mm glass coverslips were placed in 24-well plates coated with poly-D-Lysine (250µg/ml). Striatal tissues were dissected from postnatal day 0-1 (P0-P1) YAC transgenic mice or wild-type FVB/N mice in Hank's Balanced Salt Solution (HBSS, Gibco) on ice, digested in papain and further dissociated in trypsin inhibitor solution. MSNs were then plated at a density of approximately 2×10^5 cells per well, as described

(Zeron et al., 2002). Approximately 80-90% of the cells cultured in serum-free media have the characteristics of MSNs (Kovacs et al., 2001; Shehadeh et al., 2006; Zeron et al., 2004).

2.2.5.2 Embryonic striatal and hippocampal neuronal cultures

Embryonic striatal and hippocampal cultures were prepared by dissecting striatal and hippocampal tissue respectively from 17- to 18-day-old rat embryos using methods described previously (Li et al., 2002a).

2.2.5.3 Cortical and striatal co-cultures

Cortical and striatal co-cultures were prepared from 17- to 18-day-old rat embryos. Striatal cells were transfected at days *in vitro* (DIV) 0 with yellow fluorescent protein (YFP) plasmid on a β-actin promoter (a gift from A. M. Craig, University of British Columbia, Vancouver) in 100 μl of electroporation buffer (Mirus Inc.) by nucleofection (Amaxa Inc), according to manufacturer's instructions. Transfected striatal cells were plated with untransfected cortical cells at a ratio of 1:1 on a 24-well plate pre-coated with poly-D-lysine with 2×10^5 cells in total per well.

2.2.6 Immunoprecipitation

HEK293T cells (30–32 hrs after transfection), or cultured striatal neurons at 9-10 DIV, or hippocampal neurons at 17-20 DIV pretreated for 1 hour with varying

concentrations of Tat-NR2B9c and Tat-NR2BAA (control peptide) in the medium, or homogenized 4 or 8 week-old YAC transgenic mice striatal tissues, were harvested and lysed in 0.8% TritonX-100 + 0.1% SDS or 1% NP-40-containing lysis buffer (50 mM Tris-pH7.4, 150 mM NaCl, 1 mM EDTA, 1 mM EGTA) with protease and phosphatase inhibitors (1 mM PMSF, 2 μg/mL aprotinin, 2 μg/mL leupeptin, 4 μg/mL pepstatin A, 30 mM NaF, 40 mM β–glycerophosphate, 20 mM sodium pyrophosphate, 1 mM sodium orthovanadate, and 10 μM ZVAD if immunoprecipitating htt), and solubilized by ultrasonication. The lysates were pre-cleared with equilibrated (pre-washed three times with lysis buffer) 50% Protein A/G beads for 1 hour at 4^0C, and then incubated by constant rotating overnight with 50% Protein A/G beads and antibodies (or without antibody for no antibody controls). Beads of each sample were then washed with Tris Wash Buffer (50 mM Tris-pH 7.4, 150 mM NaCl, 1 mM EDTA, 1 mM EGTA, 1% Triton in Milli-Q water) and heated at 95-99^{0}C in Protein Sample Buffer (PSB; 125 mM Tris-pH6.8, 2% SDS, 10% Glycerol, 72 mg/mL Dithiothreitol, with Pyronin Y in Milli-Q water).

2.2.7 Western blotting

Paired samples were run on 8% Sodium dodecyl sulfate-polyacrylamide gel electrophoresis (SDS-PAGE) and then transferred from gels to polyvinylidene difluoride (PVDF) membranes (Bio-Rad) and subjected to immunoblotting. The blot was cut into two parts along the 150 kDa marker and probed with anti-GluN2B (or GluN2A, or htt)

and anti-PSD-95 antibodies respectively. Protein bands were visualized with the enhanced chemiluminescence (ECL) Western Blotting Detection System (GE Healthcare Bio-Sciences). For the anti-PSD-95 immunoprecipitation experiments, cut top blots were probed with anti-GluN2A antibodies first and visualized with Horseradish Peroxidase - ECL system and then reprobed for GluN2B and visualized using Alkaline Phosphatase (AP) − Lumi-Phos WB chemiluminescent system (Pierce, Rockford, IL, USA). Densitometry of resulting bands was performed using ImageJ.

To measure the co-immunoprecipitation (co-IP) of associated proteins, the levels of associated PSD-95 were normalized to the levels of GluN2B (or GluN2A) subunit co-immunoprecipitated with anti-GluN2B (or anti-GluN2A) in the same lane of the gel; alternatively, levels of GluN2A or GluN2B were normalized to PSD-95 co-immunoprecipitated with anti-PSD-95 antibodies. In both sets of experiments band densities were compared between treatment conditions on the same blot and same exposures. Notably, similar amounts of GluN2 and PSD-95 proteins were solubilized using either 0.8% TritonX-100 + 0.1% SDS or 1% NP-40 detergents, and the relative ratios of GluN2 subunits co-immunoprecipitated with PSD-95 after treatment with the different Tat peptides were similar for the two detergents (comparing results from n=7 − 13 experiments in each detergent).

Densitometry of resulting bands was analyzed using ImageJ or Scion Image software. The band densities for YAC72 and YAC128 were normalized to those of either WT or YAC18 (controls) that were run on the same gel because of variability in antibody

sensitivity and exposure times between experiments.

2.2.8 NMDA-induced cytotoxicity

Postnatal mouse striatal neurons (DIV 9) or embryonic rat hippocampal neurons (DIV 18 or 19) or co-cultured rat cortical and striatal neurons (DIV14), cultured in 24-well plates were pretreated for 1 hour with various concentrations of Tat-NR2B9c or Tat-NR2BAA peptide, then incubated in warm balanced salt solution (BSS, pH7.4) with or without 500μM NMDA for 10 min, or directly incubated with or without 100μM or 500μM NMDA in the medium for 10 min in some experiments. After NMDA treatment, hippocampal and striatal cultured neurons were washed once with warm plating medium and then incubated in conditioned PM (without Tat peptides or N-Arg) for 24 hours; co-cultured striatal and cortical neurons were maintained for just 6 hours after NMDA before fixing and assessing cell death in order to preserve the YFP signal. Then cells were washed with PBS once and fixed with 4 % paraformaldehyde (PFA) for 30 minutes.

2.2.9 Terminal deoxynucleotidyl transferase dUTP nick end labeling (TUNEL) assay and assessment of apoptosis

Fixed cultured neuronal cells were numbered according to different conditions and coded before staining to ensure that the operator was blinded during the subsequent processing and analysis of immunofluorescence. Neuronal cells were further permeabilized with 0.25% TritonX-100 in PBS with 0.5% sodium citrate on ice for 2 min,

then washed once with PBS and incubated in PBS with 16 μg/mL RNase at room temperature (RT) for 30 min. After washing once with PBS, neuronal cells were incubated in TUNEL (Roche) reagent (at a ratio of label:enzyme = 9:1) in the dark for 1hr, followed by one wash with PBS and staining with 8 μM propidium iodide (PI) or 10 μM Hoechst 33342 for nuclear staining. Coverslips were then washed with PBS and mounted on slides with Fluoromount-G. The second day after staining, the percentage of apoptotic cell death was assessed by counting the numbers of TUNEL positive cells in the green fluorescent channel which also showed condensed and blebbed nuclear morphology in the red (or blue) fluorescent channel, then dividing by the total number of PI (or Hoechst) positive cell nuclei in the red (or blue) fluorescent channel and multiplying by 100. A total of 1000 neurons were counted per condition. The percentage of apoptotic cell death of neuronal cells untreated or exposed to BSS alone normally ranged from 3-30%, and was subtracted as a baseline from each of the other conditions in the same experiment.

Co-cultured striatal and cortical neurons were permeabilized with 0.5% Triton X-100 in PBS with 0.5% sodium citrate on ice for 5 min after fixation, and then washed once with 0.03% Triton X-100 in PBS (PBST) and incubated in PBST with 4% Normal Goat Serum (NGS) for 45 min with shaking at RT. After one wash with PBST, cells were immuno-stained with chicken polyclonal anti-green fluorescent protein (GFP) antibody (1:1000; catalog #ab13970; Abcam), followed by three washes with PBST then anti-chicken Alexa Fluor 488 (1:1000; A-11039; Invitrogen), with 1 h shaking at RT for each staining. After GFP staining, co-cultured cells were washed three times in PBST

then incubated for 10 min with 10 μM Hoechst 33342 at RT and washed again in PBST. Coverslips were then mounted on slides with Fluoromount-G. The percentage of apoptotic striatal cells co-cultured with cortical neurons was assessed by counting the numbers of YFP-positive striatal cells that showed condensed and blebbed nuclear morphology in the blue fluorescent channel and then dividing by the total number of YFP-positive cells in the green fluorescent channel and multiplying by 100. A total of 100 YFP-positive striatal neurons were counted per condition.

2.2.10 Small interfering RNA (siRNA) knock-down

The control ("scrambled" siRNA, sc-36869; or non-targeting siRNA, D-001950-01), PSD-95 siRNA (sc-42012, pools of three target-specific 19-25 nt siRNAs), and NE-Dlg (SAP102) siRNA (sc-42007, pools of three target-specific 19-25 nt siRNAs) were purchased from Santa Cruz (Santa Cruz, CA, USA) or Dharmacon (Thermo Fisher, Chicago, IL, USA). At DIV 7 or 8, cultured MSNs were transfected with siRNA by DharmaFECT® siRNA transfection reagent 3 (Dharmacon/Thermo Fisher, Chicago, IL, USA, T-2003-01), in complete medium containing B-27 (Trushina et al., 2006). On DIV 9 or 10, MSNs were treated as described in section 2.2.8 (*NMDA induced cytotoxicity),* and fixed on DIV 10 or 11, then forwarded to immunostaining. For detecting the knock-down efficiency by western blotting, 35 mm dishes of MSNs with or without siRNA transfection were directly harvested 72 hrs later on DIV 10 or 11.

2.2.11 Data analysis

Figures, tables, and statistical analyses were generated using Microsoft Excel, Northern Eclipse, ImageJ, Origin, Prism, Adobe Photoshop or Adobe Illustrator software. Data or bars are presented as the mean±SEM. Significant differences were determined using the unpaired or paired, two-tail Student's t-test, one-way ANOVA or two-way ANOVA, as appropriate.

2.3 Results

2.3.1 Expression level of PSD-95 is similar in striatal tissue of 2 month-old WT and YAC mice

As a first step, I assessed the expression level of PSD-95 in 8 week-old YAC mice striatal tissue as part of my co-immunoprecipitation study. For each experiment, one-tenth volume of lysate collected from the striatal tissue of WT, YAC18, YAC72, and YAC 128 mice was separated by SDS-PAGE and transferred to PVDF membranes. Blots were probed with anti-PSD-95 antibody first, then stripped and probed with anti-actin antibody as a loading control. As shown in Fig. 1A and B, no significant difference was found in expression levels of PSD-95 across YAC genotypes (18, 72, 128) and WT mouse striatal tissue at this age. The data suggest that mutant huntingtin does not affect PSD-95 expression at the transcriptional or translational levels.
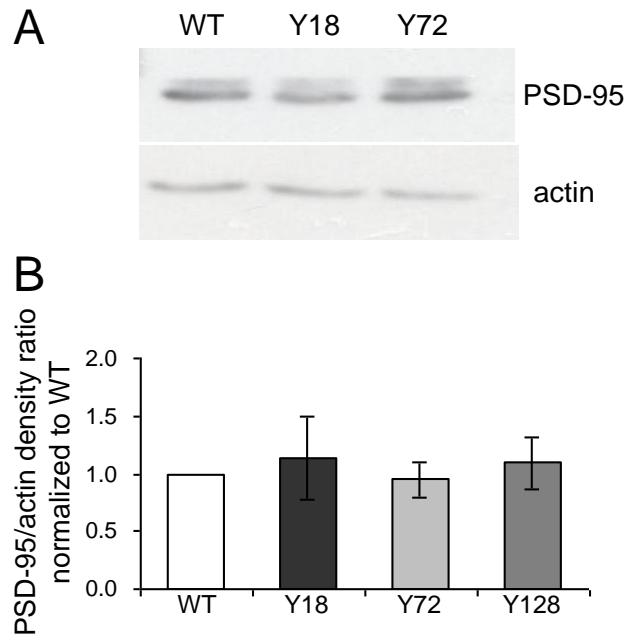
Figure 1. Expression levels of PSD-95 in 8 week-old WT, and YAC mouse striatal tissue.

A) Representative western blot showing expression levels of PSD-95 in 8 week-old WT, YAC18 and YAC72 mouse striatal tissue. Actin was probed as a loading control. **B)** The PSD-95/actin density ratios are similar across WT and all three genotypes (data from each genotype has been normalized to WT). No significant difference by one-way ANOVA, $p > 0.05$; n=6 for WT, YAC18, and YAC72; n=3 for YAC128.

2.3.2 Association of htt with PSD-95 in striatal tissue of 2 month-old WT and YAC mice

Previous studies in transfected heterologous cells and human brain tissue have demonstrated that htt associates with PSD-95 via the polyproline and SH3 domains, respectively, and that polyQ expansion weakens that interaction (Sun et al., 2001). We tested these observations in the YAC transgenic mouse model of HD. Brain lysates were immunoprecipitated with MAB2166, or anti-human huntingtin antibody HD650. As a negative control, protein A or G Sepharose beads alone were also incubated with tissue lysates, and no PSD-95 or htt bands were detected (shown in Fig. 2A). The blots were cut along 160 kDa and probed with anti-htt antibodies and anti-PSD-95 antibodies separately. As predicted from the previous studies in heterologous cells and human brain tissue, we also found co-association of htt and PSD-95 was decreased significantly in striatal tissue from YAC128 transgenic mice compared with YAC18 (Fig. 2A). In the example blot, there is a clear decrease in co-IP of PSD-95 with htt for YAC128 but not for YAC72; this reflects the group data (shown in the bar graph below the blot, Fig. 2B) in that the YAC72 results were quite variable and not significantly different from WT.

Notably, the representative blot in Fig. 2A showed no molecular weight difference of htt bands in immunoprecipitates between genotypes, using the anti-human htt (HD650) antibody for immunoprecipitation and probing. The reason is unknown, but we do see a molecular weight difference of htt bands between genotypes when using the anti-htt (MAB2166, Chemicon) antibody for immunoprecipitation and probing. However, a study

using this HD650 antibody for immunoprecipitation and MAB2166 for probing has

demonstrated the appropriate molecular weight difference for htt detected in brain tissues

from YAC128 and YAC18 (Warby et al., 2005).
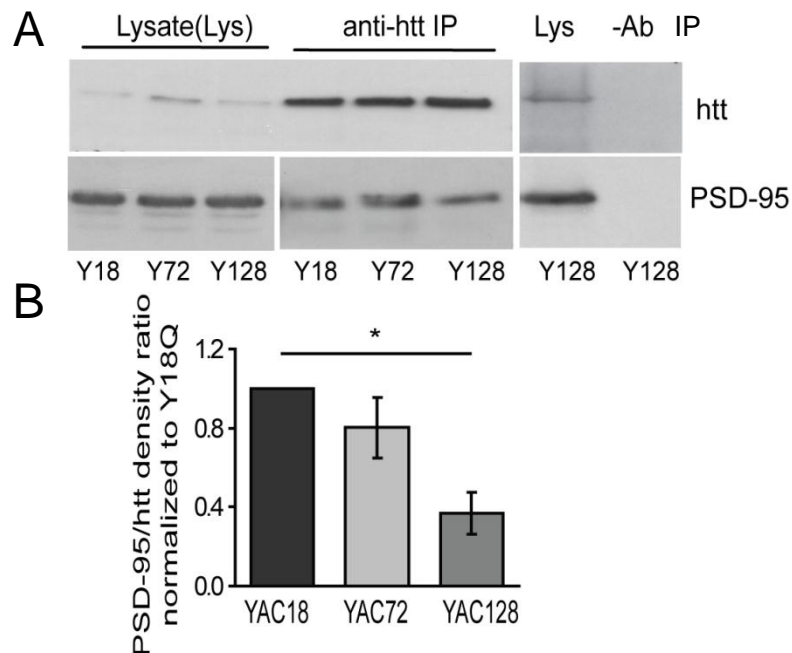
Figure 2. Association of huntingtin with PSD-95 decreases as polyQ length of htt increases.

A) Representative blot showing PSD-95 association with htt depends on polyQ length of htt in YAC transgenic mouse striatal tissues. Lysates from 4-8 week-old mouse striatal tissue were immunoprecipitated with MAB2166 or HD650 (an anti-human htt specific antibody). The blot was cut into two parts along the 160 kDa marker and probed with anti-htt (HD650 was used in this example) and anti-PSD-95 antibody respectively. **B)** Pooled data showing the mean band density ratio of PSD-95 to huntingtin for pooled data is shown below the blot (in each experiment, YAC72 and/or YAC128 were run on same gel as YAC18 and band density ratios were normalized to those in YAC18 lane). Significant by one-way ANOVA and Bonferroni posttests, *$p<0.05$ (n=3).

2.3.3 Different effect of mutant htt expression on interaction of GluN2 subunits with PSD-95

PSD-95 interacts with both GluN2A and GluN2B subunits (Niethammer et al., 1996; Sans et al., 2000), and interaction of GluN2B with these MAGUKs has been shown to regulate NMDAR surface expression and synaptic localization (Chung et al., 2004; Prybylowski et al., 2005; Roche et al., 2001), as well as excitotoxicity (Aarts et al., 2002). Previously, we have shown that in cultured MSNs from YAC transgenic mice, NMDAR-mediated apoptosis increases with htt polyQ length (Shehadeh et al., 2006; Zeron et al., 2002), and that GluN2B-contaning NMDAR surface expression is significantly increased in YAC72 compared with WT MSNs (Fan et al., 2007). Since htt, PSD-95 and GluN2 subunit of NMDAR might be associated together as a group, I set out to determine whether the PSD-95/GluN2 interaction is altered by the expanded polyQ of htt.

2.3.3.1 Mutant htt expression enhances interaction of GluN2B subunits with PSD-95

To determine whether mutant htt expression alters interaction between GluN2B-containing NMDARs and PSD-95, we immunoprecipitated GluN2B from striatal tissue of YAC transgenic mice and probed for GluN2B and PSD-95. As illustrated in Fig. 3, we found that association between GluN2B and PSD-95 significantly increased with increasing polyQ length (PSD-95/GluN2B band density ratio was 0.69 ± 0.13 for WT, 1.14 ± 0.23 for YAC72 and 1.47 ± 0.27 for YAC128 MSNs). Those data suggest that mutant htt enhances the interaction of PSD-95 with GluN2B by an unknown mechanism

and could presumably affect NMDAR localization, stability and function.
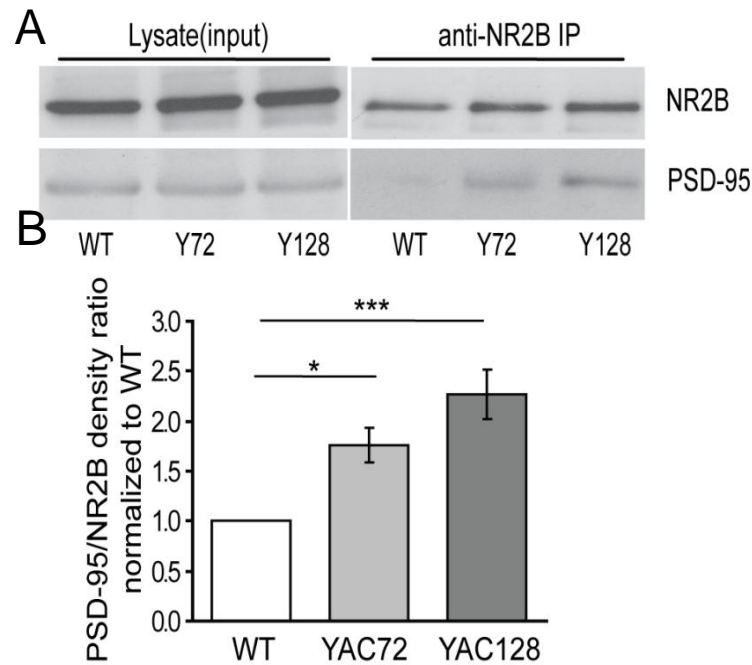
Figure 3. Mutant htt expression enhances interaction of GluN2B with PSD-95.

A) Representative blot showing that mutant htt expression alters the association of PSD-95 with GluN2B (NR2B) in vivo. GluN2B was immunoprecipitated from lysates of 8 week-old WT and YAC transgenic mouse striatal tissue using an anti-GluN2B antibody (Affinity Bioreagents) and proteins were subjected to western blot analysis. The blot was cut into two parts along the 160 kDa marker and probed with anti-GluN2B and anti-PSD-95 antibody, respectively. **B)** Pooled data for the mean band density ratio of PSD-95 to GluN2B is shown (in each experiment, YAC72 and/or YAC128 were run on same gel as WT and band density ratios were normalized to those in WT lane). Significant by one-way ANOVA and Bonferroni posttests, *$p<0.05$, ***$p<0.001$ (n=8 for WT; n=7 for YAC72 and YAC128).

2.3.3.2 Mutant htt expression does not alter interaction of GluN2A subunits with PSD-95

To test whether the mutant htt enhanced GluN2B/PSD-95 binding is subunit-specific, I repeated the co-immunoprecipitation experiment using anti-GluN2A antibody with striatal tissue of YAC transgenic mice at the same age. As shown in Fig. 4, the enhanced interaction of PSD-95 with the NMDAR is specific for the GluN2B-type, as the binding of GluN2A and PSD-95 was similar for WT and all YAC genotypes.
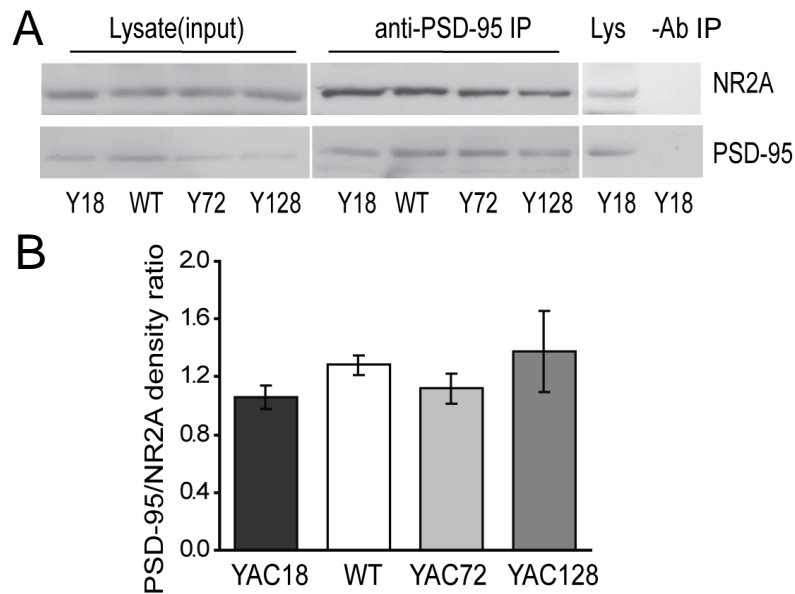
Figure 4. Association of PSD-95 with GluN2A is not altered by htt polyQ repeat length.

A) Representative blot showing that co-immunoprecipitation of PSD-95 with GluN2A (NR2A) in 8 week-old YAC mouse striatal tissue is not altered by htt polyQ repeat length.

B) Pooled data for the mean band density ratio of PSD-95 to GluN2A is shown. There is no significant difference by one-way ANOVA, $p > 0.05$ (n=3 for YAC18, n=5 for WT and YAC72, n=4 for YAC128).

2.3.4 Tat-NR2B9c peptide perturbs GluN2B interaction with PSD-95

We hypothesized that polyQ-expanded htt in a complex with MAGUKs and NMDARs functionally alters the interaction between GluN2B and PSD-95, thereby contributing to the enhanced NMDAR toxicity previously described in YAC mutant transgenic mouse MSNs (Fan et al., 2007; Shehadeh et al., 2006; Zeron et al., 2002). To test this hypothesis, we utilized a Tat-fused peptide identical to the C-terminal 9 amino acids of GluN2B (Tat-NR2B9c) to disrupt GluN2B binding to PDZ-containing proteins, as previously described (Aarts et al., 2002). In that study, 100 micromolar Tat-NR2B9c was required to disrupt PSD-95 binding to GluN2B in rat forebrain lysates *ex vivo*.

2.3.4.1 Tat-NR2B9c peptide perturbs GluN2B interaction with PSD-95 in transfected HEK cells

To determine the peptide concentration range required to uncouple GluN2B from PSD-95 in live cells, we treated transfected HEK293T cells for 1 hour with various peptide concentrations. In experiments in HEK293 cells, we found that compared with treatment with the control peptide Tat-NR2BAA, both 0.2 and 1 micromolar Tat-NR2B9c significantly reduced the amount of PSD-95 that co-immunoprecipitated with GluN2B by ~40% (Fig. 5).
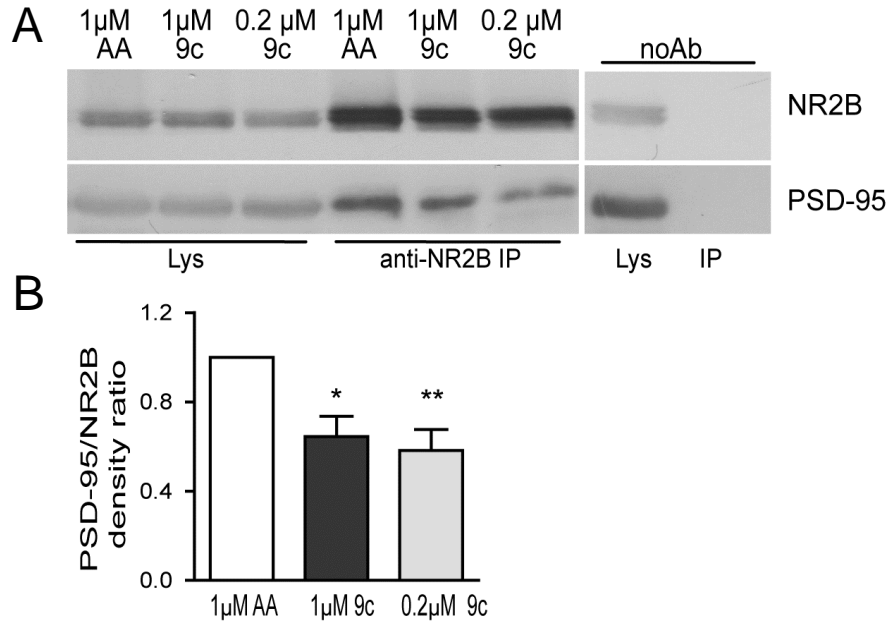
Figure 5. Association of GluN2B with PSD-95 is perturbed by 200nM and 1µM Tat-NR2B9c in transfected HEK293T cells.

A) Representative blot showing that 200nM and 1µM Tat-NR2B9c perturbs co-IP of GluN2B with PSD-95 in 293T cells. 293T cells expressing GluN2B and PSD-95 were pretreated with 200nM or 1µM Tat-NR2B9c or Tat-NR2BAA peptides for 1hr. Cell lysates were incubated with anti-GluN2B antibody. The blot was cut into two parts along the 160 kDa marker and probed with anti-GluN2B and anti-PSD-95 antibodies, respectively. **B)** Pooled data showing PSD-95/GluN2B band density ratio decreased 36±9% by 1µM Tat-NR2B9c, *$p < 0.05$, n=5; and 42±9% by 200nM Tat-NR2B9c, **$p < 0.01$, n=6; normalized to 1µM Tat-NR2BAA and tested by one-sample t-test, in transfected HEK cells.

2.3.4.2 Tat-NR2B9c peptide perturbs GluN2B interaction with PSD-95 in cultured MSNs

I also tested the efficacy of 1 micromolar and 200 nanomolar Tat-NR2B9c in uncoupling GluN2B and PSD-95 in live, cultured YAC128 MSNs. Similar to results in transfected HEK293T cells, we found a reduction by ~50% in the amount of PSD-95 that co-immunoprecipitated with GluN2B compared to neurons treated with Tat-NR2BAA for both 1 micromolar (Fig. 6A) and 200 nanomolar peptide concentrations (Fig. 6B, reprobed SAP102 bands in the same experiment also shown) in YAC 128 MSNs. The pooled data of the reduction in PSD-95 and SAP102 to GluN2B band intensity ratios (normalized to paired Tat-NR2BAA at same concentration) by both 200 nanomolar and 1 micromolar Tat-NR2B9c concentrations in cultured MSNs from YAC128 mice are shown in Fig. 6C.

A

Lysate(input)　　anti-NR2B IP

NR2B

PSD-95

-Ab　AA　9c　　-Ab　AA　9c

B Lysate(input)　anti-NR2B IP

NR2B

PSD-95

SAP102

AA　9c　　AA　9c

C

MAGUK/NR2B density ratio normalized to AA

□ 200nM Tat-2B9c
▨ 1μM Tat-2B9c

0.8
0.6
0.4
0.2
0.0

PSD-95　　SAP102
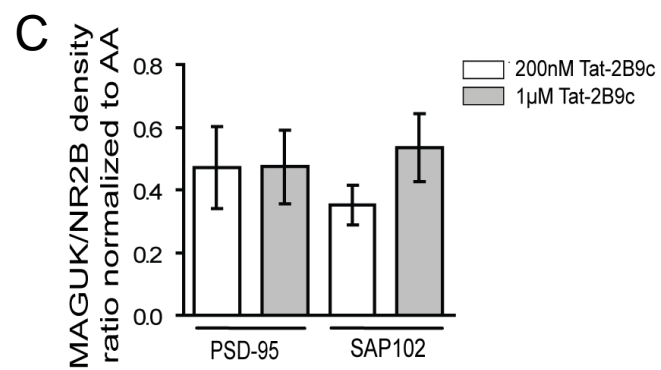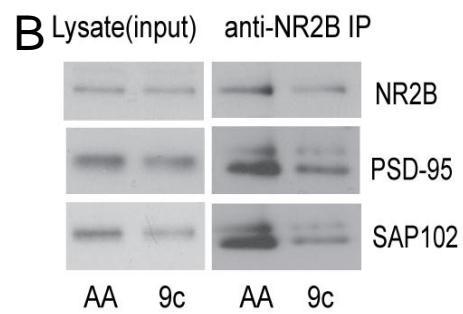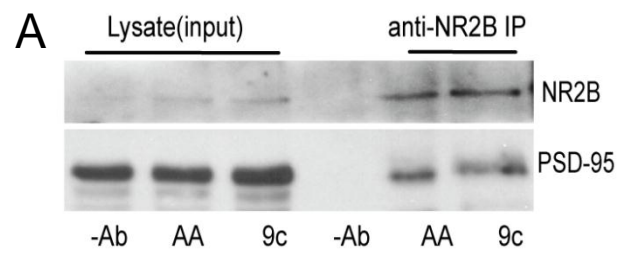
Figure 6. Tat-NR2B9c peptide perturbs GluN2B interaction with PSD-95 in cultured YAC128 MSNs.

A) Representative blot showing that 1μM Tat-NR2B9c disrupts co-IP of GluN2B with PSD-95 in YAC128 cultured MSNs. **B)** Representative blot showing that 200nM Tat-NR2B9c disrupts co-IP of GluN2B with both PSD-95 and SAP102 in YAC128 cultured MSNs. **A-B)** The concentration of Tat-NR2BAA used in each experiment matched that of the Tat-NR2B9c. **C)** The pooled data of the reduction of either PSD-95 or SAP102 ("MAGUK") to GluN2B band intensity ratio by both 200 nanomolar and 1 micromolar Tat-NR2B9c concentrations (normalized to its paired Tat-NR2BAA at the same concentration as Tat-NR2B9c). For the four bars from left to right, $*p< 0.05$, n=4; $**p<0.01$, n=3; $*p<0.05$, n=3 and $*p< 0.05$, n=8, compared with its paired Tat-NR2BAA at the same concentration (not shown, all equal to 1), by paired one-sample t-test, respectively.

When repeated in cultured MSNs from WT mice, I found a similar reduction of ~65% in the amount of PSD-95 that co-immunoprecipitated with GluN2B in neurons pretreated with 200 nanomolar Tat-NR2B9c compared to those treated with Tat-NR2BAA (Fig. 7). The PSD-95/GluN2B association ratio is 1.08 ± 0.03 for Tat-NR2BAA treated neurons, and 0.37 ± 0.09 for Tat-NR2B9c treated neurons (n=3 batches of cultures and paired experiments, $p<0.05$ by paired student t-test). Together with the result in YAC128 MSNs, I conclude that Tat-NR2B9c peptide has similar efficiency in disrupting the GluN2B/PSD-95 interaction in WT and mutant htt-expression neurons.
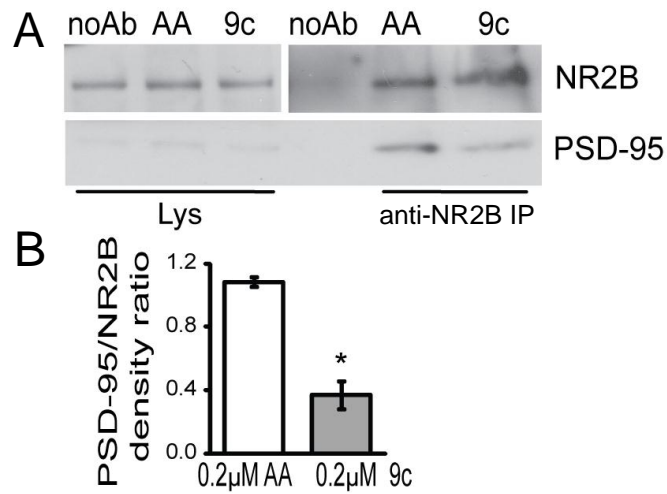
Figure 7. Tat-NR2B9c peptide perturbs GluN2B interaction with PSD-95 in cultured WT MSNs.

A) Representative blot showing co-immunoprecipitation of GluN2B with PSD-95 in cultured postnatal mouse striatal neurons following 1h pretreatment of 200nM Tat-NR2B9c or Tat-NR2BAA. **B)** Pooled data for PSD-95/GluN2B mean $\pm$ SEM band density ratios are shown. Significant by paired student t-test, $*p<0.05$ (n=3).

2.3.4.3 Tat-NR2B9c peptide perturbs GluN2B interaction with PSD-95 in primary cultured hippocampal neurons

Previous studies showed that submicromolar concentrations of Tat-NR2B9c peptide significantly reduced NMDAR-mediated toxicity in cultured cortical and hippocampal neurons (Aarts et al., 2002). However, the apparent concentration required to disrupt binding between GluN2B subunits and PSD-95 in brain lysates was 1000-fold higher. Although a subsequent study using an *in vitro* binding assay showed that the IC$_{50}$ values for inhibiting GluN2B binding to PSD-95 is ~ 8 μM (Cui et al., 2007), the Tat-NR2B9c effective concentration was not determined in live neuronal cultures.

We tested the potency of Tat-NR2B9c in disrupting interactions between GluN2B and PSD-95 in mature primary hippocampal neuronal cultures. Cultures were treated with 250 nM or 1 μM Tat-NR2B9c or its control peptide Tat-NR2BAA in the medium for 1 hour, then lysed and immunoprecipitated with antibodies against GluN2B. First, we found that PSD-95/GluN2B binding was reduced by ~ 50% with both 250 nM and 1 μM Tat-NR2B9c pretreatment, compared to the control peptide (Fig. 8). Furthermore, when we repeated the experiments using the anti-PSD-95 antibody to immunoprecipitate GluN2B, we found again that 250 nM Tat-NR2B9c significantly reduced association of PSD-95 with GluN2B when compared with Tat-NR2BAA (Fig. 9, GluN2B/PSD-95 ratio after treatment with Tat-NR2B9c was normalized to ratio after treatment with Tat-NR2BAA in paired experiments). There was a trend towards reduction in co-IP with PSD-95 after treatment with 1 μM Tat-NR2B9c (as illustrated in representative blot

shown in Fig. 9), but the experimental number was too low for quantification. These results are consistent with the protective effects of Tat-NR2B9c against NMDAR toxicity in cortical and hippocampal neurons, which have been reported to occur at $50 - 100$ nM concentrations of Tat-NR2B9c (Aarts et al., 2002). This result, together with the data in cultured striatal neurons, indicates that Tat-NR2B9c is able to disrupt GluN2B/PSD-95 binding in both cultured hippocampal and striatal neurons at similar concentrations.
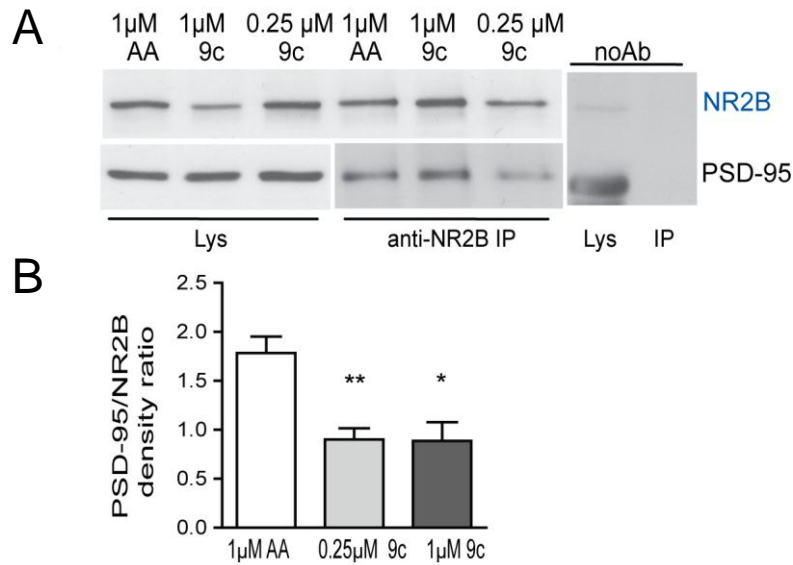
Figure 8. PSD-95 immunoprecipitated with anti-GluN2B antibody is reduced by both 1µM and 0.25µM Tat-NR2B9c pretreatments in primary hippocampal neuronal cultures.

A) In the example blot, there is a clear decrease in co-IP of PSD-95 with GluN2B for 0.25 µM Tat-NR2B9c that is less obvious for 1 µM Tat-NR2B9c; in fact, after quantification, this particular blot gave a ~30% reduction of PSD-95/GluN2B ratio by comparing 1 µM Tat-NR2B9c to Tat-NR2BAA. **B)** Pooled data for PSD-95/GluN2B mean band density ratios are shown below representative blot. Significant by one-way ANOVA and Bonferroni posttests, *$p<0.05$, **$p<0.01$ (n=8, 7, 4 for 1µM Tat-NR2BAA, 0.25µM and 1µM Tat-NR2B9c respectively).
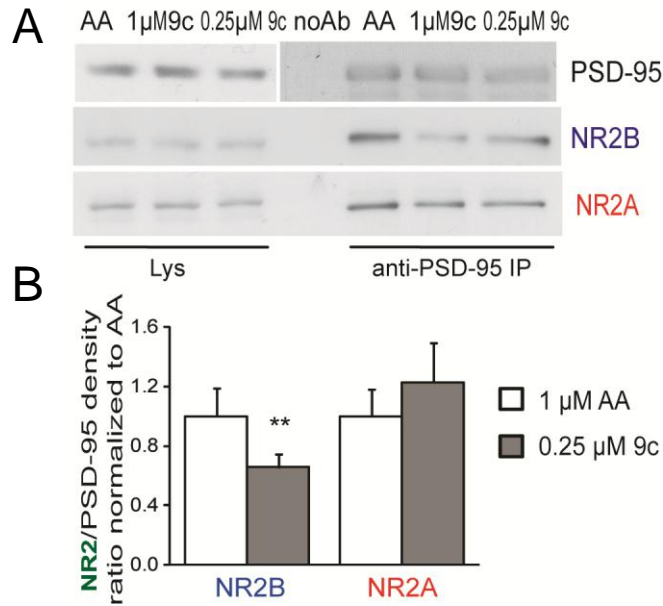
Figure 9. GluN2B but not GluN2A immunoprecipitated with anti-PSD-95 antibody is reduced by 0.25μM Tat-NR2B9c pretreatments in primary hippocampal neuronal cultures.

A) Representative blots showing 1 hour 0.25μM Tat-NR2B9c pretreatment of primary hippocampal cultures, followed by immunoprecipitation of PSD-95, disrupts co-IP of GluN2B/PSD-95 but not GluN2A/PSD-95. **B)** Pooled data for GluN2/PSD-95 mean ± SEM band density ratio (data was normalized to its paired Tat-NR2BAA control, set equal to 1). Note that 1 hour 0.25μM Tat-NR2B9c pretreatment disrupts co-IP of GluN2B/PSD-95 ($p<0.01$ by paired one-sample t-test, n=8) but not GluN2A/PSD-95 ($p>0.05$ by paired one-sample t-test, n=5). GluN2B and GluN2A were probed on the same blots for n=8 experiments, but 3 could not be quantified for GluN2A because of low sensitivity of the GluN2A antibody. Due to limited number of experiments, the 1μM Tat-NR2B9c data were not quantified.

2.3.5 The effect of Tat-NR2B9c on NMDA-induced apoptosis

Interaction between NMDARs and PDZ-containing proteins, especially PSD-95, has

been postulated to contribute to NMDAR-mediated excitotoxicity by anchoring signaling

proteins such as nNOS in close proximity with NMDAR-mediated calcium influx (Aarts

et al., 2002; Sattler and Tymianski, 2000). As well, the number, stability and localization

of surface NMDARs would be expected to regulate calcium influx in response to

excitotoxic insults and therefore affect the level of NMDA-induced apoptosis.

2.3.5.1 Tat-NR2B9c reduces NMDA-induced apoptosis in YAC72 and YAC128 MSNs but not WT MSNs

Cultured MSNs were treated with Tat peptides to determine whether Tat-NR2B9c

could protect these neurons from NMDA-induced toxicity. I chose to use a concentration

of 200 nanomolar rather than 1 micromolar, since I found 200 nanomolar to be the lowest

effective concentration for reducing surface NMDAR expression (see J. Fan's master's

thesis and (Fan et al., 2009), Fig. 6C; also, in pilot experiments, 50 nanomolar

Tat-NR2B9c showed no effect on NMDA-induced surface expression or toxicity – data

not shown). Plates of WT, YAC72 and YAC128 MSNs were processed in parallel to

assess the proportion of apoptotic cells, using the TUNEL stain to identify apoptotic

neurons and the PI stain to identify all nuclei (representative photomicrograph shown in

Fig. 10A and used in J. Fan's master's thesis).

Remarkably, I found that 200 nanomolar Tat-NR2B9c significantly reduced

NMDA-induced cell death in YAC72 and YAC128 MSNs (by ~35% compared with

treatment with NMDA alone or in combination with 200 nanomolar Tat-NR2BAA, as shown in Fig. 10B and J. Fan's master's thesis). Moreover, the proportion of NMDA-induced apoptotic neurons in Tat-NR2B9c-treated YAC72 and YAC128 MSNs was equivalent to that observed for WT MSNs under all three experimental conditions (Tat-NR2B9c had no apparent effect on NMDA-induced apoptosis in WT MSNs). Similar to previous findings from our lab (Shehadeh et al., 2006), I found that the proportion of apoptotic MSNs in groups treated with NMDA alone (without peptides) was significantly higher for YAC72 and YAC128 MSNs compared with WT MSNs (approximately 19% for WT, 31% for YAC72, and 31% for YAC128 MSNs). Importantly, treatment with Tat-NR2BAA had no significant effect on NMDA-treated MSNs. Furthermore, 200 nanomolar Tat-NR2B9c or Tat-NR2BAA alone did not cause significant apoptosis (data not shown). As a control for specificity of the neuroprotective effect of Tat-NR2B9c, we found that 1-hr pre-treatment with 200 nanomolar Tat-NR2B9c did not alter the extent of apoptosis induced by 10 micromolar staurosporine in cultured YAC72 MSNs (Fig. 10C and was also used in J. Fan's master's thesis).

A

TUNEL   PI

NMDA + 200nM 9c

NMDA + 200nM AA

B

C
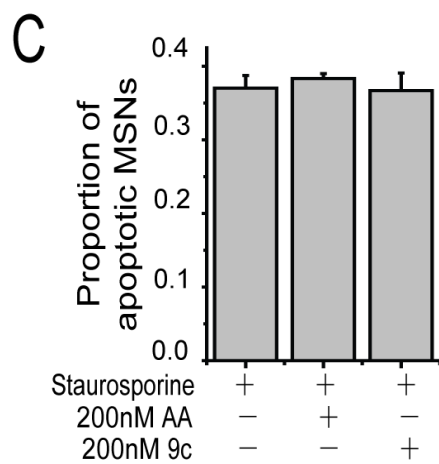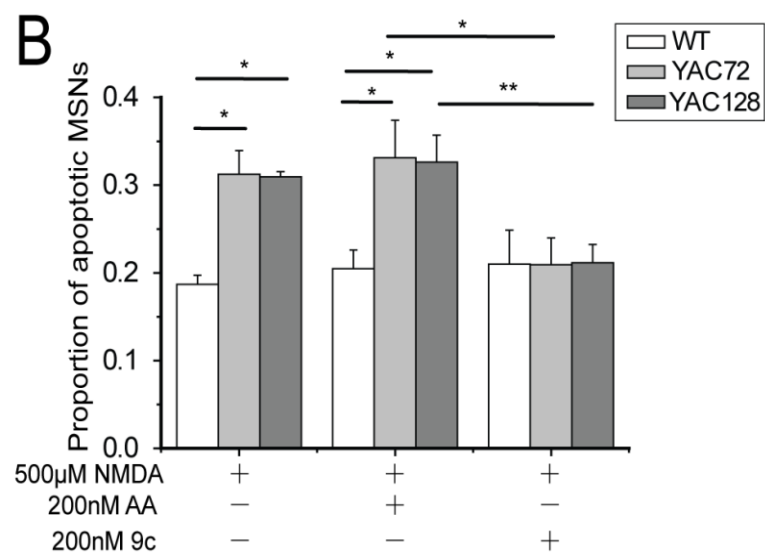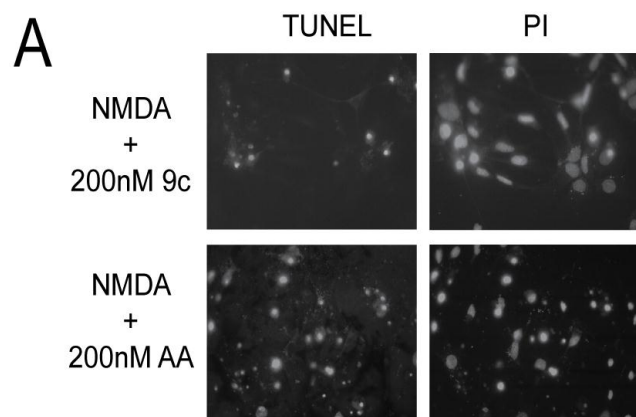
Figure 10. Tat-NR2B9c reduces NMDA-induced toxicity in YAC72, YAC128, but not WT cultured MSNs.

A) Representative photomicrographs showing TUNEL and PI stained YAC128 MSNs pretreated with 200nM Tat-NR2B9c (upper panel) or Tat-NR2BAA (lower panel) for 1hr prior to 10-min exposure to NMDA. **B)** 1-hr pre-treatment with 200nM Tat-NR2B9c peptide reduces NMDA-induced toxicity in YAC72 and YAC128, but not WT cultured MSNs. Average proportion of apoptotic MSNs following pre-treatment with 200nM Tat-NR2B9c and exposure to 500 μM NMDA showed a 37.4±2.7% reduction for YAC72, and 33.6±6.6% reduction for YAC128, compared to 200nM Tat-NR2BAA pretreatment and 500 μM NMDA exposure (mean values calculated after subtraction of percent apoptosis in NMDA-untreated condition for each experiment). Tested by two-way ANOVA, significant for both genotype and treatment, n=4; $F_{2,50}$=6.34, $p<0.005$ for genotype; $F_{5,50}$=63.9, $p<0.0001$ for treatment (*$p<0.05$, **$p<0.01$, by Bonferroni posttests). **C)** 200nM Tat-NR2B peptide 1-hr pretreatment has no effect on 10μM staurosporine-induced cell death of cultured YAC72 MSNs. Mean values calculated after subtraction of percent apoptosis in staurosporine-untreated condition for each experiment, n=3, no significant difference between three groups treated with staurosporine by one-way ANOVA and post-tests.

2.3.5.2 *Tat-NR2B9c protects against NMDA-induced apoptosis in cultured hippocampal neurons but not in mono-cultured or co-cultured WT MSNs*

PSD-95 has been suggested to contribute to NMDAR-mediated cell death by anchoring nNOS in close proximity with NMDAR-mediated calcium influx (Aarts et al., 2002; Sattler and Tymianski, 2000). Tat-NR2B9c peptide has been shown to reduce NMDA-induced excitotoxicity in cultured cortical neurons, presumably by interfering with either the GluN2/PSD-95, or PSD-95/nNOS, interaction (Aarts et al., 2002; Sattler and Tymianski, 2000). We therefore pretreated cultured hippocampal neurons with Tat peptides to determine whether Tat-NR2B9c could protect these neurons from NMDA-induced toxicity. We found that 200nM Tat-NR2B9c significantly reduced NMDA-induced cell death in cultured hippocampal neurons (by ~50% compared with treatment with NMDA alone), and that higher concentrations of Tat-NR2B9c did not provide any further protection (Fig. 11). Notably, the concentration (200nM) of Tat-NR2B9c at which maximum protection (approximately 50%) against NMDA receptor-mediated toxicity is observed correlates well with the concentration (250nM) that disrupts GluN2B/PSD-95 coupling by approximately 50%. Furthermore, treatment of neuronal cultures with Tat-NR2B9c alone at concentrations ranging from 50 – 2000nM did not affect the baseline level of neuronal apoptosis (data not shown).
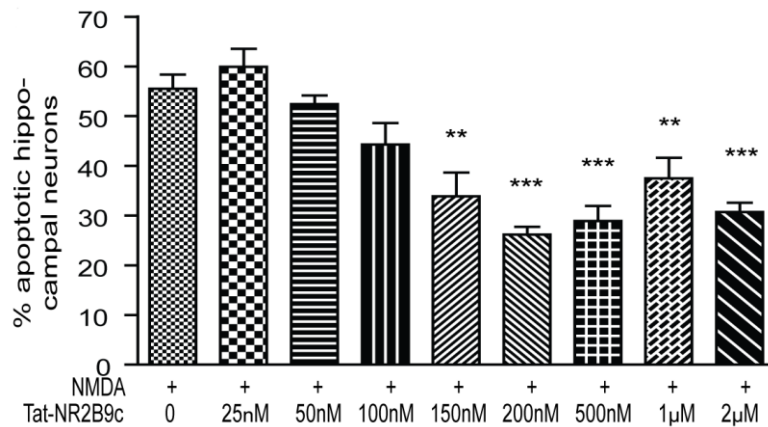
Figure 11. Dose effect of Tat-NR2B9c 1-h pretreatment on 500μM NMDA-induced neuronal death in cultured hippocampal neurons.

Basal percent apoptosis in NMDA-untreated condition was subtracted to calculate percent apoptosis value for each experiment. N= 6, 4, 4, 5, 3, 6, 4, 5, 3 independent experiments from different culture batches, respectively, for each condition from left to right. Significant by one-way ANOVA, **$p<0.01$, ***$p<0.001$, compared with NMDA alone, by Bonferroni posttests.

One possible explanation for the lack of protective effect is that cultured postnatal murine neurons respond differently than embryonic rat neurons to excitotoxic insults. Therefore, we repeated experiments using the Tat-NR2B9c peptide at a range of concentrations in embryonic rat striatal cultures. Peptide concentrations as high as $1\,\mu M$ produced no effect on NMDA toxicity in these embryonic rat striatal neurons (Fig. 12).
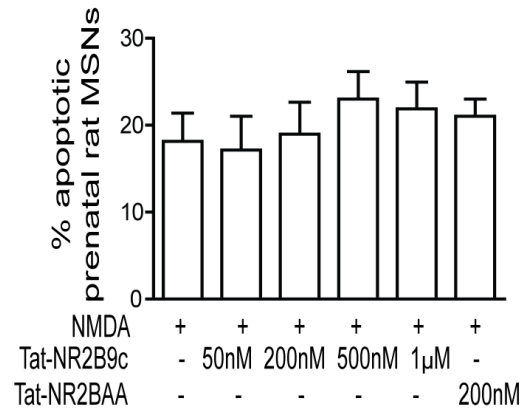
Figure 12. Dose effect of Tat-NR2B9c pretreatment on NMDA-induced apoptosis in embryonic rat cultured striatal neurons.

Basal percent apoptosis in NMDA-untreated condition was subtracted to calculate percent apoptosis value for each experiment. No significance was detected by one-way ANOVA, $p>0.05$, compared with NMDA alone, by Bonferroni posttests. N= 5 independent experiments from different culture batches in which all treatments were performed in parallel in each experiment.

Another concern why cultured striatal neurons might appear resistant to rescue by Tat-NR2B9c is because those used in the above experiments are relatively immature (DIV 9-10) and have few excitatory synapses, due to the paucity of glutamatergic input (~3% of neurons are VGluT-positive in these cultures) (Shehadeh et al., 2006); therefore, the role of PSD-95 in excitotoxicity may be lessened. To test whether striatal neurons that receive appropriate glutamatergic input and are more mature can be rescued by Tat-NR2B9c from NMDA-induced excitotoxicity, we tested this peptide at 200nM and $1\,\mu M$ concentrations in embryonic rat striatal-cortical co-cultures at DIV 14. As previously reported (Segal et al., 2003), these striatal neurons appeared far more spiny than striatal neurons in mono-culture, although this was not quantified. Similar to results in the striatal mono-cultures, we found no protection by Tat-NR2B9c peptide against $100\,\mu M$ or $500\,\mu M$ NMDA-induced toxicity in these more mature, cortically innervated striatal neurons (Fig. 13, data not shown for $500\,\mu M$ NMDA). We conclude that the NMDAR/PSD-95 interaction does not contribute significantly to NMDAR-mediated toxicity observed in WT cultured striatal neurons, unlike in hippocampal and cortical neurons, probably due to intrinsic protein network and signaling differences of these neurons.
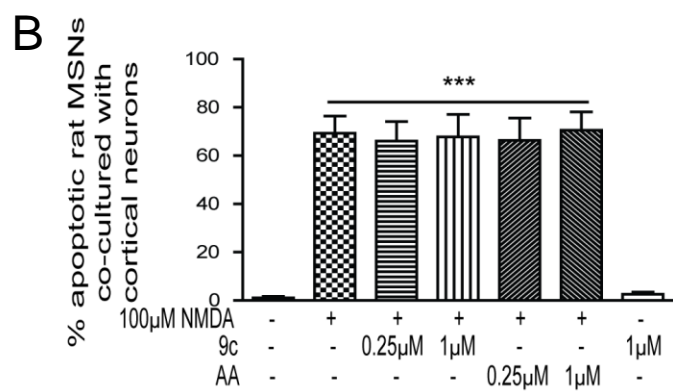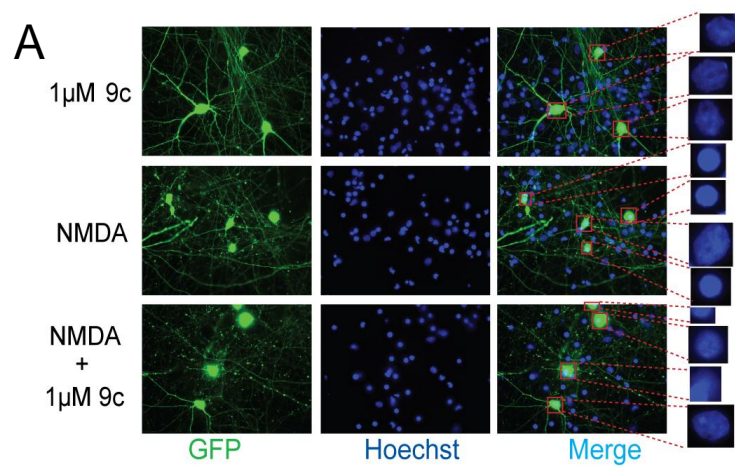
Figure 13. Tat-NR2B9c pretreatment does not protect against NMDA-induced neuronal death in rat striatal neurons co-cultured with cortical cells.

A) Representative photomicrographs showing YFP transfected (striatal cells) and Hoechst stained prenatal rat co-cultured striatal and cortical neurons treated with 1 μM Tat-NR2B9c alone, 100 μM NMDA alone, and 1 μM Tat-NR2B9c plus 100 μM NMDA. Note the beading and/or loss of neuronal processes in the green channel in the middle and bottom panels, in addition to condensed nuclear morphology. **B)** Mean ± SEM percentage apoptotic neurons pretreated with 200nM or 1μM Tat-NR2B9c shows no protection against NMDA toxicity in DIV 14 rat prenatal striatal neurons co-cultured with cortical neurons. Significant when tested by one-way ANOVA, $p<0.001$, when comparing conditions with NMDA treatment to untreated and Tat-NR2B9c only groups, by Bonferroni posttests. N= 4 experiments from different culture batches.

2.3.6 Knock-down of PSD-95 but not SAP102 reduces NMDA-induced apoptosis in YAC72 and YAC128 MSNs but not WT MSNs

SAP102 is a member of the PSD-95 family of MAGUK proteins and shows high homology with PSD-95 in the SH3 as well as PDZ domains (Kim and Sheng, 2004). SAP102 co-immunoprecipitated with htt in striatal tissue from all genotypes of YAC transgenic mice, but no significant differences in co-association of SAP102 and htt were found between genotypes (Fan et al., 2009).

There is always concern about the specificity of Tat-NR2B9c peptide, as it disrupts NMDAR interaction with potentially all MAGUK members, especially with PSD-95 and SAP102 (Cui et al., 2007). To test whether PSD-95 is necessary for elevated NMDA-induced toxicity in YAC HD MSNs, we used siRNA to knock down expression of PSD-95 (see Fig. 14A). After 72 hrs treatment with siRNA, MSNs were exposed to 500 micromolar NMDA with or without 200 nanomolar Tat-NR2B9c. We found that the NMDA-induced toxicity in YAC128 MSNs was reduced to WT levels by PSD-95 siRNA (Fig. 14B and C) and that the effect of Tat-NR2B9c peptide was not additive to that of PSD-95 knock-down. As a control, we found that the non-targeting siRNA did not alter NMDA-induced toxicity in either WT or YAC128 MSNs.

A

WT   YAC128

control   PSD-95   control   PSD-95
siRNA Untreated siRNA   siRNA Untreated siRNA

PSD-95

actin

B

WT   YAC128

NMDA + control siRNA

NMDA + PSD-95 siRNA

TUNEL   Hoechst   TUNEL   Hoechst

C

Legend:
- NMDA
- N + PSD-95 siRNA
- N + PSD-95 siRNA + 9c
- N + control siRNA
- N + control siRNA + 9c
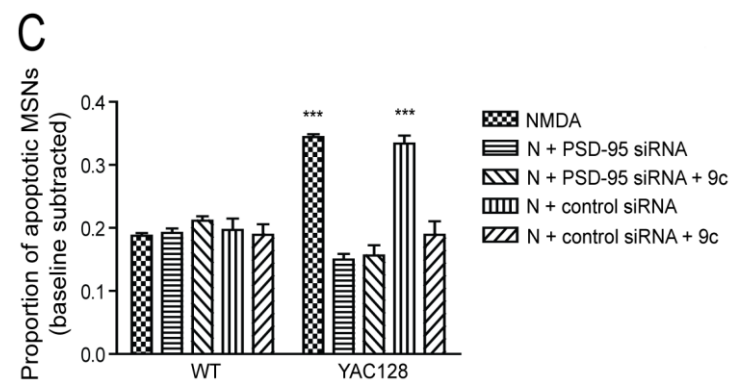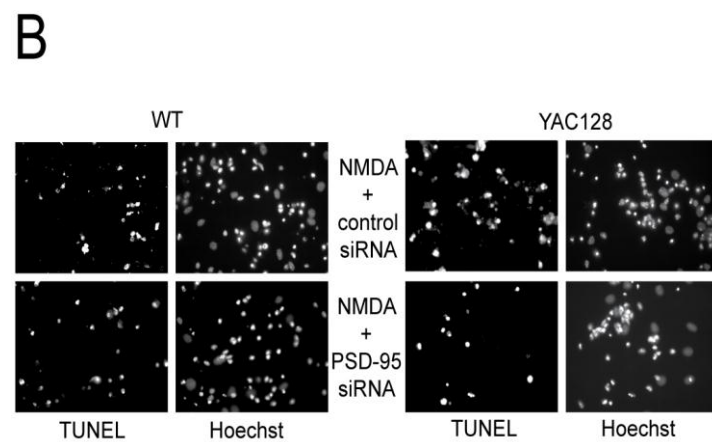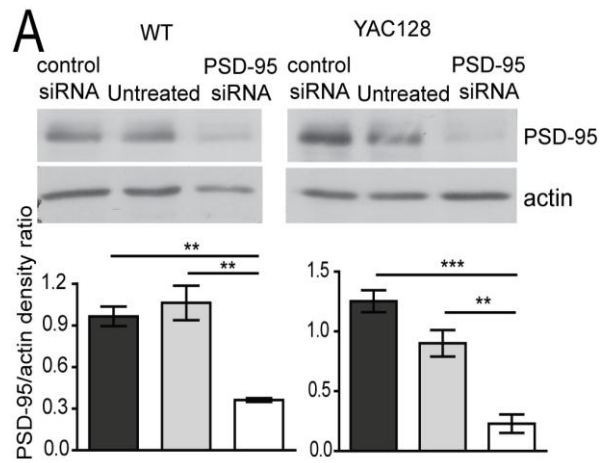
Figure 14. Knock-down of PSD-95 reduces NMDA-induced neuronal death in YAC128 but not WT MSNs.

A) Representative western blots and pooled data showing the knock-down of PSD-95 expression in WT and YAC128 MSNs 72 hours following addition of PSD-95 siRNA but not control siRNA to culture medium. **p<0.01, ***p<0.001, by one-way ANOVA and Bonferroni posttests (n=3 for WT, and YAC128). **B)** Representative photomicrographs showing TUNEL and Hoechst stained WT and YAC128 MSNs pretreated with control siRNA (upper panel) or PSD-95 siRNA (lower panel) 72 hrs prior to 10-min challenge of NMDA. **C)** The effect of PSD-95 knock-down by siRNA on NMDA-induced toxicity in WT and YAC128 MSNs. Average proportion of apoptotic MSNs are shown (mean values calculated after subtraction of percent apoptosis in NMDA-untreated condition for each experiment). Two-way ANOVA revealed significant difference for genotype, treatment and interaction, n=3; $F_{1,20}=22$, $p<0.001$ for genotype; $F_{4,20}=25$, $p<0.001$ for treatment; $F_{4,20}=29$, $p<0.001$ for interaction (***$p<0.001$ by Bonferroni posttests).

To rule out the contribution of SAP102 to the enhanced NMDA-induced toxicity in YAC HD MSNs, I then used siRNA to knock down expression of SAP102 (see Fig. 15A for representative blots). Knock-down of SAP102 expression levels, measured by SAP102/actin ratio, ranged from ~30% to 80% and was significant for both WT and YAC128 in comparing lysates from control siRNA versus SAP102 siRNA-treated cultured MSNs, n=3 and $p<0.05$ by paired t-test for each genotype (data not shown). In contrast, SAP102 siRNA had no effect on NMDA-induced toxicity in both WT and YAC128 MSNs (Fig. 15B), while Tat-NR2B9c peptide still reduced NMDA-induced toxicity of YAC128 to that of WT in both the presence and absence of SAP102 knock-down.
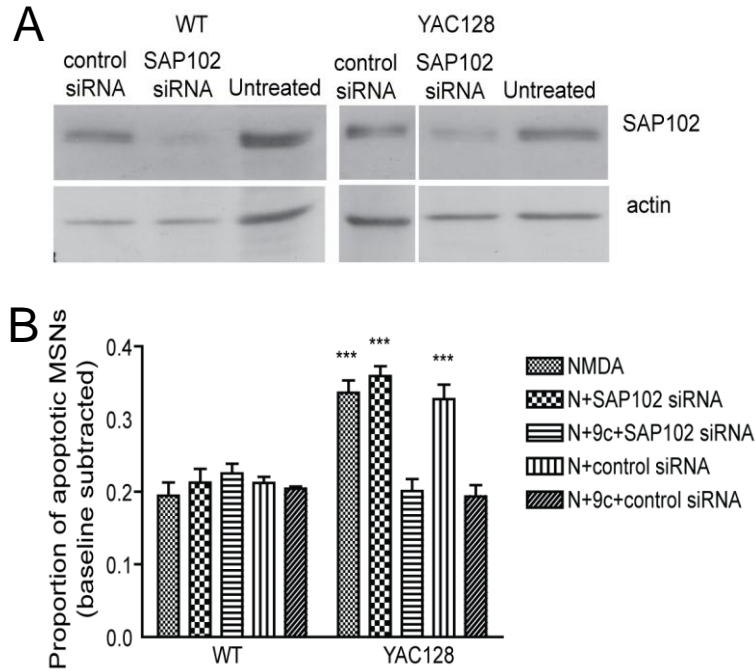
Figure 15. Knock-down of SAP102 has no protection against NMDA-induced neuronal death in YAC128 and WT MSNs.

A) Representative western blots showing the knock-down of SAP102 expression in WT and YAC128 MSNs 72 hours following addition of SAP102 siRNA but not control siRNA to culture medium (n=3 for WT, and YAC128). **B)** The effect of SAP102 knock-down on NMDA-induced toxicity in WT and YAC128 MSNs. Average proportion of apoptotic MSNs are shown (mean values calculated after subtraction of percent apoptosis in NMDA-untreated condition for each experiment). Two-way ANOVA revealed significant difference for genotype, treatment and interaction, n=3 for WT and n=4 for YAC128; $F_{1,25}=52$, $p<0.001$ for genotype; $F_{4,25}=11$, $p<0.001$ for treatment; $F_{4,25}=14$, $p<0.001$ for interaction (***$p<0.001$ by Bonferroni posttests).

2.4 Discussion

Altered NMDA receptor function and increased neuronal sensitivity to excitotoxicity have been proposed as candidate mechanisms for selective neuronal dysfunction and degeneration in HD based on studies in human autopsy brain tissue, as well as cellular and animal models of HD (Albin et al., 1990; Chen et al., 1999b; Fan and Raymond, 2007; Ferrante et al., 1993; Young et al., 1988; Zeron et al., 2002). Attention has focused on GluN2B-containing NMDARs, which are enriched in striatal tissue (Christie et al., 2000; Landwehrmeyer et al., 1995; Li et al., 2003b) and show specificity for regulation by mutant huntingtin in heterologous cell lines and cultured MSNs (Chen et al., 1999b; Fan et al., 2007; Song et al., 2003; Tang et al., 2005; Zeron et al., 2001; Zeron et al., 2002). Here, we demonstrate that polyQ expansion in huntingtin increases interaction between GluN2B-containing NMDARs and PSD-95. Moreover, a peptide that interferes with GluN2B binding to PSD-95, as well as siRNA knock-down of PSD-95, rescue the increased NMDA-induced toxicity in MSNs expressing polyQ-expanded htt, restoring excitotoxic susceptibility to WT levels. Together, our results provide evidence that the GluN2B interaction with MAGUKs plays an important role in enhanced excitotoxicity in YAC HD MSNs. Notably, the peptide used in our studies to uncouple NMDARs from PSD-95 has previously been shown to protect against ischemic neuronal damage in a rodent model of stroke (Aarts et al., 2002).

2.4.1 Interaction of PSD-95 with GluN2B modulates mutant htt enhancement of NMDAR apoptosis

PSD-95 binds directly to htt, and binding is reduced with increasing htt polyQ length (Sun et al., 2001), leading to the hypothesis that expression of polyQ-expanded htt could augment the GluN2B/PSD-95 interaction. Here, we show increased amounts of PSD-95 co-immunoprecipitated with GluN2B from YAC HD mouse striatal tissue, providing direct evidence for an altered GluN2B/PSD-95 interaction. Previous work showed that glutamate-induced excitotoxicity in an NMDAR-transfected neuronal cell line is enhanced by mutant htt expression (Sun et al., 2001), and that this toxicity is influenced by PSD-95-dependent src family kinase-mediated GluN2B phosphorylation (Song et al., 2003). However, these studies did not directly demonstrate that interaction between GluN2B and PSD-95 contributed to mutant htt-enhanced excitotoxicity in striatal neurons.

We have shown that pre-treatment of live, cultured MSNs with a peptide that significantly reduces (by ~50%) the interaction between GluN2B and PSD-95/SAP102 also decreases NMDAR-mediated apoptosis in YAC72 and YAC128 MSNs to WT levels. This effect was specific for NMDA excitotoxicity, since Tat-NR2B9c had no effect on staurosporine-induced apoptosis ((Fan et al., 2009) and J. Fan, master's thesis). Notably, 200 nanomolar Tat-NR2B9c reduces NMDAR surface expression equally well in WT and YAC72 MSNs (the surface to internal GluN1 ratio after treatment with Tat-NR2B9C normalized to that after Tat-NR2BAA treatment was 0.73 ± 0.04 for WT and 0.82 ± 0.03 for YAC72; n=4 and $p<0.05$ by paired t-test for each genotype) ((Fan et al., 2009) and J.

Fan, Master's thesis), whereas the effect on toxicity was exclusive to YAC HD MSNs and not observed in WT MSNs. Therefore, we propose that the Tat-NR2B-mediated reduction in NMDA-induced apoptosis is predominantly a consequence of uncoupling NMDAR activation from downstream, cell death-signaling proteins that would normally be anchored near the receptors by PSD-95 or other MAGUKs. Based on the known association between PSD-95 and the cell death-signaling protein nNOS, and our data showing increasing GluN2B/PSD-95 co-association with htt polyQ expansion, we hypothesized that the GluN2B/PSD-95/htt complex (rather than GluN2B/SAP102/htt) is critical for enhanced excitotoxicity in the YAC transgenic HD mouse model. Indeed, siRNA knock-down of PSD-95, but not of SAP102, reduced NMDAR-mediated toxicity in YAC128 MSNs, with no effect in WT, a result similar (and not additive) to the effect of Tat-NR2B9c. These data are consistent with a critical role of the GluN2B/PSD-95/htt complex in enhanced excitotoxicity in mutant htt-expressing MSNs.

2.4.2 Role of GluN2B interactions with PSD-95 family members in HD

In the YAC transgenic mouse models expressing human htt with expanded polyQ, the middle age onset of motor and cognitive deficits, along with neuronal degeneration that is relatively striatal MSN-specific (Hodgson et al., 1999; Slow et al., 2003; Van Raamsdonk et al., 2005b), are tightly linked with enhanced susceptibility to NMDAR-mediated excitotoxicity; mice expressing htt with 128 polyQ truncated after exon 2 – ("short-stop") (Slow et al., 2005) or modified to eliminate cleavage by caspase-6

("C6R") (Graham et al., 2006a) lack the HD motor and cognitive phenotype, show no striatal degeneration, and are resistant to NMDAR-mediated toxicity.   However, because of the adverse side effects associated with direct NMDAR inhibition, therapy targeted to proteins or molecular mechanisms that mediate the enhanced NMDAR death signaling in HD may be more specific, effective and have fewer side effects. The fact that the Tat-NR2B9c peptide eliminated the excess NMDAR toxicity in YAC72 and YAC128 MSNs without affecting cell death in WT MSNs suggests that uncoupling NMDARs from PSD-95 (and/or other MAGUKs) may be a target for therapy in HD.

2.4.3 Sensitivity of GluN2A and GluN2B to Tat-NR2B9c interference with binding to PSD-95

We found that a 1-hour treatment of live cultured neurons with 250nM Tat-NR2B9c reduces the GluN2B/PSD-95 interaction by ~50%, but does not interfere with GluN2A/PSD-95 binding (Fig. 9), while 1 μM Tat-NR2B9c is required to disrupt the GluN2A/PSD-95 interaction to the same extent (data not shown, see Fig 1A and C in (Fan et al., 2010)). Our results contrast with a report that the Tat-NR2B9c IC50 value is lower for PSD-95 PDZ2 binding to GluN2A than for GluN2B – 0.5 μM and ~8 μM, respectively (Cui et al., 2007). However, the in vitro assay used in that study does not reproduce physiological conditions in live neurons. Specifically, the GluN2 PDZ ligand binding affinity may be affected by other protein binding partners or post-translational modifications close to this domain. For example, phosphorylation of Ser1480 by casein

kinase II (CK2) within the GluN2B C-terminal PDZ ligand (ESDV) disrupts interaction of GluN2B with the PDZ domains of PSD-95 and SAP102 (Chung et al., 2004). Furthermore, binding of proteins to sites near the distal C-terminal ESDV, such as GluN2B 1472-1475 YEKL and GluN2A 1320-1321 dileucine (LL) that mediate binding to the AP2 complex (Lau and Zukin, 2007; Lavezzari et al., 2004), could affect PDZ-containing protein interaction with ESDV differently in GluN2A and GluN2B. In addition, a recent study identified distinct accessory PDZ binding motifs within GluN2A and GluN2B, which may differentially modulate PSD-95 interaction with these two subunits (Cousins et al., 2009).

Our data demonstrate that 4-fold higher concentrations of Tat-NR2B9c are needed to achieve similar disruption of the GluN2A/PSD-95 compared with GluN2B/PSD-95 complex (1 μM vs. 0.25 μM, respectively) in live cultured hippocampal neurons. Consistent with this finding, a previous study showed ex vivo treatment with 10 μM Tat-NR2B9c reduced co-immunoprecipitation of PSD-95 with GluN2B, but not with GluN2A, in rat forebrain tissue lysates (Aarts et al., 2002). Furthermore, in vivo intrastriatal injection of 500 μM Tat-NR2B9c selectively dissociated the GluN2B/PSD95 but not GluN2A/PSD-95 complex (Gardoni et al., 2006a), and 1 μM Tat-NR2B9c peptide disrupted PSD-95 co-immunoprecipitation with GluN2B but not GluN2A in hippocampal slices (Gardoni et al., 2009b). Because of the differences in methods of application of Tat peptides and membrane fractions analyzed, it is difficult to directly compare results with those of our study. In particular, the effective concentration of Tat-NR2B9c required to

disrupt GluN2A/PSD-95 binding may not have been achieved by intrastriatal peptide injection or incubation of acute brain slices with 1 μM peptide in the previous studies.

It is interesting that treatment of live hippocampal neurons with Tat-NR2B9c concentrations of 250nM and 1 μM produced identical results in dissociating 50% of PSD-95 from GluN2B. Although additional PDZ binding sites proximal to the C-terminal PDZ ligand in GluN2B (Cousins et al., 2009) may contribute to limiting the efficacy of Tat-NR2B9c in disrupting PSD-95 binding, another factor may be that there are distinct populations of NMDARs with respect to subcellular compartments, to which Tat-NR2B9c has differential access. These populations could correspond to surface extrasynaptic versus synaptic receptors, as well as those in intracellular membranous compartments such as the Golgi or endosomes. It is possible that lower concentrations of Tat-NR2B9c (e.g., < 1 μM) are largely excluded from the postsynaptic density. Consistent with this idea, further increase in Tat-NR2B9c to 10 μM reduces PSD-95 co-IP with GluN2B by 70 ± 13% (n=4). Lower concentrations of Tat-NR2B9c may access mainly surface extrasynaptic NMDARs and those in intracellular vesicular compartments; both of these populations have been shown to interact with PSD-95, PSD-93, and SAP102 (Petralia et al., 2010; Sans et al., 2003). In fact, a recent study indicates surface NMDARs in hippocampal neurons are distributed equally between extrasynaptic and synaptic sites, and a substantial proportion of the surface extrasynaptic NMDARs co-localize with PSD-95 family members (Petralia et al., 2010). However, the fact that maximal protection by Tat-NR2B9c against NMDA-induced toxicity in hippocampal

neurons was also ~50% in our paradigm may be, in part, explained by the contribution of NMDAR cell death signaling via JNK pathways, independent of the NMDAR/PSD-95/nNOS complex (Soriano et al., 2008).

2.4.4 Distinct roles of PSD-95 and SAP102 in HD

The highly homologous MAGUK proteins SAP102 and PSD-95 both bind GluN2 subunits and associate in a complex with htt, yet show differential interactions with polyQ-expanded htt and play distinct roles in mhtt-induced alterations of NMDAR trafficking and signaling (data shown in J. Fan's master's thesis). Although PSD-95 and SAP102 bind GluN2 and htt through PDZ and SH3 domains, respectively, other regions of these MAGUKs likely affect the strength of this binding. Both PDZ1 and PDZ2 contribute to MAGUK interactions with GluN2 subunits (Kornau et al., 1995), while regions upstream of the GluN2 C-terminal PDZ ligand, that differ between GluN2A and GluN2B, contribute to interaction of these subunits with PSD-95 (Cousins et al., 2008) and may explain differences in strength of binding to various MAGUKs (Cui et al., 2007). Similarly, sequence differences around the SH3 domain of PSD-95 and SAP102 may contribute to differential interaction of these two MAGUKs with the polyproline of htt.

2.4.5 Summary

The interaction between NMDARs and PSD-95/nNOS has emerged as a major contributor to excitotoxicity in cultured cortical and hippocampal neurons, as well as to

ischemic damage in a rodent stroke model (Aarts et al., 2002; Sattler and Tymianski, 2000; Sattler et al., 1999; Soriano et al., 2008). Here, we demonstrate for the first time that the interaction between NR2B-containing NMDARs and PSD-95 increases in striatal tissue expressing huntingtin with expanded polyQ. Moreover, a peptide at a concentration that interferes with NR2B binding to SAP102 and PSD-95 rescues the enhanced NMDA-induced toxicity in MSNs expressing polyQ-expanded htt, as well as in WT hippocampal cultures, but not in WT striatal cultures. Together, our results provide evidence that the NR2B interaction with MAGUKs plays an important role in enhanced excitotoxicity in YAC HD MSNs. However, the mechanisms underlying neuronal-specific or HD-specific protection against NMDA toxicity by disruption of the NMDAR/PSD-95 remain unknown.

3 Contribution of signaling pathways downstream of PSD-95 and NMDAR association in HD pathology[2]

3.1 Introduction

Members of the PSD-95 family of MAGUKs act as scaffolds that facilitate signaling by tethering enzymes close to glutamate receptors (Fujita and Kurachi, 2000). The GluN2A or GluN2B C-terminal tSXV motif binds to the second PDZ domain in PSD-95 family members (Kornau et al., 1995; Niethammer et al., 1996). This interaction has been shown to contribute to toxic signaling downstream of NMDAR activation; a peptide that interferes with the binding of MAGUKs to NMDARs rescues hippocampal and cortical neurons from NMDA-induced excitotoxicity *in vitro* and ischemic neuronal death *in vivo* (Aarts et al., 2002; Soriano et al., 2008). Neuronal protection mediated by this peptide correlates well with reduced activation of nNOS, which also binds to the PDZ2 of PSD-95. Less is known about the mechanisms of excitotoxic death in striatal neurons, which are the targets of neurodegeneration in a variety of neurological disorders as well as in response to ischemia. Therefore, one goal of experiments described in this

---

[2] Part of this chapter has been published: J. Fan, C. M. Cowan, L. Y. J. Zhang, M. R. Hayden, and L. A. Raymond. Interaction of postsynaptic density protein-95 with N-Methyl-D-Aspartate Receptors influences excitotoxicity in the YAC mouse model of Huntington's disease. *J Neurosci.* Sep 2; 29(35): 10928-38, 2009. Article content reproduced here with permission from Society of Neuroscience. Copyright 2009. Other parts in: J. Fan, O. C. Vasuta, L. Y. J. Zhang, L. Wang, A. George, L. A. Raymond. N-Methyl-D-Aspartate receptor subunit- and neuronal-type dependence of excitotoxic signaling through postsynaptic density 95. *J Neurochem.* 115, 1045-56, 2010. Article content reproduced here with permission from John Wiley and sons. Copyright 2010. Additional parts are included in a manuscript under review at the *Neurobiology of Disease*.

chapter was to begin to investigate the signaling pathways downstream of NMDA receptor activation mediating apoptotic death in cultured striatal neurons.

PSD-95 may contribute to NMDAR-mediated excitotoxicity by stabilizing surface NMDAR expression and anchoring signaling proteins such as nNOS near NMDAR-mediated calcium influx (Roche et al., 2001; Sattler and Tymianski, 2000; Sattler et al., 1999). The NMDAR-PSD-95-nNOS pathway is critical for excitotoxic cell death in a rodent stroke model (Aarts et al., 2002), and this pathway is down regulated with development of resistance to NMDAR toxicity in the N171-82Q transgenic mouse model of HD (Jarabek et al., 2004). As shown in the previous chapter and other publications(Graham et al., 2009; Shehadeh et al., 2006; Tang et al., 2005; Zeron et al., 2002), YAC72 and YAC128 HD mouse models show enhanced susceptibility to excitotoxicity at early stage of disease. Notably, in striatal tissue from these YAC mice, GluN2B binding with PSD-95 is increased with increasing htt polyQ length and contributes to elevated NMDA toxicity in cultured MSNs (Fan et al., 2009). However, the mechanism by which mutant htt-enhanced NMDAR/PSD-95 binding contributes to increased striatal NMDA toxicity in HD is not known.

MAPKs form a superfamily of serine/threonine protein kinases that are highly responsive to diverse extracellular signals in adult mammalian neurons, including activation of NMDARs (Haddad, 2005; Wang et al., 2007; Wang et al., 2004). In particular, the ERK, p38, and JNK MAPKs are differentially activated by glutamate receptor subtypes, play distinct roles in regulating synaptic plasticity, gene expression,

and neuronal survival, and have emerged as targets for neurodegenerative diseases (Haddad, 2005; Harper and Wilkie, 2003; Wang et al., 2004).

Activation of extrasynaptic NMDARs triggers nuclear translocation of the death-program transcription factor FoxO3a, which can be reduced by either p38 or JNK inhibitors in hippocampal neurons (Dick and Bading, 2010). Consistent with this finding, recent data show that two distinct excitotoxic pathways contribute to NMDA-induced cell death in cortical neurons: one via p38 MAPK, which relies on NMDAR-PSD-95 binding and can be disrupted by Tat-NR2B9c without impacting pro-survival signaling; and the other via JNK, which is not PSD-95- dependent and also plays a role in non-neuronal cell death (Soriano et al., 2008). To investigate the mechanism of Tat-NR2B9c protection in YAC HD mice, we determined whether p38 MAPK and/or JNK pathways downstream of NMDAR-PSD-95 signaling is altered by mutant htt expression and contributes to enhanced excitotoxicity in MSNs of YAC HD mice.

3.2 Methods and materials

3.2.1 Brain slices preparation and treatment

To minimize suffering, 2 month old WT and YAC128 mice were killed by decapitation following deep halothane vapour anaesthesia. The brains were rapidly removed and immersed in oxygenated (95% O_2–5% CO_2), chilled (~ 4 ℃) artificial cerebrospinal fluid (ACSF). Parasagittal cortico-striatal slices 300μm thick were cut on a vibratome (Leica VT1000) and placed in a 10cm culture dish containing continuously oxygenated ACSF at RT for > 1 h prior to treatment. Slices were transferred to a 6cm culture dish containing continuously oxygenated ACSF with 200nM Tat peptides for a 1-h pretreatment and then a 10-min 500μM NMDA treatment at RT. Slices were washed in ACSF for 5 min prior to harvest.

3.2.2 Tissue and brain slices sample preparation and lysis

Brains of 8 weeks-old WT and YAC mice or brain slices after treatments were quickly dissected to obtain striatal tissues on ice in cold PBS with 5mM EDTA and EGTA and homogenized in 1% NP-40-containing lysis buffer (50 mM Tris-pH8.0, 150 mM NaCl, 1 mM EDTA, 1 mM EGTA, 1 mM PMSF, 2 μg/mL aprotinin, 2 μg/mL leupeptin, 4 μg/mL pepstatin A, 30 mM NaF, 40 mM β–glycerophosphate, 20 mM sodium pyrophosphate, 1 mM sodium orthovanadate, in Milli-Q water) containing protease (Santa Cruz biotechnology, Santa Cruz, CA, U.S.A.), and phosphatase (Roche diagnostics, Laval, QC, Canada) inhibitor cocktails. The slice samples were solubilized by

ultrasonication and rotated > 2 hrs at 4 ℃.

3.2.3 Western blotting

The total protein concentration of the striatal tissue lysates, slice lysates, as well as

PSD and non-PSD fractions was assessed using the Bicinchoninic Acid (BCA) protein

assay (Pierce, Rockford, IL, USA). Samples containing 8-12 μg protein were heated

(5-10min, 95-97 ℃) in 3X protein sample buffer (6 % SDS, 0.4 mM Tris pH 6.8, 30 %

glycerol, pyronin y, 70 mg/ml dithiothreitol). Proteins were separated in 8% (w/v)

SDS-PAGE gels and transferred to PVDF membranes using semi-dry or traditional

electrophoresis (BioRad, Hercules, CA, USA). After transfer, membranes were incubated

overnight at 4 ℃ with one of the following primary antibodies: goat anti-actin antibody

(sc-1616; Santa Cruz, CA, USA; 1:1500 dilution), rabbit anti-phospho-p38

(Thr180/Tyr182) (D3F9) antibody (#4511; Cell Signaling, MA, USA; 1:200 dilution),

rabbit anti-phospho-c-Jun (Ser73) (D47G9) antibody (#3270; Cell Signaling, MA, USA;

1:200 dilution). Then blots were incubated with HRP-coupled secondary antibody

(Amersham, Pittsburgh, PA, USA; 1:8000 dilution; 1-2hs, room temperature). Blots were

subsequently visualized using ECL, (Amersham) and exposure to film (BioLab, Kodak).

Some of the blots were then directly reprobed by incubating at 4 ℃ overnight with one of

the following antibodies: mouse anti-PSD-95 (75-028, Neuromab, Davis, CA, USA;

1:2000 dilution); mouse anti-synaptophysin (S5768, Sigma, Ontario, Canada; 1:1000

dilution); mouse anti-p38α/β (A-12) (sc-7972, Santa Cruz, CA, USA; 1:200 dilution);

mouse anti-c-Jun (B-1) (sc-166540, Santa Cruz, CA, USA; 1:200 dilution).   Proteins were visualized using AP-conjugated secondary antibody (S372B, Promega, Madison, WI, USA; 1:10,000 dilution) and the Lumi-phos WB chemiluminescent substrate (Pierce, Rockford, IL, USA) detection system.

We used phospho-c-Jun/c-Jun as a read-out for JNK activation, because others have shown that phospho-JNK antibodies detect a pool of active JNK1 under basal conditions in CNS neurons, which does not influence c-Jun phosphorylation or reflect elevation of stress activated JNK signaling (Coffey et al., 2002). For some experiments detecting p38 activation in striatal tissues, the lysates were divided into two equal parts and loaded to the same gel with the molecular weight markers loaded in between. The blots were then cut along ~40-45 KD molecular weight and also along the molecular weight marker ladder. The parts of blots were probed using mouse anti-phospho-p38 (Thr180/Tyr182) (28B10) (#9216; Cell Signaling, MA, USA; 1:200 dilution) antibodies or mouse anti-p38α/β (A-12) (sc-7972) antibodies, and goat anti-β-Tubulin (N-20) (sc-9935, Santa Cruz, CA, USA; 1:1000 dilution) antibody as a loading control. For data analysis, the densities of bands were quantified using Image-J (NIH).

3.2.4 Co-immunoprecipitation

Parasagittal cortico-striatal slices of 6-8 week-old WT and YAC128 mice were pretreated for 1 hour with 200nM Tat-NR2B9c or Tat-NR2BAA (control peptide) or nothing in the ACSF, then the striatum tissue was harvested and lysed in 0.8%

TritonX-100 + 0.1% SDS or 1% NP-40-containing lysis buffer with protease and phosphatase inhibitors, and solubilized by ultrasonication. The lysates were pre-cleared with equilibrated 50% Protein A/G beads for 1 hour at 4 ℃, and then incubated by constant rotating overnight with 50% Protein A/G beads and anti-PSD-95 antibodies (or without antibody for no antibody controls). Beads of each sample were then washed with Tris Wash Buffer (50 mM Tris-pH 7.4, 150 mM NaCl, 1 mM EDTA, 1 mM EGTA, 0.8% TritonX-100 + 0.1% SDS or 1% NP40 in Milli-Q water) and heated at 95-99 ℃ in 3X PSB.

Paired samples were run on 8% SDS-PAGE and then transferred from gels to PVDF membranes and subjected to immunoblotting. The blot was cut into two parts along the 150 kDa marker and probed with anti-GluN2B (Affinity BioReagents, Rockford, IL, USA, MA1-2014) and anti-PSD-95 (Affinity BioReagents, Rockford, IL, USA, MA1-045) antibodies respectively. Protein bands were visualized with HRP-ECL system (GE Healthcare Bio-Sciences, Piscataway, NJ, USA). Densitometry of resulting bands was performed using ImageJ.

To measure the co-IP of associated proteins, the levels of associated GluN2B were normalized to the levels of PSD-95 immunoprecipitated with anti-PSD-95 in the same lane of the gel. In both sets of experiments band densities were compared between treatment conditions on the same blot and same exposures. Notably, similar reduction of the co-IP of GluN2B and PSD-95 proteins after Tat-NR2B9c pretreatment compared to after Tat-NR2BAA pretreatment were observed using either WT or YAC128 brain slices

(comparing results from n=3 experiments with each genotype).

3.2.5 NMDA-induced toxicity

Postnatal mouse striatal neurons (DIV 9) cultured in 24-well plates were pretreated for 1 hour with 200nM Tat-NR2B9c, and/or 100μM or 1mM Nω-Nitro-L-arginine (N-Arg, nNOS inhibitor, from Sigma-Aldrich), and/or SB-239063 (p38 inhibitor, from Sigma-Aldrich), and/or SP-600125 (JNK inhibitor, from Sigma-Aldrich), then incubated with or without 500μM NMDA for 10 min. After NMDA treatment, striatal cultured neurons were washed once with warm plating medium and then incubated in conditioned plating medium (without Tat peptides or p38, JNK inhibitors) for 24 hours. Then cells were washed with PBS once and fixed with 4 % PFA for 30 minutes.

3.2.6 TUNEL assay and assessment of apoptosis

Fixed neuronal cultures on coverslips were numbered according to different conditions and coded before staining to ensure that the operator was blinded during the subsequent processing and analysis of immunofluorescence. Striatal neuronal cultures were stained with TUNEL (Roche) reagent and 10μM Hoechst 33342, and the percentage of apoptotic cell death was assessed as described previously (Fan et al., 2009) as well as in the method of Chapter 2.

3.2.7 Cyclic guanosine monophosphate (cGMP) assay

On DIV 9, cultured MSNs were pretreated 1 hr with N-Arg and/or Tat-NR2B9c, or Ifenprodil (IFN), then incubated in warm BSS with or without 500 μM NMDA for 1 min, then immediately forwarded to Amersham cGMP Enzymeimmunoassay Biotrak (EIA) System kit (GE Healthcare, UK, RPN226), as per manufacturer's instructions. The concentrations of cGMP in 96-well plates were determined by a microplate-reader (Multiskan Ascent, Labsystems) at 630nm.

3.2.8 Data analysis

Figures, tables, and statistical analyses were generated using Microsoft Excel, ImageJ, Prism, Adobe Photoshop or Adobe Illustrator software. Data or bars are presented as the mean±SEM. Significant differences were determined using the unpaired or paired, two-tail Student's t-test, one-way ANOVA or two-way ANOVA, as appropriate.

3.3 Results

3.3.1 nNOS inhibitor reduces NMDA-induced apoptosis in YAC72 and YAC128 MSNs but not WT MSNs

PSD-95 has been postulated to contribute to NMDAR-mediated excitotoxicity by anchoring signaling proteins such as nNOS in close proximity with NMDAR-mediated calcium influx (Aarts et al., 2002; Sattler and Tymianski, 2000). Furthermore, a previous study showed that NO released from nNOS-interneurons could promote release of intracellular calcium from mitochondria in MSNs (Horn et al., 2002), and thus contribute to NMDA-induced cell death. Therefore, we treated cultured MSNs with an nNOS inhibitor (N-Arg) and/or Tat peptides to determine whether the effect of Tat-NR2B9c is equivalent to that of an nNOS inhibitor on NMDA-induced toxicity. Interestingly, we found that the nNOS inhibitor has a similar effect as 200 nanomolar Tat-NR2B9c on NMDA-induced cell death in WT, YAC72 and YAC128 MSNs, and the combination of these two treatments did not show any significant additive effect (as shown in Fig. 16A and B). This finding suggested that inhibition of nNOS signaling could contribute to the protection afforded by Tat-NR2B9c against NMDAR-dependent toxicity in YAC HD MSNs.

A

WT   YAC128

TUNEL   Hoechst   Merge   TUNEL   Hoechst   Merge

NMDA

NMDA
+
N-Arg

NMDA
+
9c + N-Arg

B

Proportion of apoptotic MSNs

- NMDA
- N+9c
- N+9c+N-Arg
- N+N-Arg

WT   YAC72   YAC128

***
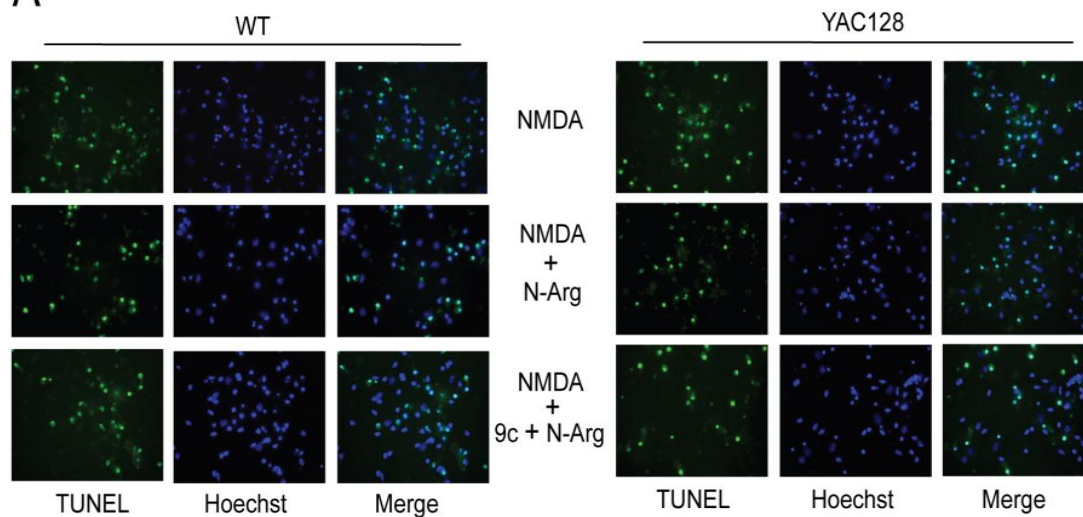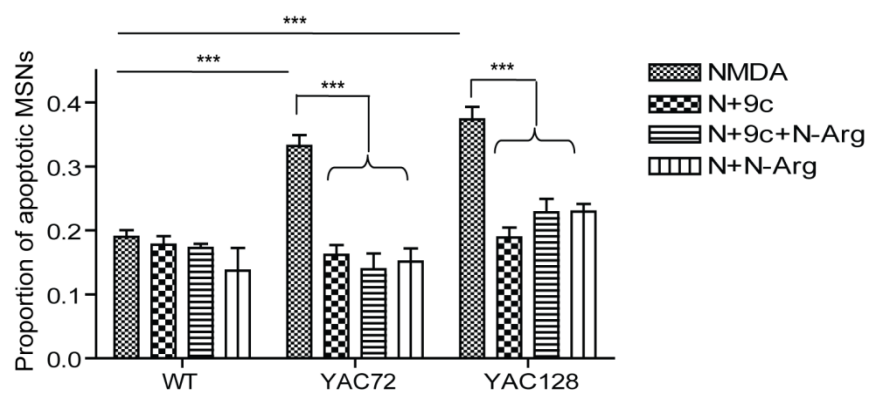
Figure 16. Protection against NMDAR-mediated neuronal death by N-Arg (nNOS inhibitor) and Tat-NR2B9c in cultured YAC72 and YAC128, but not WT striatal neurons.

A) Representative photomicrographs showing TUNEL and Hoechst stained WT and YAC128 MSNs pretreated with 100 μM N-Arg (middle panel), and 200nM Tat-NR2B9c plus 100 μM N-Arg (lower panel) for 1hr prior to 10-min exposure to NMDA. **B)** Average proportion of apoptotic MSNs following pre-treatment with 100μM N-Arg and/or 200nM Tat-NR2B9c and exposure to 500μM NMDA showed a similar reduction in YAC72 and YAC128 MSNs, and no significant reduction in WT MSNs (mean values calculated after subtraction of percent apoptosis in NMDA-untreated condition for each experiment). Tested by two-way ANOVA, significant for both genotype and treatment, n=6; $F_{1,42}=48$, $p<0.0001$ for genotype; $F_{5,42}=70$, $p<0.0001$ for treatment $F_{5,42}=9$, $p<0.0001$ for interaction (***$p<0.001$, by Bonferroni post-tests).

3.3.2 Protection against NMDAR-mediated death by Tat-NR2B9c and nNOS inhibitor in primary cultured hippocampal neurons

Tat-NR2B9c peptide has been shown to reduce NMDA-induced excitotoxicity in cultured cortical neurons, presumably by interfering with either the GluN2/PSD-95, or PSD-95/nNOS, interaction (Aarts et al., 2002; Sattler and Tymianski, 2000). However, WT postnatal mouse cultured MSNs were not protected against NMDA toxicity by treatment with 100μM N-Arg and/or 200nM Tat-NR2B9c (Fig. 16). To confirm that this lack of protection is due to neuronal-type differences and not experimental factors, we treated cultured hippocampal neurons with Tat peptides and/or N-Arg to determine whether Tat-NR2B9c could protect these neurons from NMDA-induced toxicity and whether this protection is occluded by, or additive to, that afforded by the nNOS inhibitor.

As previously shown (Fig. 11), we confirmed that 200nM Tat-NR2B9c significantly reduced NMDA-induced cell death in cultured hippocampal neurons (by ~50% compared with treatment with NMDA alone). Furthermore, the percentage of NMDA-induced apoptotic neurons in the Tat-NR2B9c-treated condition was equivalent to that observed with 100 μM of the nNOS inhibitor, N-Arg (Fig. 17A, B). Combined pre-treatment with Tat-NR2B9c and N-Arg showed slightly more protection against NMDA-induced apoptosis, but this was not significantly different from Tat-NR2B9c or N-Arg treatment alone. Both 100 μM (Fig. 17A, B) and 500 μM (Fig. 11) NMDA caused a similar percentage of cell death (~ 60%) in hippocampal cultures.

We conclude that the NMDAR/PSD-95/nNOS pathway does not contribute

significantly to NMDAR-mediated toxicity observed in cultured WT striatal neurons,

unlike in hippocampal and cortical neurons.

A

Hoechst   TUNEL

NMDA

N + 200nM 9c

N + N-Arg

N + 200nM 9c + N-Arg

B

NMDA	+	+	+	+
N-Arg	-	-	+	+
200nM 9c	-	+	+	-

115
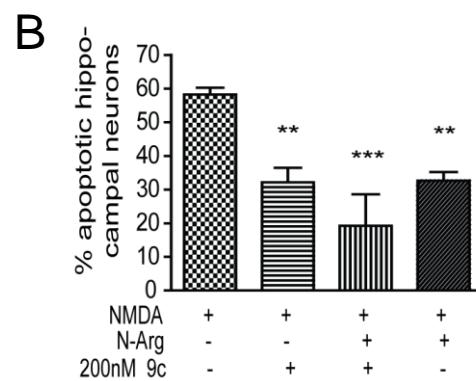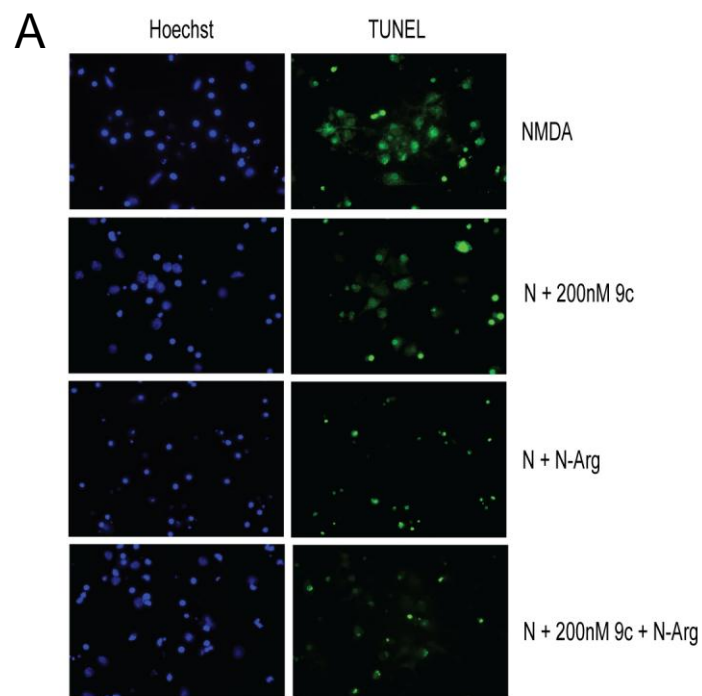
Figure 17. Protection against NMDAR-mediated death by N-Arg (nNOS inhibitor) and Tat-NR2B9c in primary cultured hippocampal neurons.

A) Representative photomicrographs showing TUNEL and Hoechst stained hippocampal neurons pretreated with 200nM Tat-NR2B9c alone, 100 μM N-Arg alone, and 200nM Tat-NR2B9c plus 100 μM N-Arg for 1hr prior to and during 10-min exposure to 100μM NMDA. **B)** Bar graphs showing mean percentage apoptotic neurons under each condition. Note that Tat-NR2B9c (200nM) and N-Arg (100μM), alone or in combination, provide similar protection (approximately 50%) against NMDA toxicity. Mean values were calculated by subtraction of percent apoptosis in NMDA-untreated condition for each experiment. N=3 independent experiments from different batches of hippocampal cultures. Significant when tested by one-way ANOVA, $**p<0.01$, $***p<0.001$, compared with NMDA alone, by Bonferroni posttests. Nω-Nitro-L-arginine, N-Arg; NMDA, N.

3.3.3 NMDA-induced nNOS activity is independent of NMDAR/PSD-95 interaction in cultured striatal neurons from WT and YAC72

To further assess a role for nNOS signaling in the effect of Tat-NR2B9c on NMDA toxicity, we repeated these treatments and measured the cGMP production as a read-out for nNOS activity. We found that NMDA-stimulated cGMP production was abolished by 100 micromolar N-Arg, partially reduced by ifenrodil, and not significantly affected by either 200 nanomolar or 1 micromolar Tat-NR2B9c (as shown in Fig. 18A, B). Thus, interference with the nNOS pathway cannot explain the protective effect of Tat-NR2B9c on NMDA toxicity in YAC HD MSNs.

A

B
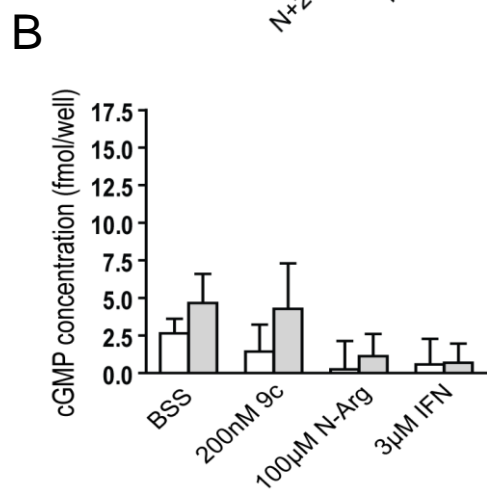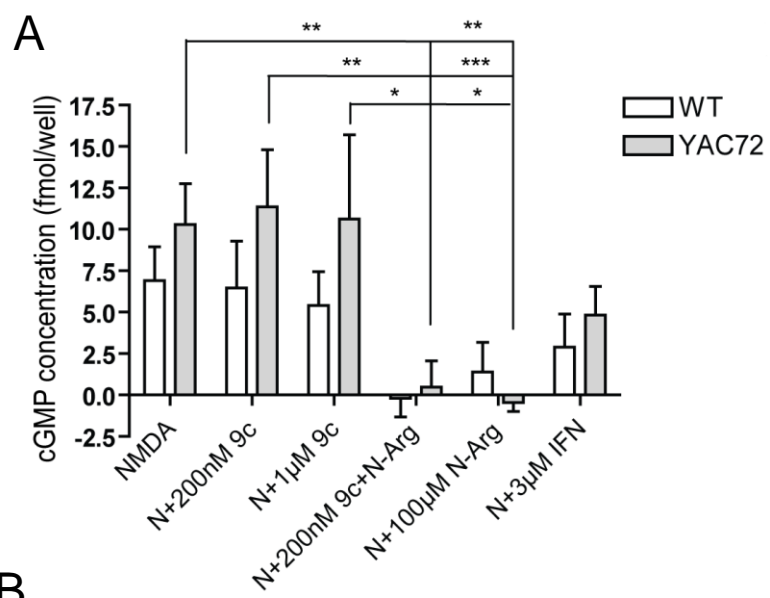
Figure 18. The NMDA-induced cGMP assay on cultured WT and YAC72 MSNs.

A) The 500µM NMDA-induced cGMP production in WT and YAC72 MSNs following treatment with 100µM N-Arg and/or 200nM/1µM Tat-NR2B9c, or 3µM Ifenprodil (IFN). Significance was tested by two-way ANOVA, n=5 for WT and n=6 for YAC72; $F_{1,46}=3$, $p>0.05$ for genotype; $F_{5,46}=6$, $p<0.0001$ for treatment; $F_{5,46}=0.7$, $p>0.05$ for interaction (*$p<0.05$, **$p<0.01$, ***$p<0.001$, by Bonferroni post-tests). **B)** Basal cGMP production in WT and YAC72 MSNs following treatment with 100µM N-Arg and/or 200nM/1µM Tat-NR2B9c, BSS, or 3µM Ifenprodil. Significance tested by two-way ANOVA, n=5 for WT and n=6 for YAC72; $F_{1,33}=1$, $p>0.05$ for genotype; $F_{3,33}=1$, $p>0.05$ for treatment; $F_{3,33}=0.2$, $p>0.05$ for interaction.

3.3.4 Increased basal activation of p38 and JNK MAPK in striatal tissues of pre-symptomatic YAC128 mice

Previous studies have shown that stimulation of extrasynaptic NMDARs activates cell death pathways, including p38-MPAK and JNK (Hardingham, 2006; Soriano and Hardingham, 2007), whereas synaptic NMDAR stimulation signals cell survival. However, NMDAR activation of the p38 MAPK cell death pathway is dependent on the GluN2B-PSD-95 interaction whereas the JNK pathway is not (Soriano et al., 2008). Here, I tested whether the increased interaction between PSD-95 and GluN2B-containing NMDARs might result in altered baseline activity levels of p38 and/or JNK cell death pathways in YAC128 striatal tissue.

We found that the basal levels of both activated p38 and JNK MAPKs were elevated in YAC128 mice striatal tissue compared with YAC18 at 8-weeks of age (Fig. 19 and 20). Activated p38 levels in the YAC128 striatum were significantly higher than the other three genotypes, including YAC72 mice, which also exhibit features of the HD phenotype, though at older ages and to a milder extent than YAC128 mice (Hodgson et al., 1999; Slow et al., 2003) (Fig. 19A, B). In contrast, activated JNK levels are elevated in the striatum of both YAC72 and YAC128 mice compared YAC18 levels (Fig. 20A, B). These data demonstrate a positive correlation between JNK activation and the polyQ length of huntingtin, consistent with the impaired ability of the JNK activator MLK2 to bind huntingtin as the polyQ length increases (Liu et al., 2000).
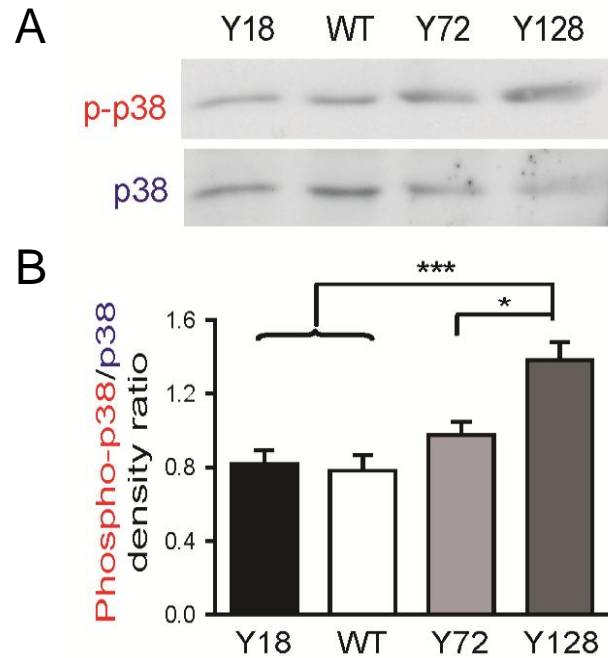
Figure 19. Basal activation of p38 MAPK in striatal tissues from pre-symptomatic WT and YAC mice.

A) Representative blot showing basal level of p38 activation in striatal tissue from 2 month-old WT and YAC mice. **B)** Pooled data showing basal level of p38 activation is elevated in striatal tissue from 2 month-old YAC128 mice. Phospho-p38/p38 band density ratios were calculated by normalizing to Tubulin. $P<0.0001$ by one-way ANOVA and *$p<0.05$, ***$p<0.001$ by Bonferroni's Multiple Comparison Test, n=8.
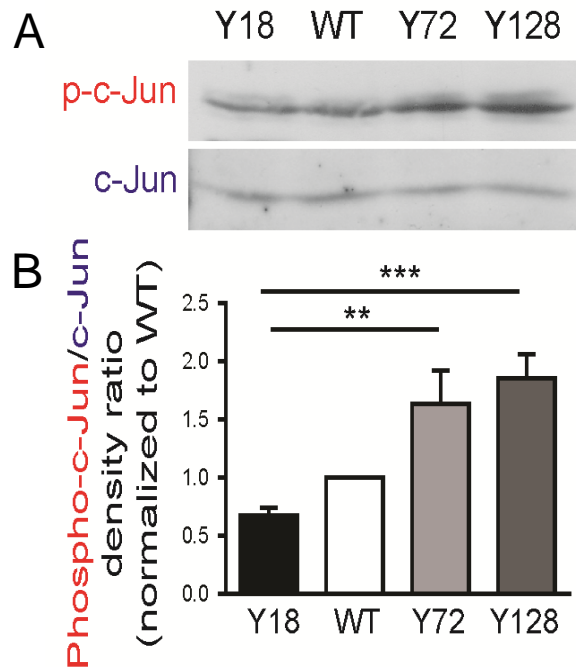
Figure 20. Basal activation of JNK MAPK in striatal tissues from presymptomatic WT and YAC mice.

A) Representative blots showing basal level of JNK activation in striatal tissues from 2 month-old WT and YAC mice. **B)** Pooled data showing basal level of JNK activation is elevated in striatal tissues from 2 month-old mutant htt-expressing mice. JNK activation is measured by phospho-c-Jun/c-Jun band density ratio (normalized to WT). Significant by one-way ANOVA ($p<0.001$) and Bonferroni post-test, $**p<0.01$, $***p<0.001$, n=7. P-c-Jun, phospho-c-Jun.

3.3.5 NMDA-induced activation of p38 but not JNK MAPK depends on NMDAR/PSD-95 interaction in striatum of YAC128 mice

NMDAR stimulation activates MAPK in cultured striatal neurons, which can be blocked by an inhibitor of p38 MAPK (Vincent et al., 1998). It has been found recently that the p38 MAPK death pathway is downstream of NMDAR-PSD-95 signaling either through nNOS or SynGAP in hippocampal and cortical neurons (Cao et al., 2005; Ghatan et al., 2000; Kim et al., 1998; Rumbaugh et al., 2006). Moreover, Tat-NR2B9c disrupts NMDAR signaling to p38 MAPK in cortical neurons while having no effect on JNK activation (Soriano et al., 2008). However, it remains unknown whether the NMDAR/PSD-95 interaction is required for NMDA-induced p38 MAPK activation in striatal tissue, which is the most affected brain region in HD, as the classical NMDAR/PSD-95/nNOS toxic signaling has been found to play a less important role in cultured striatal neurons than in hippocampal neurons (Fan et al., 2010). Therefore, we investigated whether NMDA-induced p38 and/or JNK MAPK activation is enhanced, and whether their activations are dependent on the NMDAR/PSD-95 interaction, in striatal tissue of YAC128 mice compared to WT mice.

WT and YAC128 mice were sacrificed at 8-weeks of age, and acute parasagittal corticostriatal slices were prepared for NMDA treatment, with or without 1-hr Tat-NR2B9c pretreatment. We first confirmed that one hour treatment with 200nM Tat-NR2B9c of acute cortico-striatal slices from 6-8 week-old WT and Y128 mice reduced the association of GluN2B with PSD-95 in striatal tissue by ~ 50% (Fig. 21), similar to what was observed in neuronal cultures. Striatal tissue was then analyzed for

phospho-c-Jun/c-Jun (measures JNK activity) and phospho-p38/p38 by western blotting.

We found that at five minutes following a 10-min incubation with 500 μM NMDA, both p38 and JNK were activated ~1.5-fold compared to baseline levels (not shown) in the striatum of corticostriatal slices from both WT and YAC128 mice (Fig. 22 and 23). Notably, NMDA-induced p38 activation was reduced (~50%) by 200nM Tat-NR2B9c in YAC128 striatal tissue, but not in WT (Fig. 22), consistent with the lack of protection by Tat-NR2B9c against NMDAR toxicity in WT cultured MSNs (Fan et al., 2010). In contrast, NMDA-induced JNK activation was not altered by Tat-NR2B9c in either genotype (Fig. 23). These data indicate that JNK activation by NMDA in striatal tissue does not depend on NMDAR/PSD-95 binding, which is consistent with previous findings in AtT20 and cortical cells (Soriano et al., 2008). As a control peptide, Tat-NR2BAA had no effect on NMDA-induced activation of either p38 or JNK in striatal tissues of WT and YAC128 mice. We have also collected data from cortical tissues and found a similar trend as in striatal tissue, but no significance was detected due to larger variability.
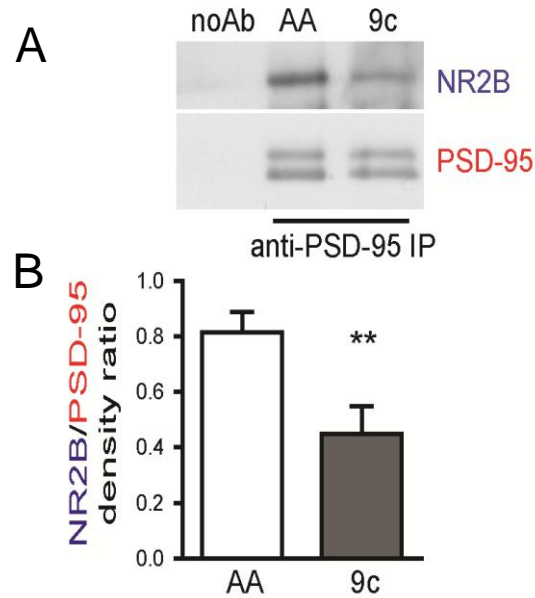
Figure 21. Tat-NR2B9c reduces the co-IP of GluN2B with PSD-95 in striatal neurons of cortico-striatal slices from 8 week-old WT and Y128 mice.

A) Representative blot showing one hour pretreatment with 200nM Tat-NR2B9c reduced the co-immunoprecipitation of GluN2B with PSD-95 (using an anti-PSD-95 antibody) in striatal tissue of cortico-striatal slices from 8 week-old WT and Y128 mice. **B)** Pooled data for mean $\pm$ SEM band density ratio of GluN2B to PSD-95 is shown. Significant by two-tailed paired t-test, **$p<0.01$ (n=6).
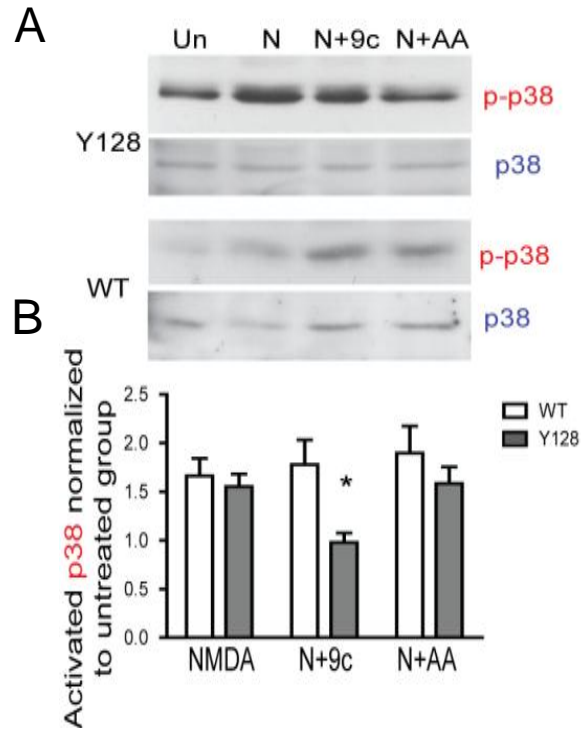
Figure 22. NMDA-induced activation of p38 is dependent on GluN2B/PSD-95 coupling in striatal neurons of cortical-striatal slices from YAC128 mice.

A) Representative blots showing NMDA-induced p38 activation after one hour pretreatment of 200nM Tat-NR2B9c in striatal tissue in cortical-striatal slices from 2 month-old WT and YAC128. **B)** Pooled data showing that one hour pretreatment of 200nM Tat-NR2B9c reduced NMDA-induced p38 activation in striatal tissue in cortical-striatal slices from 2 month-old Y128 but not WT mice. The p-p38/p38 density ratio was normalized to untreated group (not shown) as fold change. Both treatment ($F_{2,40}$=5.65) and interaction between genotype and treatment ($F_{2,40}$=5.39) are significant (**p<0.01) when tested by two-way ANOVA, *p<0.05, by Bonferroni post-tests, n=10 for Y128, and 12 for WT.
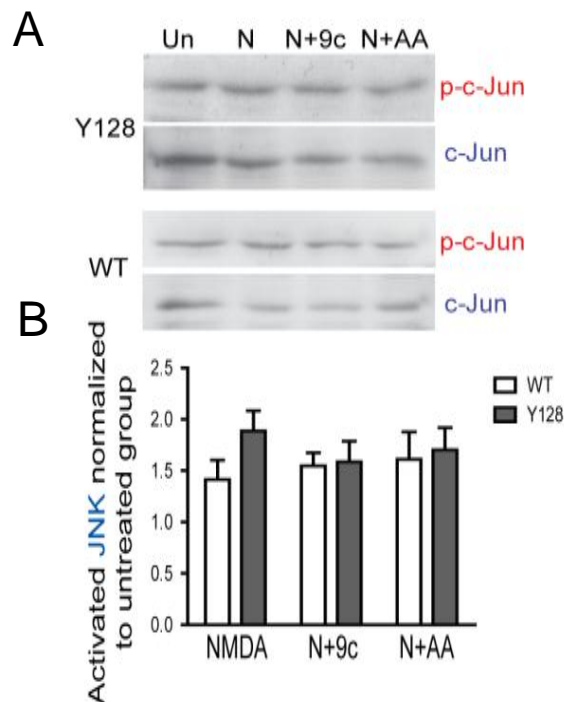
Figure 23. NMDA-induced activation of JNK is independent of GluN2B/PSD-95 coupling in striatal neurons of cortical-striatal slices from WT and YAC128 mice.

A) Representative blots showing NMDA-induced JNK activation (measured by phospho-c-Jun/c-Jun ratio) after one hour pretreatment of 200nM Tat-NR2B9c in cortical-striatal slices from 2 month-old WT and Y128 mice. **B)** Pooled data showing NMDA-induced JNK activation is not affected by one hour pretreatment of 200nM Tat-NR2B9c in cortical-striatal slices from 2 month-old WT and Y128 mice. No significance detected by two-way ANOVA, n=12 for Y128, 9 for WT.

3.3.6 Protection against NMDAR-mediated death by p38 inhibitor and JNK inhibitor in primary cultured striatal neurons

It has been reported recently in hippocampal neurons that selective stimulation of extrasynaptic NMDARs leads to activation of p38-MAPK, which promotes cell death (Xu et al., 2009), and that this p38 MAPK activation depends on NMDAR interaction with PSD-95 and nNOS (Soriano et al., 2008). NMDAR activation also stimulates JNK activation, leading to cell death, but this pathway is PSD-95-independent (Soriano et al., 2008). Since disruption of the GluN2B and PSD-95 interaction selectively reduces NMDAR-mediated p38 activation in striatal tissue of YAC128 and not WT mice, and also Tat-NR2B eliminates the enhanced NMDA-induced toxicity found in YAC128 MSNs (Fan et al., 2009), we hypothesized that excessive, PSD-95-dependent activation of p38-MAPK contributes to the increased NMDAR toxicity in YAC128 striatum.

To test this hypothesis, we pretreated WT and YAC128 DIV 9 cultured striatal neurons with the p38 inhibitor (SB-239063) or JNK inhibitor (SP-600125), with or without Tat-NR2B9c peptide. NMDA toxicity was assessed by TUNEL assay and Hoechst-stained nuclear morphology. We found that the p38 inhibitor reduced NMDAR-mediated cell death in cultured MSNs from YAC128 mice to the level observed in WT MSNs, and also occluded the Tat-NR2B9c peptide protective effect. Notably, this inhibitor provided no protection against NMDA-induced toxicity in WT cultured MSNs (Fig. 24). In addition, 0.2% DMSO alone did not cause significant apoptosis (data not shown).

A

WT MSNs   Y128 MSNs

NMDA

NMDA +
SB239063
(p38 inhibitor)

NMDA + 9c
+
SB239063

TUNEL   Hoechst   TUNEL   Hoechst

B

Legend:
- NMDA
- N+10μM SB
- N+20μM SB
- N+1/500 DMSO
- 20μM SB
- N+9c+20μM SB
- N+9c
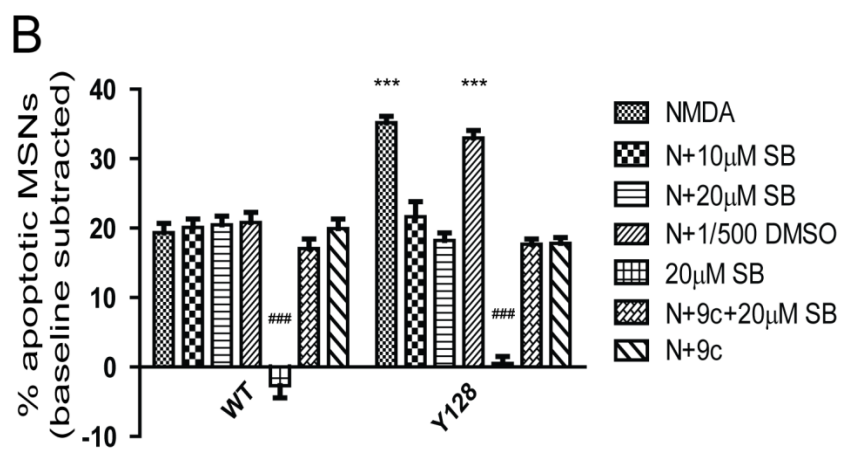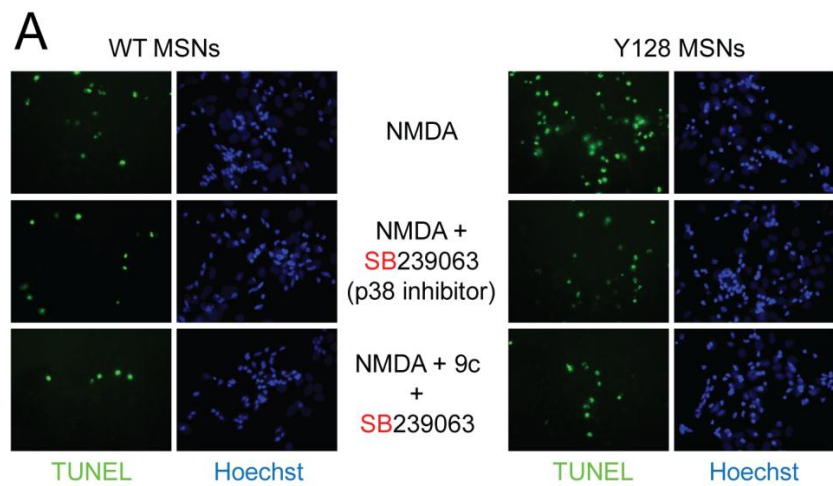
Figure 24. Protection against NMDAR-mediated death by p38 inhibitor in primary cultured striatal neurons of YAC128 but not WT mice.

A) Representative photomicrographs showing TUNEL and Hoechst stained cultured WT and YAC128 MSNs treated for 1 hr with p38 inhibitor and/or Tat-NR2B9c prior to 10-min challenge with NMDA. **B)** P38 inhibitor reduced NMDA-induced cell death in cultured MSNs of YAC128 to the level of WT, and occluded the Tat-NR2B9c peptide protective effect. Pooled mean average percentages of apoptotic MSNs are shown after subtraction of percent apoptosis in NMDA-untreated condition for each experiment. Two-way ANOVA revealed significant difference for genotype, treatment and interaction, $p<0.001$, n= 3 to 6 (***$p<0.001$ by Bonferroni post-test). N, NMDA; 9c, Tat-NR2B9c; SB, SB-239063.

In contrast, the JNK inhibitor (SP-600125) reduced NMDA-induced cell death in cultured MSNs from both WT and YAC128 mice, and the protective effect was additive to that of Tat-NR2B9c (Fig. 25A, B). Consistent with our hypothesis, these data in cultured striatal neurons suggest that activation of p38 contributes to mutant htt-mediated enhancement of GluN2B-PSD-95 toxic signaling. In contrast, NMDA-induced JNK activation contributed to toxicity in both WT and YAC128 MSNs, and appeared to be independent of PSD-95/GluN2B association.

A

WT MSNs   Y128 MSNs

NMDA

NMDA +
SP600125
(JNK inhibitor)

NMDA + 9c
+
SP600125

TUNEL   Hoechst   TUNEL   Hoechst

B

NMDA
N+1μM SP
N+9c+1μM SP
N+5μM SP
N+9c+5μM SP
5μM SP
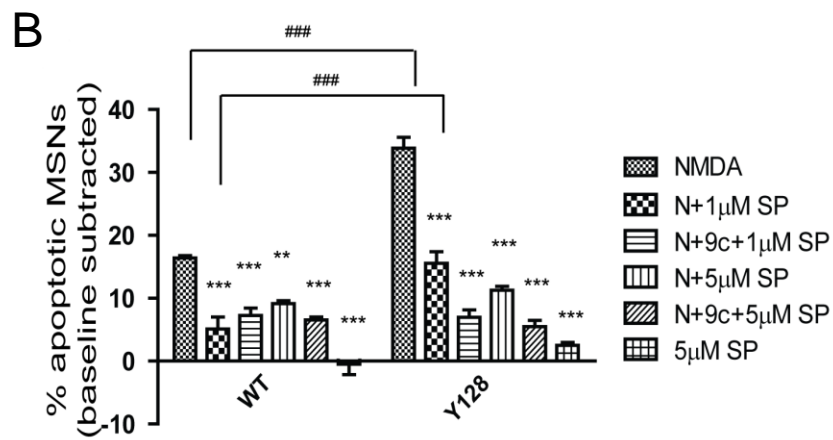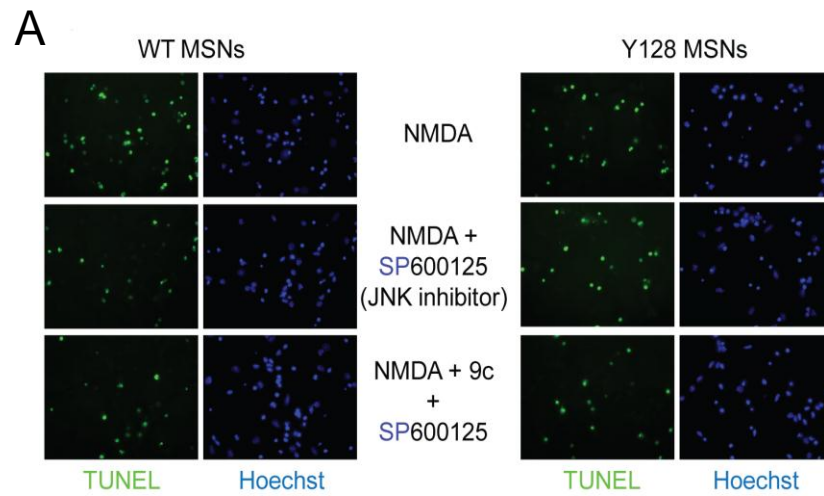
Figure 25. Protection against NMDAR-mediated death by JNK inhibitor in primary cultured striatal neurons of both WT and YAC128 mice.

A) Representative photomicrographs showing TUNEL and Hoechst stained cultured WT and YAC128 MSNs treated with JNK inhibitor and/or Tat-NR2B9c for 1 hr prior to 10-min challenge of NMDA. **B)** JNK inhibitor reduced NMDA-induced cell death in cultured MSNs of both WT and YAC128, and is additive to Tat-NR2B9c. Pooled mean average percentages of apoptotic MSNs are calculated after subtraction of percent apoptosis in NMDA-untreated condition for each experiment. $P<0.001$ by two-way ANOVA for genotype, treatment and interaction, n=3 to 4, except n=2 for 5μM SP600125-only condition; ***$p<0.001$ compared to NMDA treated groups of each genotype respectively, ###$p<0.001$, by Bonferroni's post-test. SP, SP600125.

3.4 Discussion

The NMDAR/PSD-95 interaction was shown previously to be a key contributor to excitotoxicity in cultured striatal neurons of a murine HD model (Fan et al., 2009), as well as in cultured WT rat cortical or hippocampal neurons, and to ischemic damage in a rodent stroke model (Aarts et al., 2002; Sattler and Tymianski, 2000; Sattler et al., 1999; Soriano et al., 2008). However, the cellular mechanisms underlying neuroprotection by disruption of the NMDAR/PSD-95 complex in the YAC HD mouse model remained unclear. Here, I reported that pre-treatment with Tat-NR2B9c at a concentration disrupting the GluN2B/PSD-95 interaction significantly reduced NMDAR-mediated cell death in wild-type hippocampal but not striatal cultures, and that similar, non-additive effects were obtained with an nNOS inhibitor. Our results confirmed that GluN2B/PSD-95/nNOS plays an important role in mediating death signaling in hippocampal neurons while it is not required in striatal neurons, which raises the question – what is/are the pathway(s) responsible for NMDAR-dependent toxicity in striatal neurons.

3.4.1 Cell death pathways downstream of NMDAR activation in striatal versus hippocampal neurons

3.4.1.1 NMDAR/PSD-95/nNOS pathway plays different role in hippocampal and striatal neurons

Hippocampal (or cortical) and striatal neurons express many similar proteins but may differ in terms of protein expression levels, subcellular compartmentalization, and/or

protein-protein interactions, potentially contributing to differences in pathways downstream of NMDAR signaling to cell death or thresholds of common pathways. One difference is that GluN2B is enriched in striatal tissue (Christie et al., 2000; Landwehrmeyer et al., 1995; Li et al., 2003b), while GluN2A- and GluN2B-type NMDARs are both common in adult hippocampal cells (Monyer et al., 1994; Wenzel et al., 1997). Unlike hippocampal neurons, we found that cultured striatal neurons are not protected by Tat-NR2B9c, in spite of the fact that these two neuronal populations show similar Tat-NR2B9c efficacy in disrupting GluN2B/PSD-95 binding. Our data are consistent with a previous study showing that Tat-NR2B9c protection against middle cerebral artery occlusion-induced ischemia is more robust in cortex than striatum (Aarts et al., 2002). Moreover, in pilot studies we found that intraperitoneal injection of Tat-NR2B9c does not protect against quinolinate-induced (NMDAR-mediated) lesions in murine striatum (BR Leavitt, J Fan, LA Raymond, unpublished results). Consistent with the lack of protection by Tat-NR2B9c in cultured striatal neurons, nNOS inhibition also did not protect against NMDA-induced toxicity. Moreover, in previous work I have shown that although NMDA stimulates nNOS activity in wild-type murine striatal cultures, as assessed by changes in cGMP levels, this increase was not affected by pre-treatment with Tat-NR2B9c (Fig. 18). We conclude that NMDAR-mediated apoptotic signaling occurs through distinct pathways in hippocampal and striatal neurons.

The fact that the GluN2B/PSD-95/nNOS pathway is not a major contributor to NMDA-induced toxicity in cultured striatal neurons may be due, in part, to the absence of

nNOS in the striatal GABAergic medium-sized spiny neurons (MSNs), which make up ~90% of all striatal neurons. On the other hand, the striatal cultures used in our experiments include ~ 4% nNOS-expressing interneurons (Shehadeh et al., 2006), and a previous study showed that NO released from such neurons could induce intracellular calcium release from mitochondria in MSNs (Horn et al., 2002). However, GluN2B expression is undetectable in those nNOS interneurons (Zucker et al., 2005), and in our striatal cultures the nNOS inhibitor N-Arg fully reverses NMDA-induced cGMP production whereas Tat-NR2B9c has no effect, indicating nNOS activation by NMDA occurs independently of the PSD-95/GluN2B interaction. Moreover, the NMDA-induced cGMP and NO production in these WT striatal cultures is apparently insufficient to trigger cell death signaling, since we have shown that nNOS inhibitors fail to block NMDA-induced toxicity.

In contrast to WT striatal MSNs, inhibition of nNOS mimicked the protective effect of Tat-NR2B9c in striatal neurons from YAC HD mice. The effect of nNOS inhibition was not additive to that of the Tat-NR2B9c peptide. These results suggest a role for nNOS in enhanced NMDA excitotoxicity in YAC72 and YAC128 MSNs. However, Tat-NR2B9c failed to influence NMDA-stimulated nNOS activity (reflected by cGMP production) in either WT or YAC72 MSNs. We conclude that nNOS activation by NMDA occurs independently of PSD-95/GluN2B interaction and cannot explain the protective effect of Tat-NR2B9c on excitotoxicity in YAC HD MSNs. On the other hand, NMDAR-activated signaling pathways that depend on NMDAR-PSD-95 association may

converge with those that involve NMDAR-mediated nNOS activation in the same final pathway that mediates enhanced excitotoxic vulnerability of YAC HD MSNs; if so, inhibition of just one of these upstream pathways may be sufficient to abolish enhanced toxicity.

One possibility for nNOS-independent, PSD-95-dependent NMDAR cell death signaling is through the phosphatase calcineurin, which is involved in induction of the mitochondrial permeability transition and release of apoptotic factors(Springer et al., 2000). Calcineurin and PSD-95 are linked through binding with A-kinase anchoring protein (AKAP79/150) (Bhattacharyya et al., 2009; Colledge et al., 2000). Moreover, NMDAR-induced calcineurin activity is enhanced in mutant htt-expressing striatal cells and inhibition of calcineurin protects against excitotoxicity better in mutant htt-expressing than WT cells (Xifro et al., 2008).

3.4.1.2 NMDAR subunit composition in excitotoxic signaling via PSD-95 and nNOS in hippocampal neurons

Previous studies have shown that Tat-NR2B9c peptide concentrations on the order of 100nM protect cultured hippocampal and cortical neurons from NMDAR-mediated toxicity (Aarts et al., 2002; Soriano et al., 2008). However, whether this effect could be attributed to Tat-NR2B9c disrupting PSD-95 interactions between GluN2B and/or GluN2A in live neurons had not been established previously. We report that the concentration dependence of the Tat-NR2B9c neuroprotective effect in hippocampal

cultures correlates well with the concentration required to uncouple GluN2B and PSD-95 in live neurons, suggesting signaling pathways that require the GluN2B interaction with PSD-95 critically contribute to apoptotic cell death 24 hours after brief (10 min) exposures to NMDA. Notably, further increasing the Tat-NR2B9c concentration to levels required to disrupt GluN2A binding with PSD-95 did not augment protection from NMDA-induced toxicity in this paradigm. The nNOS inhibitor N-Arg provided a similar level of neuroprotection (~50%), and this effect was not additive with Tat-NR2B9c. Together, these data suggest that it is the GluN2B link through PSD-95 to activate nNOS that is critical for mediating delayed apoptotic death in cultured hippocampal neurons. Our results also support data from other studies suggesting GluN2B-type NMDARs preferentially signal to cell death pathways, including shut-off of ERK1/2 and activation of p38-MAPK (Kim et al., 2005; Liu et al., 2007; Martin and Wang, 2010; Tu et al., 2010).

3.4.1.3 NMDAR signaling to p38 and JNK MAPK death pathways in striatal neurons

NMDAR-dependent apoptosis is likely to involve the activation of stress-induced pathways such as p38 MAP kinase and c-Jun N-terminal kinase (Hardingham, 2006; Hardingham and Bading, 2003). In cultured striatal neurons, NMDAR stimulation results in p38-dependent activation of MAP kinase (Vincent et al., 1998). High concentrations of glutamate and NMDA have been shown to induce strong activation of p38 MAPK (which correlates with apoptosis) and less JNK activation in rat cerebellar granule cells

(Kawasaki et al., 1997). However, it has also been shown that glutamate, but not dopamine, activates JNK and AP-1-mediated transcription in striatal neurons (Schwarzschild et al., 1997).

Here, my work showed that high-dose NMDA stimulation of acute corticostriatal slices leads to activation of both p38 and JNK in WT and YAC128 striatum. However, Tat-NR2B9c pretreatment reduced only the p38 activation but not JNK activation, and only in YAC128 but not in WT striatum. In cultured striatal neurons, inhibition of p38 MAPK reduced NMDAR-mediated cell death of YAC128 to WT levels, and occluded the Tat-NR2B9c peptide protective effect, while p38 inhibition had no effect in cultured WT MSNs. Meanwhile, inhibition of JNK had a similar protective effect in cultured MSNs from both WT and YAC128 mice, and is additive to the protection of Tat-NR2B9c peptide.

Notably, NMDA-induced p38 MAPK activation is disrupted by Tat-NR2B9c and relies on neuronal context in cortical neurons (Soriano et al., 2008). However, it is more likely that other pathways downstream of NMDAR activation, independent of the GluN2/PSD-95 interaction, contribute importantly to striatal neuronal apoptosis. Our data support a key role of JNK in NMDA-induced death of wild-type striatal neurons, as inhibition of JNK shows significant protection in this assay.

Taken together, our results point to the conclusion that mutant htt enhancement of GluN2B-PSD-95 toxic signaling (presumably by the shift and stabilization at extrasynaptic sites), is mainly mediated by activation of p38 MAPK, while

NMDA-induced JNK activation is independent of the NMDAR/PSD-95 interaction. These findings help to explain the lack of protective effect of Tat-NR2B9c peptide in WT MSNs, but specific blockade of the elevated NMDA-induced death caused by mutant huntingtin in YAC128 MSNs.

3.4.2 Activation of p38 and JNK MAPK in striatum of HD mice

Striatal p38 MAPK can be activated by reactive oxygen species (ROS) (Hsieh and Papaconstantinou, 2002; Hsieh et al., 2003; Kulisz et al., 2002) and its crosstalk with caspases (Juo et al., 1997). Both ROS and caspase activity can be increased as a result of the altered calcium homeostasis induced by mutant huntingtin early in HD (Bezprozvanny and Hayden, 2004; Cattaneo and Calabresi, 2002). Several processes have been shown to contribute to mhtt-induced intracellular calcium dysregulation in striatal MSNs, such as enhancement of NMDAR currents, impaired mitochondrial calcium handling (Fernandes et al., 2007; Panov et al., 2002; Sawa et al., 1999), and enhanced intracellular release by IP$_3$ receptors (Tang et al., 2005; Tang et al., 2004). Notably, immunocytochemical experiments have shown that p38 is activated in the striatal neurons but not cortical neurons of R6/2 mice at 12 weeks of age (when mice show advanced signs of HD), correlating with striatal damage (Gianfriddo et al., 2004).

In our study, activated p38 levels in the YAC128 striatum at 8-weeks (presymptomatic) were significantly higher than the other three genotypes tested, including YAC72 mice, which also exhibit features of the HD phenotype, though at older

ages and to a milder extent than YAC128 mice (Hodgson et al., 1999; Slow et al., 2003). The lack of increased basal p38 activation in YAC72 MSNs compared to YAC128 MSNs could be explained, in part, by the fact that p38 can be activated by cytochrome *c* release from mitochondria, which is enhanced in YAC128 striatal neurons (Tang et al., 2005). The elevated basal levels of p38 activation in YAC128 striatum, is also in accordance with the finding of more NMDAR/PSD-95 complex at extrasynaptic locations (C. Gladding's work, manuscript in preparation; data not shown in dissertation) as more extrasynaptic NMDARs now could respond to 'spill over' events. Although there is a trend toward increased extrasynaptic NMDAR current in YAC72 compared with YAC18 MSNs, this is not significant, whereas the difference is significant in YAC128 MSNs (Milnerwood et al., 2010). Also, although the GluN2B/PSD-95 interaction is significantly enhanced in YAC72 striatum compared with WT, it is a smaller effect than seen in YAC128 mice (Fan et al., 2009).

On the other hand, it has been found that wild type huntingtin interacts with MLK2 (JNK activator), while expanded polyQ interferes with this interaction and expression of mutant huntingtin in HN33 cells induces JNK activation and apoptosis (Liu et al., 2000). Those data are consistent with my observation of increased JNK basal activation with increasing htt polyQ length in striatal tissues of YAC mice at 8 weeks of age. In my study, even though basal JNK activation is elevated early in the striatum of HD mice, its activation by NMDA stimulation contributes equally to excitotoxicity of striatal neurons of WT and YAC128 mice, and is not specific to mutant huntingtin-enhanced cell death.

However, we cannot exclude the possibility that JNK activation by cellular signals other than NMDAR stimulation contributes to HD pathogenesis.

3.4.3 Role of SynGAP in NMDA-induced activation of p38 MAPK and cell death in striatal neurons

P38 MAPK could be activated by NMDAR stimulation via downstream increases in reactive oxygen species, such as NO and H_2O_2 (Bossy-Wetzel et al., 2004; Izumi et al., 2008). Another pathway downstream of NMDAR is through binding of PSD-95 to SynGAP, known to regulate synaptic plasticity and neuronal apoptosis through p38-MAPK signaling in hippocampal neurons (Kim et al., 1998; Rumbaugh et al., 2006). The NMDA-induced p38 activation in striatum (downstream of NMDAR/PSD-95), is unlikely to be through nNOS activation as in cortical cells, since we have previously shown that Tat-NR2B9c does not block NMDA-induced nNOS activation in either WT or YAC128 MSNs (Fan et al., 2009). Indeed, the fact that PSD-95 interacts with both GluN2B subunits of the NMDA receptor and SynGAP (Kim et al., 1998) suggests synGAP as a candidate mediator of p38 MAPK activation by NMDAR stimulation; further experiments are required to address this potential mechanism.

One study observed in hippocampus that GluN2B-type NMDARs but not GluN2A-type, are selectively associated with the Ras-GAP SynGAP; moreover, selective stimulation of extrasynaptic NMDARs, which are predominantly GluN2B containing, caused a net decrease in GTP-Ras (Kim et al., 2005). Therefore, it has been suggested

that even though the signaling pathways selectively activated by extrasynaptic NMDARs are less well understood, they might involve SynGAP (Paul et al., 2003; Zhang et al., 2008) and activation of p38 MAPK, leading to neuronal death (Xu et al., 2009).

3.4.4 Possible involvement of Calpain, STEPs and in-activation of p38 MAPK in HD

Striatal-enriched protein tyrosine phosphatase (STEP) is an intracellular tyrosine phosphatase that regulates activity-dependent strength of synapses (Braithwaite et al., 2006a; Braithwaite et al., 2006b; Pelkey et al., 2002). STEP61 is a membrane-associated isoform of STEP that localizes to the endoplasmic reticulum and the postsynaptic terminal (Boulanger et al., 1995; Oyama et al., 1995), where it can dephosphorylate and inactivate ERK1/2 and p38 (Munoz et al., 2003; Paul et al., 2003; Paul et al., 2007). Synaptic and extrasynaptic NMDAR stimulation promotes the degradation of STEP61 by either ubiquitination or calpain-mediated cleavage of STEP61, respectively. Synaptic STEP61 degradation then facilitates activation of ERK1/2, whereas calpain-mediated cleavage of extrasynaptic STEP61 promotes sustained activation of p38; these two processes promote entry into pro-survival or pro-apoptotic pathways, respectively (Xu et al., 2009). Indeed, calpain has been widely implicated in neurotoxicity (Liu et al., 2008), and calpain inhibitors have been suggested to be neuroprotective (Wells and Bihovsky, 1998) in striatal neurons from WT and HD mice (Cowan et al., 2008). Moreover, calpain activity is elevated in MSNs of YAC128 mice compared with WT (Cowan et al., 2008), in a cell line expressing mutant htt (Majumder et al., 2007), and in the caudate of human

HD tissue (Gafni and Ellerby, 2002). Thus, it is possible that the increased baseline and NMDA-induced calpain activation (especially through extrasynaptic NMDARs) in YAC128 striatal tissue causes enhanced cleavage and inactivation of extrasynaptic STEP61, which in turn results in less dephosphorylation of p38 (e.g., prolonged activation) in these HD mice, contributing to increased apoptotic gene expression and neuronal death compared to WT.

It is interesting that the fold-increase above baseline in the level of NMDA-induced p38 activation in YAC128 striatum was not significantly different from that observed in WT striatal tissue. However, we have only examined p38 activation 5min after 500μM NMDA stimulation on slices; it is possible that p38 MAPK could show sustained activation in YAC128 compared with WT striatum over a longer time course. NMDA concentration is another potential factor influencing the levels of p38 phosphorylation. Here, I used a high concentration of NMDA to match conditions used in striatal culture experiments ((Fan et al., 2009) and Fig. 4); however, this was unlikely to produce a ceiling effect and occlude differences in p38 activation between WT and YAC128 MSNs because in pilot experiments, little or no activation of p38 was observed in response to 100μM NMDA (data not shown). In future experiments, it would be interesting to determine whether the time-course of NMDA-induced p38 MAPK activation is different in WT and YAC128 mice striatum, since that p38 activation decreases 30min after stimulation with high concentrations of glutamate in WT cortical neurons (Kawasaki et al., 1997) and prolonged NR2B-type NMDAR activation leads to secondary activation of

p38 MAPK in WT cortico-striatal co-cultures (Poddar et al., 2010).

3.4.5 Summary

Our findings, and the work of others, point to a possible role for p38 and JNK MAPKs in NMDAR-mediated apoptosis in striatal neurons and especially a critical contribution of NMDAR/PSD-95/p38 MAPK signaling in HD pathogenesis. The targeting of the NMDAR/PSD-95 interaction or p38 MAPK signaling may be beneficial to the development of biomarkers and treatments for HD.

4 Concluding chapter

4.1 Summary of findings

Unlike other well-known neurodegenerative diseases, such as Parkinson's disease or Alzheimer's disease, HD is thought to be a more 'straightforward' brain disorder because it is monogenic, caused by an unstable expansion of CAG repeats at the 5' end region of the *HTT* gene (Group, 1993). However, the cellular and molecular pathways that have been disrupted by this single gene mutation and lead to disease symptoms are not yet fully understood. Among the numerous efforts toward exploring mechanisms like transcriptional disturbance, proteolysis dysregulation, mitochondria disruption, synaptic dysfunction and excitotoxicity, the study of altered NMDAR function and its downstream signaling has been a unique and important direction in HD research (Davies and Ramsden, 2001; Fan and Raymond, 2007; Gutekunst et al., 1995; Hoffner et al., 2002; Li and Li, 2004b; Menalled et al., 2002; Milnerwood and Raymond, 2007; Panov et al., 2002; Ross, 2002; Rubinsztein, 2002; Sugars and Rubinsztein, 2003; Tobin and Signer, 2000).

In my Ph.D dissertation, I have explored more deeply and expanded upon the previous studies of PSD-95 in HD (Sun et al., 2001) in an attempt to understand the mechanisms underlying enhanced NMDA-induced excitotoxicity in the YAC transgenic mouse model of HD. Inspired by the preliminary work of a previous member of the lab, Dr. C.M. Cowan, I carried out studies to determine the expression level of PSD-95, and its association with NMDAR GluN2 subunits in striatal tissue of WT and YAC transgenic

mice at the earliest stages of the HD phenotype (2 months old). I found no alteration of PSD-95 expression in the YAC mice striatum at this age. However, by immunoprecipitation, I discovered that the interaction between GluN2B and PSD-95 is enhanced as the polyQ expansion of huntingtin increases (together with Dr. L.Y. J. Zhang), while on the other hand, the GluN2A/PSD-95 interaction is polyQ length-independent. I also confirmed that the association of huntingtin and PSD-95 decreases with a polyQ expansion of huntingtin in our YAC transgenic mice striatal tissue at this age, consistent with the finding in the cortex tissue of HD patients (Sun et al., 2001).

By using a previously reported peptide (Tat-NR2B9c) (Aarts et al., 2002), which reduces interaction of GluN2B and PSD-95 to ~ 50% at 200nM concentration in our primary hippocampal and MSN cultures (both WT and YAC128 MSNs), without affecting the GluN2A/PSD-95 interaction in the hippocampal neuronal cultures, I was able to test the importance of the GluN2B/PSD-95 interaction in mediating NMDA-induced toxicity in WT and YAC HD MSN cultures. After pretreatment with this Tat-NR2B9c peptide, I have found that the NMDA-induced cell death in YAC72 and YAC128 MSN cultures can be reduced to the same level as in WT MSNs, while the NMDA-induced neuronal death rate of WT MSNs remains unaffected. When testing a range of concentrations, I and others in the lab found that Tat-NR2B9c at concentrations starting from 150nM, and up to 2μM protects against NMDA-induced toxicity in rat embryonic hippocampal cultures, while it affords no protection at all in either

mono-cultured or cortical-cell-co-cultured rat embryonic MSNs. To determine whether the protective effect of Tat-NR2B9c in YAC128 MSNs was due to the disruption of GluN2B/PSD-95 or GluN2B/SAP102 interaction (as this peptide at 200nM disrupts both interactions to similar degrees), I performed siRNA-based knock-down of PSD-95 and SAP102 in cultured MSNs from WT and YAC128. I found that knocking-down of PSD-95 but not SAP102 showed the same protective effect against NMDA-induced toxicity as pretreating with Tat-NR2B9c, and occluded the effect of Tat-NR2B9c in the YAC128 MSNs, while neither siRNA protected against NMDA-induced toxicity in the WT MSNs.

These results indicate that the pro-apoptotic signaling pathways downstream of NMDAR overactivation in WT cultured striatal neurons, which were not significantly influenced by the NMDAR/PSD-95 interaction, differ from those in hippocampal or cortical neurons. However, the expression of mutant huntingtin alters the NMDAR-toxicity pathway of cultured striatal neurons, so that GluN2B/PSD-95 interactions contribute to cell death mechanisms; whether the process by which mutant htt alters NMDAR toxicity involves the enhanced interaction of GluN2B/PSDD-95 in these neurons is not known.

In order to determine the mechanism underlying the 'specific' GluN2B/PSD-95 interaction-dependent, mutant huntingtin-mediated enhancement of NMDA-induced toxicity, I have further explored the nNOS pathway as well as p38 and JNK MAPK pathways. All of these pathways have been previously reported to be toxic pathways

downstream of NMDAR in cortical neurons (Aarts et al., 2002; Dawson et al., 1991; Sattler et al., 1999; Soriano et al., 2008). In contrast to what we have learned from cortical or hippocampal neurons in stroke models, the NMDA-induced nNOS activation measured by cGMP levels in cultured WT or YAC128 MSNs cannot be reduced by Tat-NR2B9c, despite the fact that an nNOS inhibitor showed a similar protective effect as Tat-NR2B9c in YAC128 MSNs. These data suggest that nNOS activation is not required for cell death signaling downstream of the GluN2B/PSD95 interaction in striatal MSNs from either WT or YAC128 mice. In other experiments, I found that the basal levels of both p38 and JNK MAPKs activities were elevated in YAC128 striatum at 2 month of age, a time at which the GluN2B/PSD-95 association is enhanced. Both p38 and JNK were shown to be moderately activated by NMDA stimulation in the striatum of acute corticostriatal slices from 2 month-old WT and YAC128 mice to a similar extent. Interestingly, I discovered that Tat-NR2B9c pretreatment reduced only the NMDA-induced p38 activation in YAC128 but not in WT striatum, and had no effect on the NMDA-induced JNK activation in striatum from either genotype. Consistent with that finding, in cultured MSNs a p38 inhibitor reduced NMDAR-mediated cell death of YAC128 neurons to WT levels, and occluded the Tat-NR2B9c peptide protective effect; in contrast, a JNK inhibitor protected cultured MSNs from both WT and YAC128 mice against NMDA toxicity equally, and its protection was additive to that of Tat-NR2B9c.

Taken together, these findings suggest that the mutant huntingtin-triggered enhanced NMDAR-dependent toxicity is mediated by an increased GluN2B/PSD-95 interaction.

Moreover, this enhanced interaction leads to augmented downstream pro-apoptotic signaling through p38 MAPK activation, but not nNOS or JNK pathways, in striatal neurons of YAC HD mice at an early stage of disease.

4.2 Overall significance

4.2.1 Insights on the cellular and molecular mechanisms of HD

Although the NMDAR/MAGUK interaction has been shown to play a critical role in mechanisms underlying ischemic stroke (Aarts et al., 2002), L-3,4-dihydroxyphenylalanine (L-DOPA)-induced dyskinesia (Gardoni et al., 2006a), chronic inflammatory pain (Tao et al., 2008), and Alzheimer's disease in rodent models (Ittner et al., 2010), the work described in my thesis has revealed for the first time that this interaction also plays a key role in HD pathogenesis in a mouse model. My study also greatly extended the work of Sun and colleagues (Sun et al., 2001), in which the mechanism by which impaired mutant huntingtin binding with PSD-95 enhances NMDA receptor-dependent toxicity and downstream toxic signaling was not explored. Notably, a gradual loss of PSD-95, starting at a presymptomatic stage (7 weeks), was observed in the striatum of HD transgenic N171-82Q mice, which was suggested as one of the adaptive changes that possibly protected these mice from quinolinic acid (QA) excitotoxicity (Jarabek et al., 2004). In my study, similar to disrupting the NMDAR/PSD-95 complex, siRNA knock-down of PSD-95 was shown to protect cultured striatal neurons of YAC HD but not WT mice against NMDA-induced toxicity.

One important implication of my study in these YAC transgenic mice at presymptomatic stages of HD is that the enhanced GluN2B/PSD-95 interaction could potentially affect synaptic function of NMDARs and therefore learning and memory, which might contribute to the cognitive impairment that is apparent before neuronal loss

or motor deficits in HD mutation carriers. Furthermore, the balance of pro-survival and pro-death pathways downstream of NMDARs, such as p38 MAPK in my study, could be shifted due to this altered interaction, and may gradually lead to neurodegeneration through altered transcriptional regulation.

Among the most interesting findings of my research is that targeting the GluN2B/PSD-95 interaction and its downstream p38 MAPK pathway can specifically rescue the enhanced NMDA-induced toxicity caused by mutant huntingtin without disrupting the normal signaling of NMDAR in WT cells. Peptides targeting this protein-protein interaction or inhibitors to this GluN2B/PSD-95/p38 MAPK pathway will provide novel candidates for drug screening to develop new therapeutics for HD. In fact, a more stable and membrane-permeable peptide modified from Tat-NR2B9c has also been identified, and with a 40-fold higher affinity to PDZ-2 of PSD-95, that could serve as a better tool to study the role of the NMDAR/PSD-95 interaction in HD pathogenesis, as well as for potential drug development in HD (Bach et al., 2011). In combination with other drug candidates for treating HD, this peptide and a p38 inhibitor could be tried as a cocktail to provide better selectivity with fewer side effects, by using lower concentrations of each drug.

4.2.2 Contribution to the pro-apoptotic signaling study of NMDARs in striatal neurons

Although there have been numerous studies of NMDAR pro-apoptotic signaling in cortical and hippocampal neurons, my study revealed the neuronal-type specific roles of

three NMDAR-mediated excitotoxic pathways in striatal neurons: the GluN2B/PSD-95/nNOS pathway, GluN2B/PSD-95/p38 and NMDAR/JNK. First, I have confirmed that nNOS activation contributes importantly to NMDA-induced death signaling in hippocampal neurons, whereas it contributes little to NMDAR apoptotic signaling and is independent of GluN2B/PSD-95 binding in wild-type cultured striatal neurons. Further exploration indicates that NMDA-induced p38 MAPK activation is also independent of the GluN2B/PSD-95 interaction in wild-type rodent striatal tissue, and this activation does not contribute significantly to NMDA-induced cell death in wild-type rodent cultured striatal neurons, unlike results reported in mature cortical and hippocampal neurons (Kawasaki et al., 1997; Soriano et al., 2008; Waxman and Lynch, 2005b; Xiao et al., 2011). On the other hand, I also found in wild-type striatal tissue that NMDAR/PSD-95 binding is not necessary for NMDA-induced activation of JNK, which is consistent with the finding in cortical neurons, likely because this pathway is activated by mitochondrial-derived reactive oxidative species (Soriano et al., 2008). Thus, in the normal rodent brain, JNK, but not nNOS or p38 MAPK, contributes importantly to NMDA toxicity in striatal neurons. The differences in these pathways of NMDAR-dependent toxicity in striatal versus cortical or hippocampal neurons might be explained, in part, by differences in protein (including receptors, enzymes, etc.) expression or interacting context, as well as distinct inputs from circuits and the networking environment. Notably, these factors might also contribute to understanding why striatal neurons (mostly MSNs) are more affected at the early stage of HD.

In addition to elucidating downstream pathways of NMDAR toxicity, my thesis work focuses on the pro-death signaling of GluN2B-subtype NMDARs. My data support the theory that GluN2B-type NMDARs play a larger role than GluN2A-type NMDARs in signaling cell death (Chen et al., 2007; Liu et al., 2007), although it is possible that these death-signaling GluN2B-containing NMDARs are also predominantly distributed at extrasynaptic sites (Barria and Malinow, 2002; Li et al., 1998; Rumbaugh and Vicini, 1999; Stocca and Vicini, 1998; Tovar and Westbrook, 1999).

4.2.3 Significance to the understanding of PSD-95 as a mediator of NMDAR-dependent excitotoxicity in striatal MSNs

In my study, siRNA knock-down of PSD-95 provided no protection against NMDA-induced toxicity in cultured WT striatal neurons contradicts what was found previously in cortical neurons (Sattler et al., 1999). However, these data are consistent with my findings that the PSD-95-dependent nNOS or p38 MAPK activation plays little or no role in NMDA-induced toxicity in these striatal neurons, while the PSD-95-independent JNK MAPK pathway could be predominantly responsible for NMDA-induced toxicity in striatal neurons. Thus, under normal conditions, PSD-95 is not an important mediator of NMDA-induced toxicity in striatal neurons, perhaps due to as yet undetermined cell-specific regulation of its localization and interactions with receptors and other molecules at synapses. Interestingly, the lack of involvement of the PSD95/GluN2B interaction in NMDA-induced striatal toxicity is associated with a higher

NMDA-induced pro-apoptotic pathway threshold compared to cortical neurons (preliminary data from our lab has shown a right shift in the NMDA toxicity dose-response curve of striatal neurons compared to cortical neurons in corticostriatal co-cultures on div14; A.M. Kaufman and Dr. A. J. Milnerwood unpublished data). However, during pathological progression in HD, PSD-95 could serve as modulator for toxic signaling of NMDAR in striatal neurons. For example, because the interaction of PSD-95 with huntingtin is disrupted by htt polyQ expansion (Sun et al., 2001), and PSD-95 distribution is shifted to extrasynaptic sites in mutant htt-expressing MSNs (C. Gladding and L.A. Raymond, unpublished data), PSD-95 may affect the balance of survival and death through NMDAR signaling at an early stage of HD.

4.2.4 Impact on studies of MAPK pathways in striatum and striatal neurons

MAPK pathways, especially the ERK1/2 pathway, are among the most well-studied signaling pathways in cortical or hippocampal neurons, whereas much less is known about p38 or JNK MAPKs in the striatum and striatal MSNs in particular, as well as how the MAPKs are activated by NMDARs or in HD.

My observation of increased p38 MAPK activation in the striatum of YAC HD mice is in agreement with what was found in the striatal cells of R6/2 mice (Gianfriddo et al., 2004) and a study using huntingtin-transfected cells (Tsirigotis et al., 2008). In addition, my study has shown for the first time that the NMDA-induced p38 MAPK activation contributes to the death of striatal cells in HD mice. However, I have found the selective

inhibitor of p38 MAPK (SB-239063) (see (Harper and Wilkie, 2003)) had no effect on our high-dose NMDA-induced toxicity in WT striatal cells, in contrast to what was found in cortical neurons (Barone et al., 2001; Cao et al., 2005; Kawasaki et al., 1997; Legos et al., 2002; Soriano et al., 2008) and in two studies on striatal neurons using SB-203580 (Poddar et al., 2010; Vincent et al., 1998).

As for JNK, several studies have reported that polyglutamine expansion of huntingtin induces JNK activation and mediates neurotoxicity in transfected cell models of HD (Apostol et al., 2006; Apostol et al., 2008; Garcia et al., 2004; Liu et al., 2000), and that JNK is involved in HD-related neurotoxicity in a rat model (Perrin et al., 2009) as well as in neurodegeneration in a *Drosophila* model of HD (Scappini et al., 2007). Nevertheless, my study has shown for the first time *in vivo* that JNK shows enhanced activation in striatal tissue of YAC mice expressing mutant huntingtin compared with WT, and that JNK activation plays role in NMDAR-dependent toxicity in both WT and YAC HD striatal cells.

4.3 Future directions

4.3.1 The mechanism of how mutant huntingtin modifies the GluN2B/PSD-95 interaction and localization of this complex

One of the unsolved questions in my thesis study is how GluN2B/PSD-95 association was enhanced by mutant huntingtin. One possibility is that the impaired binding of the SH3 domain of PSD-95 with the poly-proline region of mutant huntingtin (Sun et al., 2001) might directly expose some domains of PSD-95 for protein-interaction or sites for phosphorylation, presumably affecting localization of PSD-95 and its association with the GluN2B-type NMDAR. The recent identification of an additional PSD-95 binding domain on GluN2B, which contains an SH3 domain binding motif, suggests that the PSD-95 SH3 domain could mediate binding in addition to that of the ESDV-PDZ1/2 interaction and help to determine the lateral mobility of NMDARs (Cousins et al., 2009). Furthermore, besides the palmitoylation of the N-terminal two cysteines of PSD-95 that are required for targeting PSD-95 to the postsynaptic membrane (Topinka and Bredt, 1998; Craven et al., 1999), it has been suggested that the SH3 domain of PSD-95 and its interactions with proteins might be important for the formation of a more stable PSD (Sturgill et al., 2009). Therefore, it would be interesting to determine whether this additional binding between GluN2B and the PSD-95 SH3 domain is competitive with the htt poly-proline to PSD-95-SH3 binding *in vitro*, and enhanced when huntingtin polyQ expansion increases.

Another interesting direction is to determine whether the Ser295 and/or Ser73 sites of

PSD-95 play any role in the mutant huntingtin-mediated enhancement of GluN2B/PSD-95 association (but not GluN2A/PSD-95) and mislocalization of PSD-95 to non-PSD sites (work of Dr. C. M. Gladding, manuscript in preparation). The Ser295 of PSD-95 has been shown to be phosphorylated by the Rac1-JNK1 signaling pathway and stabilize PSD-95 in the PSD (Kim et al., 2007). On the other hand, Ser73 phosphorylation of PSD-95 by CaMKII interferes with GluN2A/PSD-95 binding, but not GluN2B binding to PSD-95 (Gardoni et al., 2006b).

In addition, phosphorylation of GluN2B at Ser1480 by CK2 has been shown to disrupt GluN2B interaction with PSD-95 and promote NMDAR localization to extrasynaptic sites (Chung et al., 2004). Notably, our lab has found an increased expression of CK2 in YAC HD mice striatal membranes (Fan et al., 2008) and an elevated GluN2B expression level in YAC128 mice striatal non-PSD (extrasynaptic) fraction (Milnerwood et al., 2010). Thus, it will be important to know whether the GluN2B/PSD-95 interaction is enhanced and the phosphorylation of GluN2B Ser1480 at extrasynaptic sites of YAC HD mice striatal tissue compared to WT by conducting fractionation experiments.

4.3.2   Advanced study of NMDA-activated p38 and/or JNK pathways in HD

4.3.2.1 Time course study of p38 and JNK activation in striatum of acute slices after NMDA treatment

In part of my thesis study on NMDA-induced activation of p38 and JNK in acute slices from WT and YAC128 mice, I have examined p38 activation only at one time point

-- 5min after 10min 500 μM NMDA stimulation. At that time point, I found that when normalized to baseline, the fold-increase of NMDA-induced p38 activation level in YAC128 striatum was not significantly different from that observed in WT striatum, although there was a trend toward higher p38 activation levels in both the untreated baseline group and the NMDA treated group in YAC128 striatum than in WT striatum. It is possible that the time course for NMDA-induced activation of p38 is prolonged in mutant htt-expressing striatal neurons, and should be further explored in future experiments.

With regard to the time-course of p38 activation, it is interesting that STEP61 has been shown to dephosphorylate and inactivate p38 (Munoz et al., 2003; Paul et al., 2003); therefore, calpain-mediated cleavage of STEP61 during extrasynaptic NMDAR stimulation can lead to sustained activation of p38 (Xu et al., 2009). Moreover, calpain activity has been found elevated in MSNs of YAC128 mice when compared with WT (Cowan et al., 2008). Thus, we would predict that the increased calpain activation (especially resulting from extrasynaptic NMDAR stimulation) in YAC128 striatal tissue may cause enhanced cleavage and inactivation of STEP61, in turn resulting in prolonged activation of p38 and increased neuronal death in the YAC HD mice compared to WT mice; further experiments are required to test this hypothesis.

The idea that the time course of p38 activation may be modulated by a variety of protein interactions, including mutant htt expression, is supported by several studies. One study in WT cortical neurons indicated that p38 activation decreases 30min after

stimulation with high concentrations of glutamate (Kawasaki et al., 1997). Furthermore, brief NMDAR activation leads to rapid but transient activation of p38 MAPK due to GluN2B-type NMDAR-mediated dephosphorylation and activation of STEP61; on the other hand, sustained GluN2B-type NMDAR activation degrades active STEP61, leading to secondary sustained activation of p38 MAPK and signaling to neuronal death (Poddar et al., 2010). Thus, it would be both interesting and critical to compare whether the time-course of transient and/or prolonged NMDA treatment-induced p38 MAPK activation is different in WT and YAC128 mice striatum, and whether the secondary sustained p38 activation also requires the GluN2B/PSD-95 interaction.

4.3.2.2 In vivo study of Tat-NR2B9c peptide and p38 MAPK in QA lesion model of WT and YAC128 mice.

The intra-striatal injection of the NMDA receptor agonist QA in rodents has been widely used as an acute model mimicking the selective degeneration of striatal neurons in HD (Beal et al., 1991; Beal et al., 1986). To test whether disrupting the GluN2B/PSD-95 interaction or blocking p38 MAPK activation protects striatal neurons from excitotoxic insults in YAC HD mice *in vivo*, we plan to inject Tat-NR2B9c or p38 MAPK inhibitor intravenously or directly into striatum 1hr before the intra-striatal QA injection. Brains of WT (or YAC18) and YAC128 mice would then be removed 5 mins and 30 mins later to detect p38 MAPK activation in striatum using western blotting; another cohort of mice would be sacrificed 7 days following QA injection to quantify the volume of the striatal

lesion by FluoroJade B staining. If pilot experiments support a protective role of either the Tat-NR2B9c or p38 MAPK inhibitor, further behavioral tests will be conducted to determine the effects of these compounds on motor deficits of YAC128 mice at later disease stages. These studies will be carried out in collaboration with Dr. Blair Leavitt.

4.3.2.3 The role of SynGAP in GluN2B/PSD-95/p38 MAPK pathway in WT and YAC HD mice striatum.

Besides the traditional GluN2B/PSD-95/nNOS/p38 MAPK pathway, which is unlikely to be a major player in excitotoxicity in wild-type striatal neurons according to my study, the signaling of GluN2B/PSD-95 through SynGAP has been known to regulate neuronal apoptosis through p38 MAPK in hippocampal and cortical neurons (Kim et al., 1998; Rumbaugh et al., 2006). Thus, further work should be carried to test whether synGAP is the missing link between NMDAR/PSD-95 and p38 MAPK using siRNA knock-down in cultured striatal neurons.

4.3.2.4 Isoform study of p38 and JNK in NMDA-induced toxicity in striatum of HD mice.

The p38(α, β, γ and δ) and JNK(1-3) MAPK are complicated kinase families that respond to numerous stimuli to perform cell-specific and stimuli-specific functions under various distinct regulations, depending on their subcellular localizations, tissue distributions, developmental expression patterns, the interacting complexes as well as upstream kinases and downstream substrate selectivity and cross-talks (Haeusgen et al.,

2009; Mielke and Herdegen, 2000; Ono and Han, 2000; Raman et al., 2007). Notably, JNK3 is the relatively neural-specific isoform (Gupta et al., 1996) and was considered to play a pro-apoptotic role particularly in the CNS (Haeusgen et al., 2009). The role of different isoforms of p38 and JNK MAPKs are poorly understood in the HD and NMDA-induced toxicity field. Thus, instead of examining general activation of p38 and JNK MAPKs in response to NMDA-stimulation in striatum of WT and HD mice, a more thorough and detailed research into the roles of different isoforms of these MAPKs should be done if specific antibodies and inhibitors to isoforms are available. In fact, one might find more significant differences if only one of these isoforms plays a key role in the NMDAR-mediated toxicity in these neurons. The isoform-specific inhibitors will also serve as better drug candidates for testing in HD.

Bibliography

Aarts, M., et al., 2002. Treatment of ischemic brain damage by perturbing NMDA receptor- PSD-95 protein interactions. Science. 298**,** 846-50.

Al-Hallaq, R. A., et al., 2007. NMDA di-heteromeric receptor populations and associated proteins in rat hippocampus. J Neurosci. 27**,** 8334-43.

Albin, R. L., Greenamyre, J. T., 1992. Alternative excitotoxic hypotheses. Neurology. 42**,** 733-8.

Albin, R. L., et al., 1990. Abnormalities of striatal projection neurons and N-methyl-D-aspartate receptors in presymptomatic Huntington's disease. N Engl J Med. 322**,** 1293-8.

Andrew, S. E., et al., 1993. The relationship between trinucleotide (CAG) repeat length and clinical features of Huntington's disease. Nat Genet. 4**,** 398-403.

Apostol, B. L., et al., 2006. Mutant huntingtin alters MAPK signaling pathways in PC12 and striatal cells: ERK1/2 protects against mutant huntingtin-associated toxicity. Hum Mol Genet. 15**,** 273-85.

Apostol, B. L., et al., 2008. CEP-1347 reduces mutant huntingtin-associated neurotoxicity and restores BDNF levels in R6/2 mice. Mol Cell Neurosci. 39**,** 8-20.

Asztely, F., Gustafsson, B., 1996. Ionotropic glutamate receptors. Their possible role in the expression of hippocampal synaptic plasticity. Mol Neurobiol. 12**,** 1-11.

Atwal, R. S., et al., 2007. Huntingtin has a membrane association signal that can modulate huntingtin aggregation, nuclear entry and toxicity. Hum Mol Genet. 16**,** 2600-15.

Aziz, N. A., et al., 2009. Normal and mutant HTT interact to affect clinical severity and progression in Huntington disease. Neurology. 73**,** 1280-5.

Bach, A., et al., 2011. Cell-permeable and plasma-stable peptidomimetic inhibitors of the postsynaptic density-95/N-methyl-D-aspartate receptor interaction. J Med Chem. 54**,** 1333-46.

Barone, F. C., et al., 2001. Inhibition of p38 mitogen-activated protein kinase provides neuroprotection in cerebral focal ischemia. Med Res Rev. 21**,** 129-45.

Barria, A., Malinow, R., 2002. Subunit-specific NMDA receptor trafficking to synapses. Neuron. 35**,** 345-53.

Beal, M. F., 1992. Mechanisms of excitotoxicity in neurologic diseases. Faseb J. 6**,** 3338-44.

Beal, M. F., et al., 1991. Chronic quinolinic acid lesions in rats closely resemble Huntington's disease. J Neurosci. 11**,** 1649-59.

Beal, M. F., et al., 1986. Replication of the neurochemical characteristics of Huntington's disease by quinolinic acid. Nature. 321**,** 168-71.

Behrens, P. F., et al., 2002. Impaired glutamate transport and glutamate-glutamine cycling: downstream effects of the Huntington mutation. Brain. 125**,** 1908-22.

Ben-Levy, R., et al., 1998. Nuclear export of the stress-activated protein kinase p38 mediated by its substrate MAPKAP kinase-2. Curr Biol. 8**,** 1049-57.

Bergles, D. E., et al., 1999. Clearance of glutamate inside the synapse and beyond. Curr Opin Neurobiol. 9**,** 293-8.

Berliocchi, L., et al., 2005. Ca2+ signals and death programmes in neurons. Philos Trans R Soc Lond B Biol Sci. 360**,** 2255-8.

Berridge, M. J., 1998. Neuronal calcium signaling. Neuron. 21**,** 13-26.

Besancon, E., et al., 2008. Beyond NMDA and AMPA glutamate receptors: emerging mechanisms for ionic imbalance and cell death in stroke. Trends Pharmacol Sci. 29**,** 268-75.

Bezprozvanny, I., Hayden, M. R., 2004. Deranged neuronal calcium signaling and Huntington disease. Biochem Biophys Res Commun. 322**,** 1310-7.

Bhattacharyya, S., et al., 2009. A critical role for PSD-95/AKAP interactions in endocytosis of synaptic AMPA receptors. Nat Neurosci. 12**,** 172-81.

Bliss, T. V., Collingridge, G. L., 1993. A synaptic model of memory: long-term potentiation in the hippocampus. Nature. 361**,** 31-9.

Bortolotto, Z. A., et al., 1999. Roles of metabotropic glutamate receptors in LTP and LTD in the hippocampus. Curr Opin Neurobiol. 9**,** 299-304.

Bossy-Wetzel, E., et al., 2004. Molecular pathways to neurodegeneration. Nat Med. 10 Suppl**,** S2-9.

Boulanger, L. M., et al., 1995. Cellular and molecular characterization of a brain-enriched protein tyrosine phosphatase. J Neurosci. 15**,** 1532-44.

Braak, H., Braak, E., 1982. Neuronal types in the striatum of man. Cell Tissue Res. 227**,** 319-42.

Braithwaite, S. P., et al., 2006a. Regulation of NMDA receptor trafficking and function by striatal-enriched tyrosine phosphatase (STEP). Eur J Neurosci. 23**,** 2847-56.

Braithwaite, S. P., et al., 2006b. Synaptic plasticity: one STEP at a time. Trends Neurosci. 29**,** 452-8.

Brandt, J., et al., 1996. Trinucleotide repeat length and clinical progression in Huntington's disease. Neurology. 46**,** 527-31.

Brenman, J. E., et al., 1996. Interaction of nitric oxide synthase with the postsynaptic density protein PSD-95 and alpha1-syntrophin mediated by PDZ domains. Cell. 84**,** 757-67.

Brinkman, R. R., et al., 1997. The likelihood of being affected with Huntington disease by a particular age, for a specific CAG size. Am J Hum Genet. 60**,** 1202-10.

Buller, A. L., et al., 1994. The molecular basis of NMDA receptor subtypes: native receptor diversity is predicted by subunit composition. J Neurosci. 14**,** 5471-84.

Burlacu, A., 2003. Regulation of apoptosis by Bcl-2 family proteins. J Cell Mol Med. 7**,** 249-57.

Cao, J., et al., 2005. The PSD95-nNOS interface: a target for inhibition of excitotoxic p38 stress-activated protein kinase activation and cell death. J Cell Biol. 168**,** 117-26.

Cattaneo, E., Calabresi, P., 2002. Mutant huntingtin goes straight to the heart. Nat Neurosci. 5**,** 711-2.

Cattaneo, E., et al., 2001. Loss of normal huntingtin function: new developments in Huntington's disease research. Trends Neurosci. 24**,** 182-8.

Cattaneo, E., et al., 2005. Normal huntingtin function: an alternative approach to Huntington's disease. Nat Rev Neurosci. 6**,** 919-30.

Cavara, N. A., Hollmann, M., 2008. Shuffling the deck anew: how NR3 tweaks NMDA receptor function. Mol Neurobiol. 38**,** 16-26.

Centeno, C., et al., 2007. Role of the JNK pathway in NMDA-mediated excitotoxicity of cortical neurons. Cell Death Differ. 14**,** 240-53.

Cepeda, C., et al., 2001. NMDA receptor function in mouse models of Huntington disease. J Neurosci Res. 66**,** 525-39.

Chan, S. L., Mattson, M. P., 1999. Caspase and calpain substrates: roles in synaptic plasticity and cell death. J Neurosci Res. 58**,** 167-90.

Chazot, P. L., et al., 1992. Immunological detection of the NMDAR1 glutamate receptor subunit expressed in embryonic kidney 293 cells and in rat brain. J Neurochem. 59**,** 1176-8.

Chen, C., Okayama, H., 1987. High-efficiency transformation of mammalian cells by plasmid DNA. Mol Cell Biol. 7**,** 2745-52.

Chen, L., et al., 2000. Stargazin regulates synaptic targeting of AMPA receptors by two distinct mechanisms. Nature. 408**,** 936-43.

Chen, N., et al., 1999a. Subtype-dependence of NMDA receptor channel open probability. J Neurosci. 19**,** 6844-54.

Chen, N., et al., 1999b. Subtype-specific enhancement of NMDA receptor currents by mutant huntingtin. J Neurochem. 72**,** 1890-8.

Chen, Q., et al., 2007. Differential roles of NR2A- and NR2B-containing NMDA receptors in activity-dependent brain-derived neurotrophic factor gene regulation and limbic epileptogenesis. J Neurosci. 27**,** 542-52.

Chen, R. W., et al., 2003. Regulation of c-Jun N-terminal kinase, p38 kinase and AP-1 DNA binding in cultured brain neurons: roles in glutamate excitotoxicity and lithium neuroprotection. J Neurochem. 84**,** 566-75.

Chetkovich, D. M., et al., 2002. Postsynaptic targeting of alternative postsynaptic density-95 isoforms by distinct mechanisms. J Neurosci. 22**,** 6415-25.

Choi, D. W., 1992. Excitotoxic cell death. J Neurobiol. 23**,** 1261-76.

Choi, D. W., et al., 1987. Dextrorphan and levorphanol selectively block N-methyl-D-aspartate receptor-mediated neurotoxicity on cortical neurons. J Pharmacol Exp Ther. 242**,** 713-20.

Christie, J. M., et al., 2000. Native N-methyl-D-aspartate receptors containing NR2A and NR2B subunits have pharmacologically distinct competitive antagonist binding sites. J Pharmacol Exp Ther. 292**,** 1169-74.

Christopherson, K. S., et al., 1999. PSD-95 assembles a ternary complex with the N-methyl-D-aspartic acid receptor and a bivalent neuronal NO synthase PDZ domain. J Biol Chem. 274**,** 27467-73.

Chung, H. J., et al., 2004. Regulation of the NMDA receptor complex and trafficking by activity-dependent phosphorylation of the NR2B subunit PDZ ligand. J Neurosci. 24**,** 10248-59.

Clapham, D. E., 1995. Calcium signaling. Cell. 80**,** 259-68.

Colledge, M., et al., 2000. Targeting of PKA to glutamate receptors through a MAGUK-AKAP complex. Neuron. 27**,** 107-19.

Conn, P. J., Pin, J. P., 1997. Pharmacology and functions of metabotropic glutamate receptors. Annu Rev Pharmacol Toxicol. 37**,** 205-37.

Cousins, S. L., et al., 2009. Delineation of additional PSD-95 binding domains within NMDA receptor NR2 subunits reveals differences between NR2A/PSD-95 and NR2B/PSD-95 association. Neuroscience. 158**,** 89-95.

Cousins, S. L., et al., 2008. Differential interaction of NMDA receptor subtypes with the post-synaptic density-95 family of membrane associated guanylate kinase proteins. J Neurochem. 104**,** 903-13.

Cowan, C. M., et al., 2008. Polyglutamine-modulated striatal calpain activity in YAC transgenic huntington disease mouse model: impact on NMDA receptor function and toxicity. J Neurosci. 28**,** 12725-35.

Cowan, C. M., Raymond, L. A., 2006. Selective neuronal degeneration in Huntington's disease. Curr Top

Dev Biol. 75**,** 25-71.

Coyle, J. T., Puttfarcken, P., 1993. Oxidative stress, glutamate, and neurodegenerative disorders. Science. 262**,** 689-95.

Cui, H., et al., 2007. PDZ protein interactions underlying NMDA receptor-mediated excitotoxicity and neuroprotection by PSD-95 inhibitors. J Neurosci. 27**,** 9901-15.

Cull-Candy, S., et al., 2001. NMDA receptor subunits: diversity, development and disease. Curr Opin Neurobiol. 11**,** 327-35.

Cuthbert, P. C., et al., 2007. Synapse-associated protein 102/dlgh3 couples the NMDA receptor to specific plasticity pathways and learning strategies. J Neurosci. 27**,** 2673-82.

Davies, S., Ramsden, D. B., 2001. Huntington's disease. Mol Pathol. 54**,** 409-13.

Davies, S. W., et al., 1997. Formation of neuronal intranuclear inclusions underlies the neurological dysfunction in mice transgenic for the HD mutation. Cell. 90**,** 537-48.

Dawson, V. L., et al., 1991. Nitric oxide mediates glutamate neurotoxicity in primary cortical cultures. Proc Natl Acad Sci U S A. 88**,** 6368-71.

Derradji, H., Baatout, S., 2003. Apoptosis: a mechanism of cell suicide. In Vivo. 17**,** 185-92.

Dick, O., Bading, H., 2010. Synaptic activity and nuclear calcium signaling protect hippocampal neurons from death signal-associated nuclear translocation of FoxO3a induced by extrasynaptic N-methyl-D-aspartate receptors. J Biol Chem. 285**,** 19354-61.

DiFiglia, M., 1990. Excitotoxic injury of the neostriatum: a model for Huntington's disease. Trends Neurosci. 13**,** 286-9.

DiFiglia, M., et al., 1995. Huntingtin is a cytoplasmic protein associated with vesicles in human and rat brain neurons. Neuron. 14**,** 1075-81.

Dingledine, R., et al., 1999. The glutamate receptor ion channels. Pharmacol Rev. 51**,** 7-61.

Doble, A., 1999. The role of excitotoxicity in neurodegenerative disease: implications for therapy. Pharmacol Ther. 81**,** 163-221.

Dunah, A. W., et al., 2002. Sp1 and TAFII130 transcriptional activity disrupted in early Huntington's disease. Science. 296**,** 2238-43.

Duyao, M. P., et al., 1995. Inactivation of the mouse Huntington's disease gene homolog Hdh. Science. 269**,** 407-10.

El-Husseini, A. E., et al., 2000. Ion channel clustering by membrane-associated guanylate kinases. Differential regulation by N-terminal lipid and metal binding motifs. J Biol Chem. 275**,** 23904-10.

Elias, G. M., Nicoll, R. A., 2007. Synaptic trafficking of glutamate receptors by MAGUK scaffolding proteins. Trends Cell Biol. 17**,** 343-52.

Engelsen, B., 1986. Neurotransmitter glutamate: its clinical importance. Acta Neurol Scand. 74**,** 337-55.

Fan, J., et al., 2009. Interaction of postsynaptic density protein-95 with NMDA receptors influences excitotoxicity in the yeast artificial chromosome mouse model of Huntington's disease. J Neurosci. 29**,** 10928-38.

Fan, J., et al., 2010. N-Methyl-d-aspartate receptor subunit- and neuronal-type dependence of excitotoxic signaling through post-synaptic density 95. J Neurochem. 115**,** 1045-56.

Fan, M. M., et al., 2007. Altered NMDA receptor trafficking in a yeast artificial chromosome transgenic mouse model of Huntington's disease. J Neurosci. 27**,** 3768-79.

Fan, M. M., Raymond, L. A., 2007. N-methyl-D-aspartate (NMDA) receptor function and excitotoxicity in Huntington's disease. Prog Neurobiol. 81**,** 272-93.

Fan, M. M., et al., 2008. Protective up-regulation of CK2 by mutant huntingtin in cells co-expressing NMDA receptors. J Neurochem. 104**,** 790-805.

Fernandes, H. B., et al., 2007. Mitochondrial sensitivity and altered calcium handling underlie enhanced NMDA-induced apoptosis in YAC128 model of Huntington's disease. J Neurosci. 27**,** 13614-23.

Ferrante, R. J., et al., 1997. Heterogeneous topographic and cellular distribution of huntingtin expression in the normal human neostriatum. J Neurosci. 17**,** 3052-63.

Ferrante, R. J., et al., 1993. Excitotoxin lesions in primates as a model for Huntington's disease: histopathologic and neurochemical characterization. Exp Neurol. 119**,** 46-71.

Ferrer, I., et al., 2001. Differential expression of active, phosphorylation-dependent MAP kinases, MAPK/ERK, SAPK/JNK and p38, and specific transcription factor substrates following quinolinic acid excitotoxicity in the rat. Brain Res Mol Brain Res. 94**,** 48-58.

Firestein, B. L., et al., 2000. Postsynaptic targeting of MAGUKs mediated by distinct N-terminal domains. Neuroreport. 11**,** 3479-84.

Fuchs, S. Y., et al., 1998. MEKK1/JNK signaling stabilizes and activates p53. Proc Natl Acad Sci U S A. 95**,** 10541-6.

Fujita, A., Kurachi, Y., 2000. SAP family proteins. Biochem Biophys Res Commun. 269**,** 1-6.

Gafni, J., Ellerby, L. M., 2002. Calpain activation in Huntington's disease. J Neurosci. 22**,** 4842-9.

Gallo, K. A., Johnson, G. L., 2002. Mixed-lineage kinase control of JNK and p38 MAPK pathways. Nat Rev Mol Cell Biol. 3**,** 663-72.

Garcia, M., et al., 2004. Expanded huntingtin activates the c-Jun terminal kinase/c-Jun pathway prior to aggregate formation in striatal neurons in culture. Neuroscience. 127**,** 859-70.

Gardoni, F., et al., 2009a. Postsynaptic density-membrane associated guanylate kinase proteins (PSD-MAGUKs) and their role in CNS disorders. Neuroscience. 158**,** 324-33.

Gardoni, F., et al., 2009b. Decreased NR2B subunit synaptic levels cause impaired long-term potentiation but not long-term depression. J Neurosci. 29**,** 669-77.

Gardoni, F., et al., 2006a. A critical interaction between NR2B and MAGUK in L-DOPA induced dyskinesia. J Neurosci. 26**,** 2914-22.

Gardoni, F., et al., 2006b. Calcium-calmodulin-dependent protein kinase II phosphorylation modulates PSD-95 binding to NMDA receptors. Eur J Neurosci. 24**,** 2694-704.

Garner, C. C., et al., 2000. PDZ domains in synapse assembly and signalling. Trends Cell Biol. 10**,** 274-80.

Gauthier, L. R., et al., 2004. Huntingtin controls neurotrophic support and survival of neurons by enhancing BDNF vesicular transport along microtubules. Cell. 118**,** 127-38.

Gervais, F. G., et al., 2002. Recruitment and activation of caspase-8 by the Huntingtin-interacting protein Hip-1 and a novel partner Hippi. Nat Cell Biol. 4**,** 95-105.

Ghatan, S., et al., 2000. p38 MAP kinase mediates bax translocation in nitric oxide-induced apoptosis in neurons. J Cell Biol. 150**,** 335-47.

Gianfriddo, M., et al., 2004. Adenosine and glutamate extracellular concentrations and mitogen-activated protein kinases in the striatum of Huntington transgenic mice. Selective antagonism of adenosine A2A receptors reduces transmitter outflow. Neurobiol Dis. 17**,** 77-88.

Gil, J. M., Rego, A. C., 2009. The R6 lines of transgenic mice: a model for screening new therapies for Huntington's disease. Brain Res Rev. 59, 410-31.

Graham, R. K., et al., 2006a. Cleavage at the caspase-6 site is required for neuronal dysfunction and degeneration due to mutant huntingtin. Cell. 125, 1179-91.

Graham, R. K., et al., 2009. Differential susceptibility to excitotoxic stress in YAC128 mouse models of Huntington disease between initiation and progression of disease. J Neurosci. 29, 2193-204.

Graham, R. K., et al., 2006b. Levels of mutant huntingtin influence the phenotypic severity of Huntington disease in YAC128 mouse models. Neurobiol Dis. 21, 444-55.

Gray, M., et al., 2008. Full-length human mutant huntingtin with a stable polyglutamine repeat can elicit progressive and selective neuropathogenesis in BACHD mice. J Neurosci. 28, 6182-95.

Group, T. H. s. D. C. R., 1993. A novel gene containing a trinucleotide repeat that is expanded and unstable on Huntington's disease chromosomes. The Huntington's Disease Collaborative Research Group. Cell. 72, 971-83.

Gubellini, P., et al., 2004. Metabotropic glutamate receptors and striatal synaptic plasticity: implications for neurological diseases. Prog Neurobiol. 74, 271-300.

Guidetti, P., et al., 2006. Elevated brain 3-hydroxykynurenine and quinolinate levels in Huntington disease mice. Neurobiol Dis. 23, 190-7.

Guidetti, P., et al., 2004. Neostriatal and cortical quinolinate levels are increased in early grade Huntington's disease. Neurobiol Dis. 17, 455-61.

Gupta, S., et al., 1996. Selective interaction of JNK protein kinase isoforms with transcription factors. EMBO J. 15, 2760-70.

Gutekunst, C. A., et al., 1995. Identification and localization of huntingtin in brain and human lymphoblastoid cell lines with anti-fusion protein antibodies. Proc Natl Acad Sci U S A. 92, 8710-4.

Haddad, J. J., 2005. N-methyl-D-aspartate (NMDA) and the regulation of mitogen-activated protein kinase (MAPK) signaling pathways: a revolving neurochemical axis for therapeutic intervention? Prog Neurobiol. 77, 252-82.

Haeusgen, W., et al., 2009. Specific activities of individual c-Jun N-terminal kinases in the brain. Neuroscience. 161, 951-9.

Hansson, O., et al., 2001. Resistance to NMDA toxicity correlates with appearance of nuclear inclusions, behavioural deficits and changes in calcium homeostasis in mice transgenic for exon 1 of the huntington gene. Eur J Neurosci. 14, 1492-504.

Hardingham, G. E., 2006. Pro-survival signalling from the NMDA receptor. Biochem Soc Trans. 34, 936-8.

Hardingham, G. E., Bading, H., 2003. The Yin and Yang of NMDA receptor signalling. Trends Neurosci. 26, 81-9.

Hardingham, G. E., Bading, H., 2010. Synaptic versus extrasynaptic NMDA receptor signalling: implications for neurodegenerative disorders. Nat Rev Neurosci. 11, 682-96.

Hardingham, G. E., et al., 2002. Extrasynaptic NMDARs oppose synaptic NMDARs by triggering CREB shut-off and cell death pathways. Nat Neurosci. 5, 405-14.

Harjes, P., Wanker, E. E., 2003. The hunt for huntingtin function: interaction partners tell many different stories. Trends Biochem Sci. 28, 425-33.

Harper, P. S. (Ed.) 1991. Huntington's Disease, Ed.22, PS Harper ed. WB Saunders Co. Ltd., London.

Harper, S. J., Wilkie, N., 2003. MAPKs: new targets for neurodegeneration. Expert Opin Ther Targets. 7**,** 187-200.

Hartley, D. M., et al., 1993. Glutamate receptor-induced 45Ca2+ accumulation in cortical cell culture correlates with subsequent neuronal degeneration. J Neurosci. 13**,** 1993-2000.

Hebb, C., 1970. CNS at the cellular level: identity of transmitter agents. Annu Rev Physiol. 32**,** 165-92.

Heng, M. Y., et al., 2007. Longitudinal evaluation of the Hdh(CAG)150 knock-in murine model of Huntington's disease. J Neurosci. 27**,** 8989-98.

Hickey, M. A., Chesselet, M. F., 2003. Apoptosis in Huntington's disease. Prog Neuropsychopharmacol Biol Psychiatry. 27**,** 255-65.

Hilditch-Maguire, P., et al., 2000. Huntingtin: an iron-regulated protein essential for normal nuclear and perinuclear organelles. Hum Mol Genet. 9**,** 2789-97.

Hodgson, J. G., et al., 1999. A YAC mouse model for Huntington's disease with full-length mutant huntingtin, cytoplasmic toxicity, and selective striatal neurodegeneration. Neuron. 23**,** 181-92.

Hodgson, J. G., et al., 1996. Human huntingtin derived from YAC transgenes compensates for loss of murine huntingtin by rescue of the embryonic lethal phenotype. Hum Mol Genet. 5**,** 1875-85.

Hoffner, G., et al., 2002. Perinuclear localization of huntingtin as a consequence of its binding to microtubules through an interaction with beta-tubulin: relevance to Huntington's disease. J Cell Sci. 115**,** 941-8.

Hollmann, M., et al., 1993. Zinc potentiates agonist-induced currents at certain splice variants of the NMDA receptor. Neuron. 10**,** 943-54.

Horn, T. F., et al., 2002. Nitric oxide promotes intracellular calcium release from mitochondria in striatal neurons. Faseb J. 16**,** 1611-22.

Hsieh, C. C., Papaconstantinou, J., 2002. The effect of aging on p38 signaling pathway activity in the mouse liver and in response to ROS generated by 3-nitropropionic acid. Mech Ageing Dev. 123**,** 1423-35.

Hsieh, C. C., et al., 2003. Age-associated changes in SAPK/JNK and p38 MAPK signaling in response to the generation of ROS by 3-nitropropionic acid. Mech Ageing Dev. 124**,** 733-46.

Humbert, S., et al., 2002. The IGF-1/Akt pathway is neuroprotective in Huntington's disease and involves Huntingtin phosphorylation by Akt. Dev Cell. 2**,** 831-7.

Irie, M., et al., 1997. Binding of neuroligins to PSD-95. Science. 277**,** 1511-5.

Ittner, L. M., et al., 2010. Dendritic function of tau mediates amyloid-beta toxicity in Alzheimer's disease mouse models. Cell. 142**,** 387-97.

Ivanov, A., et al., 2006. Opposing role of synaptic and extrasynaptic NMDA receptors in regulation of the extracellular signal-regulated kinases (ERK) activity in cultured rat hippocampal neurons. J Physiol. 572**,** 789-98.

Izumi, Y., et al., 2008. Long-term potentiation inhibition by low-level N-methyl-D-aspartate receptor activation involves calcineurin, nitric oxide, and p38 mitogen-activated protein kinase. Hippocampus. 18**,** 258-65.

Jarabek, B. R., et al., 2004. Regulation of proteins affecting NMDA receptor-induced excitotoxicity in a Huntington's mouse model. Brain. 127**,** 505-16.

Johnson, C. D., Davidson, B. L., 2010. Huntington's disease: progress toward effective disease-modifying treatments and a cure. Hum Mol Genet. 19**,** R98-R102.

Juo, P., et al., 1997. Fas activation of the p38 mitogen-activated protein kinase signalling pathway requires ICE/CED-3 family proteases. Mol Cell Biol. 17**,** 24-35.

Kalchman, M. A., et al., 1997. HIP1, a human homologue of S. cerevisiae Sla2p, interacts with membrane-associated huntingtin in the brain. Nat Genet. 16**,** 44-53.

Kanduc, D., et al., 2002. Cell death: apoptosis versus necrosis (review). Int J Oncol. 21**,** 165-70.

Kawasaki, H., et al., 1997. Activation and involvement of p38 mitogen-activated protein kinase in glutamate-induced apoptosis in rat cerebellar granule cells. J Biol Chem. 272**,** 18518-21.

Kegel, K. B., et al., 2002. Huntingtin is present in the nucleus, interacts with the transcriptional corepressor C-terminal binding protein, and represses transcription. J Biol Chem. 277**,** 7466-76.

Kim, E., et al., 1996. Heteromultimerization and NMDA receptor-clustering activity of Chapsyn-110, a member of the PSD-95 family of proteins. Neuron. 17**,** 103-13.

Kim, E., et al., 1997. GKAP, a novel synaptic protein that interacts with the guanylate kinase-like domain of the PSD-95/SAP90 family of channel clustering molecules. J Cell Biol. 136**,** 669-78.

Kim, E., Sheng, M., 2004. PDZ domain proteins of synapses. Nat Rev Neurosci. 5**,** 771-81.

Kim, J. H., et al., 1998. SynGAP: a synaptic RasGAP that associates with the PSD-95/SAP90 protein family. Neuron. 20**,** 683-91.

Kim, M. J., et al., 2005. Differential roles of NR2A- and NR2B-containing NMDA receptors in Ras-ERK signaling and AMPA receptor trafficking. Neuron. 46**,** 745-60.

Kim, M. J., et al., 2007. Synaptic accumulation of PSD-95 and synaptic function regulated by phosphorylation of serine-295 of PSD-95. Neuron. 56**,** 488-502.

Ko, H. W., et al., 1998. Ca2+-mediated activation of c-Jun N-terminal kinase and nuclear factor kappa B by NMDA in cortical cell cultures. J Neurochem. 71**,** 1390-5.

Kohr, G., 2006. NMDA receptor function: subunit composition versus spatial distribution. Cell Tissue Res. 326**,** 439-46.

Kornau, H. C., et al., 1995. Domain interaction between NMDA receptor subunits and the postsynaptic density protein PSD-95. Science. 269**,** 1737-40.

Kovacs, A. D., et al., 2001. Cortical and striatal neuronal cultures of the same embryonic origin show intrinsic differences in glutamate receptor expression and vulnerability to excitotoxicity. Exp Neurol. 168**,** 47-62.

Krupp, J. J., et al., 1996. Calcium-dependent inactivation of recombinant N-methyl-D-aspartate receptors is NR2 subunit specific. Mol Pharmacol. 50**,** 1680-8.

Kulisz, A., et al., 2002. Mitochondrial ROS initiate phosphorylation of p38 MAP kinase during hypoxia in cardiomyocytes. Am J Physiol Lung Cell Mol Physiol. 282**,** L1324-9.

Kumar, U., et al., 1997. Expression of NMDA receptor-1 (NR1) and huntingtin in striatal neurons which colocalize somatostatin, neuropeptide Y, and NADPH diaphorase: a double-label histochemical and immunohistochemical study. Exp Neurol. 145**,** 412-24.

Kutsuwada, T., et al., 1992. Molecular diversity of the NMDA receptor channel. Nature. 358**,** 36-41.

Kyriakis, J. M., Avruch, J., 2001. Mammalian mitogen-activated protein kinase signal transduction pathways activated by stress and inflammation. Physiol Rev. 81**,** 807-69.

Landwehrmeyer, G. B., et al., 1995. NMDA receptor subunit mRNA expression by projection neurons and interneurons in rat striatum. J Neurosci. 15**,** 5297-307.

Lau, C. G., Zukin, R. S., 2007. NMDA receptor trafficking in synaptic plasticity and neuropsychiatric disorders. Nat Rev Neurosci. 8**,** 413-26.

Lavezzari, G., et al., 2004. Subunit-specific regulation of NMDA receptor endocytosis. J Neurosci. 24**,** 6383-91.

Leavitt, B. R., et al., 2001. Wild-type huntingtin reduces the cellular toxicity of mutant huntingtin in vivo. Am J Hum Genet. 68**,** 313-24.

Leavitt, B. R., et al., 2006. Wild-type huntingtin protects neurons from excitotoxicity. J Neurochem. 96**,** 1121-9.

Legendre-Guillemin, V., et al., 2002. HIP1 and HIP12 display differential binding to F-actin, AP2, and clathrin. Identification of a novel interaction with clathrin light chain. J Biol Chem. 277**,** 19897-904.

Legos, J. J., et al., 2002. The selective p38 inhibitor SB-239063 protects primary neurons from mild to moderate excitotoxic injury. Eur J Pharmacol. 447**,** 37-42.

Leist, M., Nicotera, P., 1998. Calcium and neuronal death. Rev Physiol Biochem Pharmacol. 132**,** 79-125.

Leonard, A. S., et al., 1998. SAP97 is associated with the alpha-amino-3-hydroxy-5-methylisoxazole-4-propionic acid receptor GluR1 subunit. J Biol Chem. 273**,** 19518-24.

Leveille, F., et al., 2008. Neuronal viability is controlled by a functional relation between synaptic and extrasynaptic NMDA receptors. FASEB J. 22**,** 4258-71.

Levine, M. S., et al., 2010. Location, location, location: contrasting roles of synaptic and extrasynaptic NMDA receptors in Huntington's disease. Neuron. 65**,** 145-7.

Levine, M. S., et al., 2004. Genetic mouse models of Huntington's and Parkinson's diseases: illuminating but imperfect. Trends Neurosci. 27**,** 691-7.

Levine, M. S., et al., 1999. Enhanced sensitivity to N-methyl-D-aspartate receptor activation in transgenic and knockin mouse models of Huntington's disease. J Neurosci Res. 58**,** 515-32.

Li, B., et al., 2002a. Differential regulation of synaptic and extra-synaptic NMDA receptors. Nat Neurosci. 5**,** 833-4.

Li, H., et al., 2001. Huntingtin aggregate-associated axonal degeneration is an early pathological event in Huntington's disease mice. J Neurosci. 21**,** 8473-81.

Li, J. H., et al., 1998. Developmental changes in localization of NMDA receptor subunits in primary cultures of cortical neurons. Eur J Neurosci. 10**,** 1704-15.

Li, J. Y., et al., 2003a. Huntington's disease: a synaptopathy? Trends Mol Med. 9**,** 414-20.

Li, L., et al., 2003b. Role of NR2B-type NMDA receptors in selective neurodegeneration in Huntington disease. Neurobiol Aging. 24**,** 1113-21.

Li, S. H., et al., 2002b. Interaction of Huntington disease protein with transcriptional activator Sp1. Mol Cell Biol. 22**,** 1277-87.

Li, S. H., Li, X. J., 2004a. Huntingtin-protein interactions and the pathogenesis of Huntington's disease. Trends Genet. 20**,** 146-54.

Li, S. H., Li, X. J., 2004b. Huntingtin and its role in neuronal degeneration. Neuroscientist. 10**,** 467-75.

Li, S. H., et al., 1993. Huntington's disease gene (IT15) is widely expressed in human and rat tissues. Neuron. 11**,** 985-93.

Li, X. J., et al., 1995. A huntingtin-associated protein enriched in brain with implications for pathology. Nature. 378**,** 398-402.

Lievens, J. C., et al., 2001. Impaired glutamate uptake in the R6 Huntington's disease transgenic mice. Neurobiol Dis. 8**,** 807-21.

Lin, Y., et al., 2004. Postsynaptic density protein-95 regulates NMDA channel gating and surface expression. J Neurosci. 24**,** 10138-48.

Liu, J., et al., 2008. Calpain in the CNS: from synaptic function to neurotoxicity. Sci Signal. 1**,** re1.

Liu, Y., et al., 2007. NMDA receptor subunits have differential roles in mediating excitotoxic neuronal death both in vitro and in vivo. J Neurosci. 27**,** 2846-57.

Liu, Y. F., et al., 1997. SH3 domain-dependent association of huntingtin with epidermal growth factor receptor signaling complexes. J Biol Chem. 272**,** 8121-4.

Liu, Y. F., et al., 2000. Activation of MLK2-mediated signaling cascades by polyglutamine-expanded huntingtin. J Biol Chem. 275**,** 19035-40.

Luthi-Carter, R., et al., 2002. Dysregulation of gene expression in the R6/2 model of polyglutamine disease: parallel changes in muscle and brain. Hum Mol Genet. 11**,** 1911-26.

MacDonald, M. E., Gusella, J. F., 1996. Huntington's disease: translating a CAG repeat into a pathogenic mechanism. Curr Opin Neurobiol. 6**,** 638-43.

Majumder, P., et al., 2007. Increased caspase-2, calpain activations and decreased mitochondrial complex II activity in cells expressing exogenous huntingtin exon 1 containing CAG repeat in the pathogenic range. Cell Mol Neurobiol. 27**,** 1127-45.

Mangiarini, L., et al., 1996. Exon 1 of the HD gene with an expanded CAG repeat is sufficient to cause a progressive neurological phenotype in transgenic mice. Cell. 87**,** 493-506.

Maren, S., Baudry, M., 1995. Properties and mechanisms of long-term synaptic plasticity in the mammalian brain: relationships to learning and memory. Neurobiol Learn Mem. 63**,** 1-18.

Martin, H. G., Wang, Y. T., 2010. Blocking the deadly effects of the NMDA receptor in stroke. Cell. 140**,** 174-6.

Mauceri, D., et al., 2007. Dual role of CaMKII-dependent SAP97 phosphorylation in mediating trafficking and insertion of NMDA receptor subunit NR2A. J Neurochem. 100**,** 1032-46.

Maundrell, K., et al., 1997. Bcl-2 undergoes phosphorylation by c-Jun N-terminal kinase/stress-activated protein kinases in the presence of the constitutively active GTP-binding protein Rac1. J Biol Chem. 272**,** 25238-42.

Mayer, M. L., et al., 1984. Voltage-dependent block by Mg2+ of NMDA responses in spinal cord neurones. Nature. 309**,** 261-3.

McBain, C. J., Mayer, M. L., 1994. N-methyl-D-aspartic acid receptor structure and function. Physiol Rev. 74**,** 723-60.

Menalled, L. B., et al., 2003. Time course of early motor and neuropathological anomalies in a knock-in mouse model of Huntington's disease with 140 CAG repeats. J Comp Neurol. 465**,** 11-26.

Menalled, L. B., et al., 2002. Early motor dysfunction and striosomal distribution of huntingtin microaggregates in Huntington's disease knock-in mice. J Neurosci. 22**,** 8266-76.

Mielke, K., Herdegen, T., 2000. JNK and p38 stresskinases--degenerative effectors of signal-transduction-cascades in the nervous system. Prog Neurobiol. 61**,** 45-60.

Milnerwood, A. J., et al., 2006. Early development of aberrant synaptic plasticity in a mouse model of Huntington's disease. Hum Mol Genet. 15**,** 1690-703.

Milnerwood, A. J., et al., 2010. Early increase in extrasynaptic NMDA receptor signaling and expression contributes to phenotype onset in Huntington's disease mice. Neuron. 65**,** 178-90.

Milnerwood, A. J., Raymond, L. A., 2007. Corticostriatal synaptic function in mouse models of Huntington's disease: early effects of huntingtin repeat length and protein load. J Physiol. 585**,** 817-31.

Milnerwood, A. J., Raymond, L. A., 2010. Early synaptic pathophysiology in neurodegeneration: insights from Huntington's disease. Trends Neurosci. 33**,** 513-23.

Miyashita, T., et al., 1994. Tumor suppressor p53 is a regulator of bcl-2 and bax gene expression in vitro and in vivo. Oncogene. 9**,** 1799-805.

Molz, S., et al., 2008. Glutamate-induced toxicity in hippocampal slices involves apoptotic features and p38 MAPK signaling. Neurochem Res. 33**,** 27-36.

Monyer, H., et al., 1994. Developmental and regional expression in the rat brain and functional properties of four NMDA receptors. Neuron. 12**,** 529-40.

Monyer, H., et al., 1992. Heteromeric NMDA receptors: molecular and functional distinction of subtypes. Science. 256**,** 1217-21.

Mukherjee, P. K., et al., 1999. Glutamate receptor signaling interplay modulates stress-sensitive mitogen-activated protein kinases and neuronal cell death. J Biol Chem. 274**,** 6493-8.

Muller, B. M., et al., 1996. SAP102, a novel postsynaptic protein that interacts with NMDA receptor complexes in vivo. Neuron. 17**,** 255-65.

Muller, B. M., et al., 1995. Molecular characterization and spatial distribution of SAP97, a novel presynaptic protein homologous to SAP90 and the Drosophila discs-large tumor suppressor protein. J Neurosci. 15**,** 2354-66.

Munoz, J. J., et al., 2003. Differential interaction of the tyrosine phosphatases PTP-SL, STEP and HePTP with the mitogen-activated protein kinases ERK1/2 and p38alpha is determined by a kinase specificity sequence and influenced by reducing agents. Biochem J. 372**,** 193-201.

Myers, R. H., et al., 1989. Homozygote for Huntington disease. Am J Hum Genet. 45**,** 615-8.

Naisbitt, S., et al., 1999. Shank, a novel family of postsynaptic density proteins that binds to the NMDA receptor/PSD-95/GKAP complex and cortactin. Neuron. 23**,** 569-82.

Nasir, J., et al., 1995. Targeted disruption of the Huntington's disease gene results in embryonic lethality and behavioral and morphological changes in heterozygotes. Cell. 81**,** 811-23.

Nicholls, D. G., Budd, S. L., 2000. Mitochondria and neuronal survival. Physiol Rev. 80**,** 315-60.

Nicotera, P., et al., 1999. Apoptosis and necrosis: different execution of the same death. Biochem Soc Symp. 66**,** 69-73.

Niethammer, M., et al., 1996. Interaction between the C terminus of NMDA receptor subunits and multiple members of the PSD-95 family of membrane-associated guanylate kinases. J Neurosci. 16**,** 2157-63.

Nowak, L., et al., 1984. Magnesium gates glutamate-activated channels in mouse central neurones. Nature. 307**,** 462-5.

Nucifora, F. C., Jr., et al., 2001. Interference by huntingtin and atrophin-1 with cbp-mediated transcription leading to cellular toxicity. Science. 291**,** 2423-8.

Oh, J. S., et al., 2004. Regulation of the neuron-specific Ras GTPase-activating protein, synGAP, by Ca2+/calmodulin-dependent protein kinase II. J Biol Chem. 279, 17980-8.

Oliveira, J. M., et al., 2006. Mitochondrial-dependent Ca2+ handling in Huntington's disease striatal cells: effect of histone deacetylase inhibitors. J Neurosci. 26, 11174-86.

Olney, J. W., et al., 1971. Cytotoxic effects of acidic and sulphur containing amino acids on the infant mouse central nervous system. Exp Brain Res. 14, 61-76.

Ona, V. O., et al., 1999. Inhibition of caspase-1 slows disease progression in a mouse model of Huntington's disease. Nature. 399, 263-7.

Ono, K., Han, J., 2000. The p38 signal transduction pathway: activation and function. Cell Signal. 12, 1-13.

Orrenius, S., et al., 1996. Mechanisms of calcium-related cell death. Adv Neurol. 71, 137-49; discussion 149-51.

Oyama, T., et al., 1995. Immunocytochemical localization of the striatal enriched protein tyrosine phosphatase in the rat striatum: a light and electron microscopic study with a complementary DNA-generated polyclonal antibody. Neuroscience. 69, 869-80.

Panov, A. V., et al., 2002. Early mitochondrial calcium defects in Huntington's disease are a direct effect of polyglutamines. Nat Neurosci. 5, 731-6.

Paoletti, P., Neyton, J., 2007. NMDA receptor subunits: function and pharmacology. Curr Opin Pharmacol. 7, 39-47.

Park, J., et al., 1997. Activation of c-Jun N-terminal kinase antagonizes an anti-apoptotic action of Bcl-2. J Biol Chem. 272, 16725-8.

Paul, S., et al., 2003. NMDA-mediated activation of the tyrosine phosphatase STEP regulates the duration of ERK signaling. Nat Neurosci. 6, 34-42.

Paul, S., et al., 2007. The striatal-enriched protein tyrosine phosphatase gates long-term potentiation and fear memory in the lateral amygdala. Biol Psychiatry. 61, 1049-61.

Paulsen, J. S., et al., 2008. Detection of Huntington's disease decades before diagnosis: the Predict-HD study. J Neurol Neurosurg Psychiatry. 79, 874-80.

Pelkey, K. A., et al., 2002. Tyrosine phosphatase STEP is a tonic brake on induction of long-term potentiation. Neuron. 34, 127-38.

Peng, T. I., Greenamyre, J. T., 1998. Privileged access to mitochondria of calcium influx through N-methyl-D-aspartate receptors. Mol Pharmacol. 53, 974-80.

Petersen, A., et al., 2000. Oxidative stress, mitochondrial permeability transition and activation of caspases in calcium ionophore A23187-induced death of cultured striatal neurons. Brain Res. 857, 20-9.

Petralia, R. S., et al., 2010. Organization of NMDA receptors at extrasynaptic locations. Neuroscience. 167, 68-87.

Poddar, R., et al., 2010. NR2B-NMDA receptor mediated modulation of the tyrosine phosphatase STEP regulates glutamate induced neuronal cell death. J Neurochem. 115, 1350-62.

Prybylowski, K., et al., 2005. The synaptic localization of NR2B-containing NMDA receptors is controlled by interactions with PDZ proteins and AP-2. Neuron. 47, 845-57.

Prybylowski, K., Wenthold, R. J., 2004. N-Methyl-D-aspartate receptors: subunit assembly and trafficking to the synapse. J Biol Chem. 279, 9673-6.

Raingeaud, J., et al., 1995. Pro-inflammatory cytokines and environmental stress cause p38

mitogen-activated protein kinase activation by dual phosphorylation on tyrosine and threonine. J Biol Chem. 270, **7420-6**.

Raman, M., et al., 2007. Differential regulation and properties of MAPKs. Oncogene. 26, **3100-12**.

Reddy, P. H., et al., 1998. Behavioural abnormalities and selective neuronal loss in HD transgenic mice expressing mutated full-length HD cDNA. Nat Genet. 20, **198-202**.

Regalado, M. P., et al., 2006. Transsynaptic signaling by postsynaptic synapse-associated protein 97. J Neurosci. 26, **2343-57**.

Rigamonti, D., et al., 2000. Wild-type huntingtin protects from apoptosis upstream of caspase-3. J Neurosci. 20, **3705-13**.

Rigamonti, D., et al., 2001. Huntingtin's neuroprotective activity occurs via inhibition of procaspase-9 processing. J Biol Chem. 276, **14545-8**.

Roche, K. W., et al., 2001. Molecular determinants of NMDA receptor internalization. Nat Neurosci. 4, **794-802**.

Ross, C. A., 2002. Polyglutamine pathogenesis: emergence of unifying mechanisms for Huntington's disease and related disorders. Neuron. 35, **819-22**.

Rothman, S. M., Olney, J. W., 1995. Excitotoxicity and the NMDA receptor--still lethal after eight years. Trends Neurosci. 18, **57-8**.

Roucou, X., et al., 2001. Involvement of mitochondria in apoptosis. Cardiol Clin. 19, **45-55**.

Roux, P. P., Blenis, J., 2004. ERK and p38 MAPK-activated protein kinases: a family of protein kinases with diverse biological functions. Microbiol Mol Biol Rev. 68, **320-44**.

Rubinsztein, D. C., 2002. Lessons from animal models of Huntington's disease. Trends Genet. 18, **202-9**.

Rumbaugh, G., et al., 2006. SynGAP regulates synaptic strength and mitogen-activated protein kinases in cultured neurons. Proc Natl Acad Sci U S A. 103, **4344-51**.

Rumbaugh, G., Vicini, S., 1999. Distinct synaptic and extrasynaptic NMDA receptors in developing cerebellar granule neurons. J Neurosci. 19, **10603-10**.

Sanberg, P. R., et al., 1989. The quinolinic acid model of Huntington's disease: locomotor abnormalities. Exp Neurol. 105, **45-53**.

Sanchez, I., et al., 1999. Caspase-8 is required for cell death induced by expanded polyglutamine repeats. Neuron. 22, **623-33**.

Sans, N., et al., 2000. A developmental change in NMDA receptor-associated proteins at hippocampal synapses. J Neurosci. 20, **1260-71**.

Sans, N., et al., 2003. NMDA receptor trafficking through an interaction between PDZ proteins and the exocyst complex. Nat Cell Biol. 5, **520-30**.

Sans, N., et al., 2005. mPins modulates PSD-95 and SAP102 trafficking and influences NMDA receptor surface expression. Nat Cell Biol. 7, **1179-90**.

Sastry, P. S., Rao, K. S., 2000. Apoptosis and the nervous system. J Neurochem. 74, **1-20**.

Sattler, R., Tymianski, M., 2000. Molecular mechanisms of calcium-dependent excitotoxicity. J Mol Med. 78, **3-13**.

Sattler, R., Tymianski, M., 2001. Molecular mechanisms of glutamate receptor-mediated excitotoxic neuronal cell death. Mol Neurobiol. 24, **107-29**.

Sattler, R., et al., 1999. Specific coupling of NMDA receptor activation to nitric oxide neurotoxicity by

PSD-95 protein. Science. 284**,** 1845-8.

Sawa, A., et al., 1999. Increased apoptosis of Huntington disease lymphoblasts associated with repeat length-dependent mitochondrial depolarization. Nat Med. 5**,** 1194-8.

Schluter, O. M., et al., 2006. Alternative N-terminal domains of PSD-95 and SAP97 govern activity-dependent regulation of synaptic AMPA receptor function. Neuron. 51**,** 99-111.

Schubert, D., Piasecki, D., 2001. Oxidative glutamate toxicity can be a component of the excitotoxicity cascade. J Neurosci. 21**,** 7455-62.

Schwarcz, R., et al., 1977. Loss of striatal serotonin synaptic receptor binding induced by kainic acid lesions: correlations with Huntington's Disease. J Neurochem. 28**,** 867-9.

Schwarzschild, M. A., et al., 1997. Glutamate, but not dopamine, stimulates stress-activated protein kinase and AP-1-mediated transcription in striatal neurons. J Neurosci. 17**,** 3455-66.

Schwarzschild, M. A., et al., 1999. Contrasting calcium dependencies of SAPK and ERK activations by glutamate in cultured striatal neurons. J Neurochem. 72**,** 2248-55.

Segal, M., et al., 2003. Formation of dendritic spines in cultured striatal neurons depends on excitatory afferent activity. Eur J Neurosci. 17**,** 2573-85.

Seong, I. S., et al., 2005. HD CAG repeat implicates a dominant property of huntingtin in mitochondrial energy metabolism. Hum Mol Genet. 14**,** 2871-80.

Sharp, A. H., et al., 1995. Widespread expression of Huntington's disease gene (IT15) protein product. Neuron. 14**,** 1065-74.

Shehadeh, J., et al., 2006. Striatal neuronal apoptosis is preferentially enhanced by NMDA receptor activation in YAC transgenic mouse model of Huntington disease. Neurobiol Dis. 21**,** 392-403.

Shin, J. Y., et al., 2005. Expression of mutant huntingtin in glial cells contributes to neuronal excitotoxicity. J Cell Biol. 171**,** 1001-12.

Sieradzan, K., et al., 1997. Clinical presentation and patterns of regional cerebral atrophy related to the length of trinucleotide repeat expansion in patients with adult onset Huntington's disease. Neurosci Lett. 225**,** 45-8.

Sieradzan, K. A., Mann, D. M., 2001. The selective vulnerability of nerve cells in Huntington's disease. Neuropathol Appl Neurobiol. 27**,** 1-21.

Siman, R., et al., 1989. Calpain I activation is specifically related to excitatory amino acid induction of hippocampal damage. J Neurosci. 9**,** 1579-90.

Singaraja, R. R., et al., 2002. HIP14, a novel ankyrin domain-containing protein, links huntingtin to intracellular trafficking and endocytosis. Hum Mol Genet. 11**,** 2815-28.

Slow, E. J., et al., 2005. Absence of behavioral abnormalities and neurodegeneration in vivo despite widespread neuronal huntingtin inclusions. Proc Natl Acad Sci U S A. 102**,** 11402-7.

Slow, E. J., et al., 2003. Selective striatal neuronal loss in a YAC128 mouse model of Huntington disease. Hum Mol Genet. 12**,** 1555-67.

Song, C., et al., 2003. Expression of polyglutamine-expanded huntingtin induces tyrosine phosphorylation of N-methyl-D-aspartate receptors. J Biol Chem. 278**,** 33364-9.

Soriano, F. X., Hardingham, G. E., 2007. Compartmentalized NMDA receptor signalling to survival and death. J Physiol. 584**,** 381-7.

Soriano, F. X., et al., 2008. Specific targeting of pro-death NMDA receptor signals with differing reliance on

the NR2B PDZ ligand. J Neurosci. 28**,** 10696-710.

Sornarajah, L., et al., 2008. NMDA receptor desensitization regulated by direct binding to PDZ1-2 domains of PSD-95. J Neurophysiol. 99**,** 3052-62.

Springer, J. E., et al., 2000. Calcineurin-mediated BAD dephosphorylation activates the caspase-3 apoptotic cascade in traumatic spinal cord injury. J Neurosci. 20**,** 7246-51.

Squitieri, F., et al., 2003. Homozygosity for CAG mutation in Huntington disease is associated with a more severe clinical course. Brain. 126**,** 946-55.

Starling, A. J., et al., 2005. Alterations in N-methyl-D-aspartate receptor sensitivity and magnesium blockade occur early in development in the R6/2 mouse model of Huntington's disease. J Neurosci Res. 82**,** 377-86.

Steffan, J. S., et al., 2001. Histone deacetylase inhibitors arrest polyglutamine-dependent neurodegeneration in Drosophila. Nature. 413**,** 739-43.

Stocca, G., Vicini, S., 1998. Increased contribution of NR2A subunit to synaptic NMDA receptors in developing rat cortical neurons. J Physiol. 507 (Pt 1)**,** 13-24.

Strehlow, A. N., et al., 2007. Wild-type huntingtin participates in protein trafficking between the Golgi and the extracellular space. Hum Mol Genet. 16**,** 391-409.

Sturgill, J. F., et al., 2009. Distinct domains within PSD-95 mediate synaptic incorporation, stabilization, and activity-dependent trafficking. J Neurosci. 29**,** 12845-54.

Subramaniam, S., et al., 2009. Rhes, a striatal specific protein, mediates mutant-huntingtin cytotoxicity. Science. 324**,** 1327-30.

Sugars, K. L., Rubinsztein, D. C., 2003. Transcriptional abnormalities in Huntington disease. Trends Genet. 19**,** 233-8.

Sugihara, H., et al., 1992. Structures and properties of seven isoforms of the NMDA receptor generated by alternative splicing. Biochem Biophys Res Commun. 185**,** 826-32.

Sun, Y., et al., 2001. Polyglutamine-expanded huntingtin promotes sensitization of N-methyl-D-aspartate receptors via post-synaptic density 95. J Biol Chem. 276**,** 24713-8.

Surmeier, D. J., et al., 1988. Voltage-clamp analysis of a transient potassium current in rat neostriatal neurons. Brain Res. 473**,** 187-92.

Swannie, H. C., Kaye, S. B., 2002. Protein kinase C inhibitors. Curr Oncol Rep. 4**,** 37-46.

Tang, T. S., et al., 2005. Disturbed Ca2+ signaling and apoptosis of medium spiny neurons in Huntington's disease. Proc Natl Acad Sci U S A. 102**,** 2602-7.

Tang, T. S., et al., 2003. Huntingtin and huntingtin-associated protein 1 influence neuronal calcium signaling mediated by inositol-(1,4,5) triphosphate receptor type 1. Neuron. 39**,** 227-39.

Tang, T. S., et al., 2004. HAP1 facilitates effects of mutant huntingtin on inositol 1,4,5-trisphosphate-induced Ca release in primary culture of striatal medium spiny neurons. Eur J Neurosci. 20**,** 1779-87.

Tao, F., et al., 2008. Cell-permeable peptide Tat-PSD-95 PDZ2 inhibits chronic inflammatory pain behaviors in mice. Mol Ther. 16**,** 1776-82.

Thomas, C. G., et al., 2006. Synaptic and extrasynaptic NMDA receptor NR2 subunits in cultured hippocampal neurons. J Neurophysiol. 95**,** 1727-34.

Thornberry, N. A., 1997. The caspase family of cysteine proteases. Br Med Bull. 53**,** 478-90.

Tobin, A. J., Signer, E. R., 2000. Huntington's disease: the challenge for cell biologists. Trends Cell Biol. 10**,** 531-6.

Tovar, K. R., Westbrook, G. L., 1999. The incorporation of NMDA receptors with a distinct subunit composition at nascent hippocampal synapses in vitro. J Neurosci. 19**,** 4180-8.

Trottier, Y., et al., 1995. Cellular localization of the Huntington's disease protein and discrimination of the normal and mutated form. Nat Genet. 10**,** 104-10.

Trushina, E., et al., 2006. Mutant huntingtin inhibits clathrin-independent endocytosis and causes accumulation of cholesterol in vitro and in vivo. Hum Mol Genet. 15**,** 3578-91.

Tsirigotis, M., et al., 2008. Activation of p38MAPK contributes to expanded polyglutamine-induced cytotoxicity. PLoS One. 3**,** e2130.

Tu, W., et al., 2010. DAPK1 interaction with NMDA receptor NR2B subunits mediates brain damage in stroke. Cell. 140**,** 222-34.

Van Raamsdonk, J. M., et al., 2005a. Selective degeneration and nuclear localization of mutant huntingtin in the YAC128 mouse model of Huntington disease. Hum Mol Genet. 14**,** 3823-35.

Van Raamsdonk, J. M., et al., 2005b. Cognitive dysfunction precedes neuropathology and motor abnormalities in the YAC128 mouse model of Huntington's disease. J Neurosci. 25**,** 4169-80.

Vanhoutte, P., Bading, H., 2003. Opposing roles of synaptic and extrasynaptic NMDA receptors in neuronal calcium signalling and BDNF gene regulation. Curr Opin Neurobiol. 13**,** 366-71.

Velier, J., et al., 1998. Wild-type and mutant huntingtins function in vesicle trafficking in the secretory and endocytic pathways. Exp Neurol. 152**,** 34-40.

Vincent, S. R., et al., 1998. Neurotransmitter regulation of MAP kinase signaling in striatal neurons in primary culture. Synapse. 29**,** 29-36.

von Engelhardt, J., et al., 2007. Excitotoxicity in vitro by NR2A- and NR2B-containing NMDA receptors. Neuropharmacology. 53**,** 10-7.

Vonsattel, J. P., DiFiglia, M., 1998. Huntington disease. J Neuropathol Exp Neurol. 57**,** 369-84.

Wang, J. Q., et al., 2007. Regulation of mitogen-activated protein kinases by glutamate receptors. J Neurochem. 100**,** 1-11.

Wang, J. Q., et al., 2004. Glutamate signaling to Ras-MAPK in striatal neurons: mechanisms for inducible gene expression and plasticity. Mol Neurobiol. 29**,** 1-14.

Wanker, E. E., et al., 1997. HIP-I: a huntingtin interacting protein isolated by the yeast two-hybrid system. Hum Mol Genet. 6**,** 487-95.

Warby, S. C., et al., 2005. Huntingtin phosphorylation on serine 421 is significantly reduced in the striatum and by polyglutamine expansion in vivo. Hum Mol Genet. 14**,** 1569-77.

Waxman, E. A., Lynch, D. R., 2005a. N-methyl-D-aspartate receptor subtype mediated bidirectional control of p38 mitogen-activated protein kinase. J Biol Chem. 280**,** 29322-33.

Waxman, E. A., Lynch, D. R., 2005b. N-methyl-D-aspartate receptor subtypes: multiple roles in excitotoxicity and neurological disease. Neuroscientist. 11**,** 37-49.

Wells, G. J., Bihovsky, R., 1998. Calpain inhibitors as potential treatment for stoke and other neurodegenerative diseases: recent trends and developments. Exp Opin Ther Patents. 8**,** 21.

Wenzel, A., et al., 1997. NMDA receptor heterogeneity during postnatal development of the rat brain: differential expression of the NR2A, NR2B, and NR2C subunit proteins. J Neurochem. 68**,** 469-78.

Wexler, N. S., et al., 1987. Homozygotes for Huntington's disease. Nature. 326**,** 194-7.

Wood, J. D., et al., 1996. Partial characterisation of murine huntingtin and apparent variations in the subcellular localisation of huntingtin in human, mouse and rat brain. Hum Mol Genet. 5**,** 481-7.

Wyllie, D. J., et al., 1998. Single-channel activations and concentration jumps: comparison of recombinant NR1a/NR2A and NR1a/NR2D NMDA receptors. J Physiol. 510 (Pt 1)**,** 1-18.

Xiao, L., et al., 2011. Switching of N-methyl-D-aspartate (NMDA) receptor-favorite intracellular signal pathways from ERK1/2 to p38 MAPK leads to developmental changes in NMDA neurotoxicity. J Biol Chem.

Xifro, X., et al., 2008. Calcineurin is involved in the early activation of NMDA-mediated cell death in mutant huntingtin knock-in striatal cells. J Neurochem. 105**,** 1596-612.

Xu, J., et al., 2009. Extrasynaptic NMDA receptors couple preferentially to excitotoxicity via calpain-mediated cleavage of STEP. J Neurosci. 29**,** 9330-43.

Young, A. B., et al., 1988. NMDA receptor losses in putamen from patients with Huntington's disease. Science. 241**,** 981-3.

Yu, S. P., et al., 2001. Ion homeostasis and apoptosis. Curr Opin Cell Biol. 13**,** 405-11.

Zeitlin, S., et al., 1995. Increased apoptosis and early embryonic lethality in mice nullizygous for the Huntington's disease gene homologue. Nat Genet. 11**,** 155-63.

Zeron, M. M., et al., 2001. Mutant huntingtin enhances excitotoxic cell death. Mol Cell Neurosci. 17**,** 41-53.

Zeron, M. M., et al., 2004. Potentiation of NMDA receptor-mediated excitotoxicity linked with intrinsic apoptotic pathway in YAC transgenic mouse model of Huntington's disease. Mol Cell Neurosci. 25**,** 469-79.

Zeron, M. M., et al., 2002. Increased sensitivity to N-methyl-D-aspartate receptor-mediated excitotoxicity in a mouse model of Huntington's disease. Neuron. 33**,** 849-60.

Zhang, H., et al., 2008. Full length mutant huntingtin is required for altered Ca2+ signaling and apoptosis of striatal neurons in the YAC mouse model of Huntington's disease. Neurobiol Dis. 31**,** 80-8.

Zhang, S. J., et al., 2007. Decoding NMDA Receptor Signaling: Identification of Genomic Programs Specifying Neuronal Survival and Death. Neuron. 53**,** 549-62.

Zhang, Y., et al., 2003. Sequential activation of individual caspases, and of alterations in Bcl-2 proapoptotic signals in a mouse model of Huntington's disease. J Neurochem. 87**,** 1184-92.

Zuccato, C., et al., 2003. Huntingtin interacts with REST/NRSF to modulate the transcription of NRSE-controlled neuronal genes. Nat Genet. 35**,** 76-83.

Zuccato, C., et al., 2010. Molecular mechanisms and potential therapeutical targets in Huntington's disease. Physiol Rev. 90**,** 905-81.

Zucker, B., et al., 2005. Transcriptional dysregulation in striatal projection- and interneurons in a mouse model of Huntington's disease: neuronal selectivity and potential neuroprotective role of HAP1. Hum Mol Genet. 14**,** 179-89.